

兰州理工大学

科研成果汇总

学 号： 201081191001

研 究 生： 李守东

导 师： 包广清 教授

研究方向： 电力系统优化运行

论文题目： 电制热负荷参与主动配电网
需求响应与分布式协调运行研究

学 科： 可再生能源发电与智能电网

学 院： 电气工程与信息工程学院

入学时间： 2020年9月

目 录

1. 论文检索报告	1
2. Shoudong Li, Guangqing Bao, Xiaoying Zhang, Guodong Wu, Bing Ren. Distributed response strategy of electric heating loads based on temperature queue sorting[J]. Electric Power Systems Research, 2022,211. (SCI)	4
3. Shoudong Li, Guangqing Bao, Anan Zhang. Consensus-based distributed coordinated operation of active distribution networks with electric heating loads[J]. International Journal of Electrical Power & Energy Systems, 2023,153. (SCI)	16
4. Shoudong Li, Guangqing Bao, Yanwen Hu. Distributed coordinated operation of active distribution networks with electric heating loads based on dynamic step correction ADMM[J]. Energies, 2024,17(2). (SCI)	31

机构: 兰州理工大学 电气工程与信息工程学院

姓名: 李守东 [201081191001]

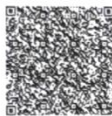
著者要求对其在国内外学术出版物所发表的科技论著被以下数据库收录情况进行查证。

检索范围:

- 科学引文索引 (Science Citation Index Expanded): 1900年-2024年

检索结果:

检索类型	数据库	年份范围	总篇数	作者篇数
SCI-E 收录	SCI-EXPANDED	2022 - 2024	3	3



委托人声明:

本人委托兰州理工大学图书馆查询论著被指定检索工具收录情况, 经核对检索结果, 附件中所列文献均为本人论著, 特此声明。

作者(签字): 李守东

完成人(签字): 刘婧

完成日期: 2024年11月6日

完成单位(盖章): 兰州理工大学图书馆信息咨询与学科服务部

(本检索报告仅限校内使用)





图书馆

文献检索报告
SCI-E 收录



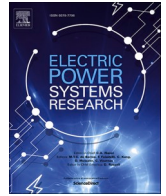
兰州理工大学图书馆 LUTLIB

报告编号: R2024-1065 SCI-E 收录

数据库: 科学引文索引 (Science Citation Index Expanded) 时间范围: 2022年至2024年	作者姓名: 李守东 作者单位: 兰州理工大学 电气工程与信息工程学院	检索人员: 刁婧 检索日期: 2024年11月6日
--	---------------------------------------	------------------------------

检索结果: 被 SCI-E 收录文献 3 篇

#	作者	地址	标题	来源出版物	文献类型	入藏号
1	LI, SD; Bao, GQ; Zhang, XY; Wu, GD; Ren, B	[Li, Shoudong; Bao, Guangqing; Zhang, Xiaoying; Wu, Guodong; Ren, Bing] Lanzhou Univ Technol, Sch Elect & Informat Engn, Lanzhou 730050, Peoples R China.; [Li, Shoudong; Ren, Bing] Lanzhou Jiaotong Univ, Sch Automat & Elect Engn, Lanzhou 730070, Peoples R China.; [Wu, Guodong] State Grid Gansu Elect Power Co, Lanzhou 730050, Peoples R China.	Distributed response strategy of electric heating loads based on temperature queue sorting	<i>ELECTRIC POWER SYSTEMS RESEARCH</i> 2022, 211: 108196.	J Article	WOS:0008-230182000-03
2	LI, SD; Bao, GQ; Zhang, AA	[Li, Shoudong; Bao, Guangqing] Lanzhou Univ Technol, Sch Elect & Informat Engn, Lanzhou 730050, Peoples R China.; [Li, Shoudong] Lanzhou Jiaotong Univ, Sch Automat & Elect Engn, Lanzhou 730070, Peoples R China.; [Bao, Guangqing; Zhang, Anan] SouthWest Petr Univ, Sch Elect & Informat Engn, Chengdu 610500, Peoples R China.	Consensus-based distributed coordinated operation of active distribution networks with electric heating loads	<i>INTERNATIONAL JOURNAL OF ELECTRICAL POWER & ENERGY SYSTEMS</i> 2023, 153: 109393.	J Article	WOS:0010-554003000-01
3	LI, SD; Bao, GQ; Hu, YW	[Li, Shoudong] Lanzhou Univ Technol, Sch Elect & Informat Engn, Lanzhou 730050, Peoples R China.; [Li, Shoudong; Hu, Yanwen] Lanzhou Jiaotong Univ, Sch Automat & Elect Engn, Lanzhou 730070, Peoples R China.; [Bao, Guangqing] Southwest Petr Univ, Sch Elect & Informat Engn, Chengdu 610500, Peoples R China.	Distributed Coordinated Operation of Active Distribution Networks with Electric Heating Loads Based on Dynamic Step Correction ADMM	<i>ENERGIES</i> 2024, 17 (2): 533.	J Article	WOS:0011-491906000-01
合计						3



Distributed response strategy of electric heating loads based on temperature queue sorting

Shoudong Li^{a,b}, Guangqing Bao^{a,*}, Xiaoying Zhang^a, Guodong Wu^{a,c}, Bing Ren^{a,b}

^a School of Electrical and Information Engineering, Lanzhou University of Technology, Lanzhou, 730050, China

^b School of Automation and Electrical Engineering, Lanzhou Jiaotong University, Lanzhou, 730070, China

^c State Grid Gansu Electric Power Company, Lanzhou, 730050, China

ARTICLE INFO

Keywords:

Electric heating loads
Demand response
Temperature queue sorting
Centralized
Distributed

ABSTRACT

In order to eliminate the adverse impact of the rapid growth of electric heating loads (EHLs) on the safe and stable operation of the power grid under the background of the development of clean heating, a distributed response strategy based on demand response technology is proposed. Based on the thermodynamic dynamic model of EHLs, its demand response capability is analyzed, and then the processes of EHLs centralized response strategy and temperature queue sorting distributed response strategy are compared. The core advantage of the distributed response strategy of temperature queue sorting is that the distributed control of EHLs is realized by setting the response threshold and recovery threshold for the two indicators of frequency and temperature, which not only takes into account the user's comfort, but also ensures the significant improvement of frequency drop under fault. A two zone test system is established, and the simulation verifies the effectiveness of the proposed response strategy. The results show that the EHLs temperature queue sorting distributed demand response strategy can effectively suppress the sharp decline of frequency in case of system failure, and avoid the impact of a large number of EHLs responses on the power grid, which plays a positive role in the safe and stable operation of the power grid.

1. Introduction

For a long time, low-frequency load shedding technology has played a vital role in ensuring the safe and stable operation of the power grid. However, with the continuous improvement of the penetration rate of new energy power and the access of diversified loads, the security and stability of the power grid has been severely challenged [1–5]. The main reason is the limited regulation capacity of the system. The demand response technology in smart grid can make use of the load response capability of the user side to improve the flexibility of the system and realize the balance between supply and demand of the system in case of system failure or disturbance [6–10].

EHLs, as a new type of flexible and adjustable load generated under the development trend of clean heating, has grown rapidly in recent years and become an important load resource on the demand side. It has considerable adjustment capacity on the premise of meeting the comfort of end users [11]. According to the statistics of Beijing electric power company, the load proportion of EHLs in Beijing's winter heating period in 2020 is up to 48.2%. Its huge regulation potential is bound to have a

far reaching impact on the dispatching operation and demand response of power grid.

In recent years, researchers have done a lot of work in temperature control load modeling and demand response control. Based on the modeling of electric water heater, reference [12] analyzed the factors affecting the response ability of electric water heater and evaluates its response ability. In terms of EHLs heating, its main load forms are electric heat storage boiler, heat pump, air conditioning, etc. As a clean heating technology under the substitution of electric energy, clean heating is realized by using electric energy through electrothermal conversion of electric heating equipment in the period of low electricity price [13]. Compared with traditional coal-fired boilers, this heating method shows obvious advantages, which can not only ensure the continuity of heating, but also reduce the power consumption cost under the guidance of peak and valley electricity price, so as to realize the peak cutting and valley filling of power grid. Reference [14] studied the optimization mode of EHLs, puts forward three optimization modes according to the difference of start and stop time, and analyzes the advantages and disadvantages of these three modes. Reference [15]

* Corresponding author.

E-mail address: 2071763385@qq.com (G. Bao).

proposed two control methods of EHLs, namely forced control and flexible control, and explained the steps of the two control methods. Reference [16] studied the impact of regenerative EHLs on the power system. When a large number of EHLs operate synchronously, it will have a serious impact on the power grid. Based on this, the operation strategy of EHLs time-sharing access system is proposed to reduce the impact of sudden load increase on the system.

EHLs belongs to time flexible load and can participate in the system frequency response in many ways. The current research mainly puts forward two control modes of EHLs frequency response: centralized and localised control. Reference [17–19] proposed a centralized control algorithm to adjust the system frequency by aggregating the loads such as electric water heaters with small power. The staff operates the central controller, which can monitor the status of all loads and input or exit loads according to external signals. Reference [20] studies the centralized constant temperature control algorithm of HVAC and electric water heater. The central controller is equipped with a temperature predictor to estimate the building temperature and switch the load operation state according to the external signal at a specific temperature level. However, the centralized control method requires complex and expensive two-way communication between the load and the upper aggregator or operator. Localized load control can realize local frequency control and avoid the complexity and delay caused by two-way communication between network operators. The basic operation of local load control is to input or exit the load when the frequency is higher or lower than the set threshold [21,22].

Some studies have also discussed the dynamic frequency control of EHLs, such as industrial asphalt tank in reference [23], household refrigerator in reference [22] and [24]. Reference [25] introduces the potential of different types of domestic loads to provide dynamic frequency response. In the above literatures, the temperature setting value of EHLs will change dynamically with the change of power grid frequency, and in the process of dynamic change, too high or too low temperature setting value will affect the user's comfort experience.

To sum up, the current research on EHLs participating in the interactive response of power grid is difficult to take into account the frequency response effect and user comfort experience. At the same time, in order to avoid the impact of a large number of EHLs accessing or exiting at the same time on the power grid frequency, based on the analysis of the demand response ability of EHLs, this paper proposes a distributed response strategy of EHLs based on temperature queue ranking. The response threshold and recovery threshold are set for the two indexes of frequency and temperature respectively, and the temperature dead zone is set at the same time. The temperature queue sorting method is used to realize the distributed control of EHLs to avoid the extreme situation of too high or too low temperature. Combined with an example, the proposed distributed response strategy is compared with EHLs non response and centralized response strategy. It shows that the distributed response strategy based on temperature queue sequencing can effectively suppress the impact of simultaneous access or exit of a large number of EHLs on power grid frequency on the premise of ensuring user comfort.

2. EHLs demand response capability analysis

2.1. EHLs model

In order to analyze the regulatory potential of EHLs, EHLs need to be modeled, and its first-order thermodynamic dynamic model [20] is

When EHLs is operating ($s^k = 1$):

$$T_{in}^{k+1} = T_{out}^{k+1} + QR - (T_{out}^{k+1} + QR - T_{in}^k)\tau \quad (1)$$

$$\tau = e^{-\Delta k/RC} \quad (2)$$

When EHLs is exiting ($s^k = 0$):

$$T_{in}^{k+1} = T_{out}^{k+1} - (T_{out}^{k+1} - T_{in}^k)\tau \quad (3)$$

Where, S^k is the EHLs switch state, 1 indicates on and 0 indicates off, T_{in} is the indoor temperature regulated by EHLs, °C, T_{out} is the outdoor temperature, °C [26], Q is the equivalent heat ratio, kW, R is the equivalent thermal resistance, °C/kW, C is the equivalent heat capacity, kJ/°C, τ is the heat dissipation coefficient, k is the control time, Δk is the control step size.

At each control time, EHLs are divided into operation and exit groups according to the operation status, which are specifically represented by the following two sets:

$$A^k = (A_1^k, A_2^k, A_3^k, \dots, A_{n_1}^k) \quad (4)$$

$$B^k = (B_1^k, B_2^k, B_3^k, \dots, B_{n_2}^k) \quad (5)$$

Where, A^k and B^k respectively represent the equipment groups running and exiting at k time. The number of EHLs in the two equipment groups is n_1 and n_2 respectively, and the total number is $n = n_1 + n_2$. When the time k changes, the number and operation status of EHLs in the A^k and B^k two equipment groups will also change.

The set temperature, upper and lower temperature limits of EHLs at time k are respectively defined as

$$T_{set}^k = (T_{set}^{1,k}, T_{set}^{2,k}, \dots, T_{set}^{i,k}, \dots, T_{set}^{n,k}) \quad (6)$$

$$T_{low}^k = (T_{low}^{1,k}, T_{low}^{2,k}, \dots, T_{low}^{i,k}, \dots, T_{low}^{n,k}) \quad (7)$$

$$T_{high}^k = (T_{high}^{1,k}, T_{high}^{2,k}, \dots, T_{high}^{i,k}, \dots, T_{high}^{n,k}) \quad (8)$$

Where, $T_{set}^{i,k}$, $T_{low}^{i,k}$ and $T_{high}^{i,k}$ are the set temperature, upper and lower temperature limits of equipment i at time k , respectively.

2.2. EHLs demand response capability

According to the EHLs model, the demand response capability of cluster load is analyzed. The power boundary of cluster load up and down regulation at $k + 1$ is

$$\begin{cases} P_{max}^{k+1} = P_{CL}^k + \sum_{T^{i,k+1} \in (T_{low}^{i,k+1}, T_{high}^{i,k+1}), S^{i,k}=0} P_{eh,i} \\ P_{min}^{k+1} = P_{CL}^k - \sum_{T^{i,k+1} \in (T_{low}^{i,k+1}, T_{high}^{i,k+1}), S^{i,k}=1} P_{ch,i} \\ P_{min}^{k+1} \leq P_{CL}^{k+1} \leq P_{max}^{k+1} \end{cases} \quad (9)$$

In Fig. 1, the red dots are the power points existing during the operation of cluster EHLs, the blue dotted line is the power boundary of cluster EHLs, and the orange shaded area indicates the reduced power consumption of cluster EHLs under the demand response strategy after the duration Δk .

As can be seen from Fig. 1, the four parameters of cluster EHLs are: P_{min}^{k+1} and P_{max}^{k+1} associated with comfort, the power P_{CL-u}^{k+1} consumed by cluster EHLs in case of no response, and the power P_{CL}^{k+1} consumed by cluster EHLs in case of response. At the same time, it can be seen that when the operating power is close to the upper boundary, the down regulation capacity of cluster EHLs is large, when the operating power is far from the upper boundary, the up regulation capacity of cluster EHLs is large.

The response reduction capacity, up and down regulation capacity of cluster EHLs are expressed as Eqs. (10)-(12) respectively.

$$\Delta P_{CL}^{k+1} = P_{CL-u}^{k+1} - P_{CL}^{k+1} \quad (10)$$

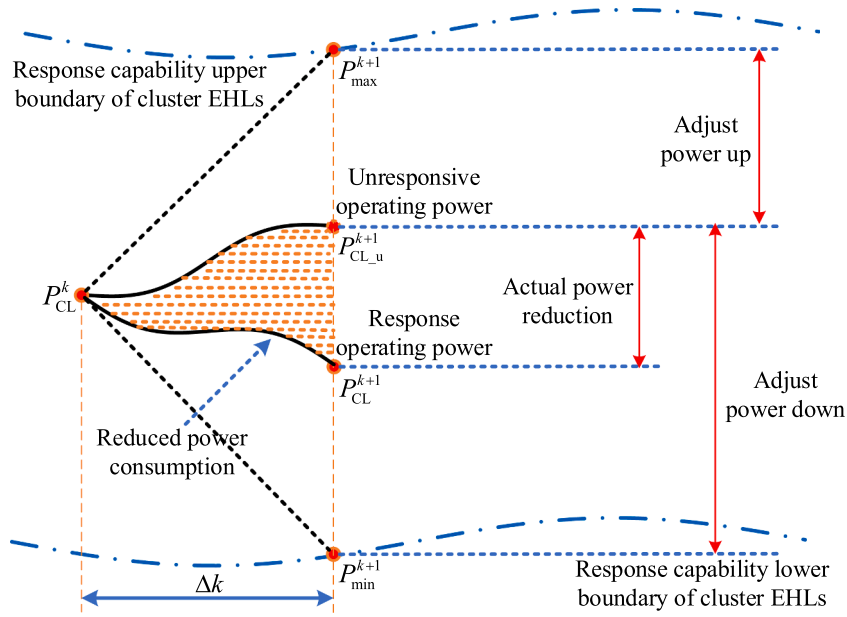


Fig 1. Demand response capability boundary of EHLs.

$$\Delta P_{up}^{k+1} = P_{max}^{k+1} - P_{CL_u}^{k+1} \quad (11)$$

$$\Delta P_{down}^{k+1} = P_{CL_u}^{k+1} - P_{min}^{k+1} \quad (12)$$

The response reduction capacity ΔP_{CL}^{k+1} represents the reduced power consumption of cluster EHLs under controlled conditions at time $k + 1$, ΔP_{up}^{k+1} and ΔP_{down}^{k+1} respectively represent the power consumption that can be increased when the cluster EHLs is up regulated and the power consumption that can be reduced when the cluster EHLs is down regulated.

3. EHLs demand response strategy

The principle of EHLs demand response strategy is to timely adjust the operation state of EHLs according to the real-time measured system frequency value and frequency change, so as to reduce the adverse factors of power grid frequency change on system safety and stability. Fig. 2 shows the basic process of EHLs demand response strategy.

As shown in Fig. 3, when the power grid frequency is lower than the response threshold f_{off} set by EHLs, the EHLs currently in operation will exit operation to reduce the power load, so that the power grid frequency can be restored immediately. When the grid frequency gradually rises to the recovery threshold f_{on} with the exit of EHLs, EHLs will be put into operation again. When the grid frequency is between f_{on} and f_{off} , EHLs will maintain the original operation state. Where the frequency response threshold f_{off} is that when the system frequency drops to the critical value f_{off} , EHLs needs to exit operation to improve the system frequency. This critical value f_{off} of frequency is called the frequency response threshold. Where the frequency recovery threshold f_{on} is that when the system frequency recovers to the critical value f_{on} , EHLs needs to be put into operation again to ensure the user's heating temperature. This critical value f_{on} of frequency is called the frequency recovery threshold.

3.1. Centralized frequency demand response strategy

In the centralized frequency demand response strategy, it is not necessary to consider the energy supply temperature of the end user, but only to detect whether the system frequency value is lower than the response threshold or higher than the recovery threshold. On this basis, it is necessary to realize real-time communication between EHLs and the

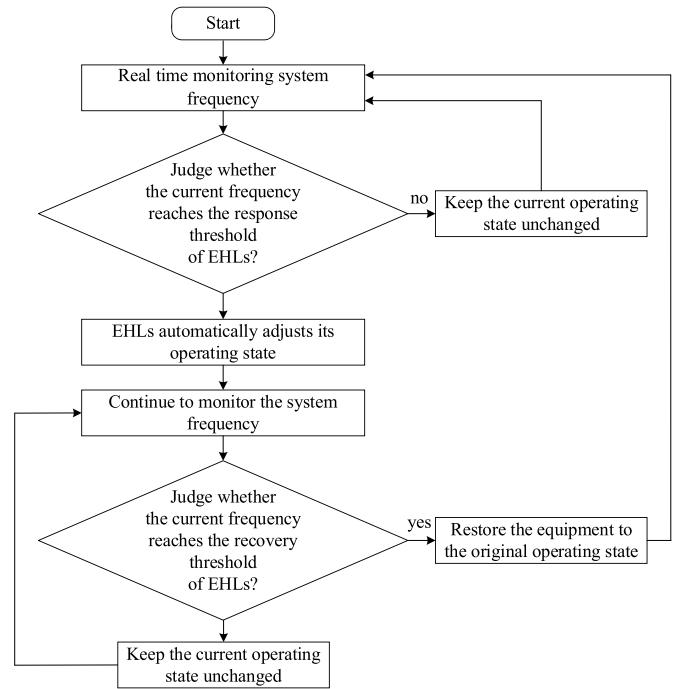


Fig 2. Demand response strategy process of EHLs.

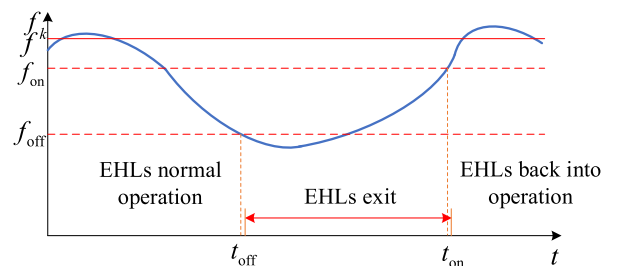


Fig 3. Schematic diagram of EHLs demand response strategy.

dispatching center. The emergence of intelligent control terminal and grid friendly control equipment provides technical possibility for it to respond to the communication requirements of control [27], as shown in Fig. 4. The dispatching center detects the system operating frequency in real time (generally within the range of plus or minus 0.2 Hz of the rated frequency), and sends control commands to the EHLs intelligent control terminal according to the frequency detection results. If the system frequency drops to the EHLs response threshold, EHLs will receive the control command to start responding.

If the frequency of the system at time k is f^k , the frequency response threshold of EHLs is f_{off} and the frequency recovery threshold is f_{on} . If the system frequency $f^k \leq f_{off}$ is detected, the dispatching control center will send the control command to the EHLs, and the EHLs running in the system will exit the operation after receiving the response command. If the system frequency $f^k \geq f_{on}$ is detected, the dispatching control center will send the input command to the EHLs, and all exited EHLs in the system will return to the previous input state after receiving the control command.

Fig. 5 shows the response of 10 EHLs equipment when the system operation frequency decreases.

It can be seen from Fig. 5 that under the centralized frequency response strategy, the response of EHLs has nothing to do with the terminal energy supply temperature, but only depends on the operating frequency of the system. If the system operation frequency is lower than the set frequency response threshold, all EHLs in operation will exit operation. The specific performance is as follows: 10 EHLs equipment have experienced four operating states ($k, k + 1, k + 2$ and $k + 3$). At time k , the system operating frequency is higher than the response threshold f_{off} , so 10 EHLs equipment still maintain the operating state without meeting the frequency response conditions. However, at time $k + 1, k + 2$ and $k + 3$, the system operation frequency is lower than the response threshold f_{off} . At this time, 10 EHLs equipment meet the frequency response conditions and exit the operation.

3.2. Temperature queue sorting distributed demand response strategy

The distributed demand response strategy of temperature queue sorting is based on the centralized frequency demand response strategy and considering the user's comfort, the queue sorting method based on temperature index is added to realize the distributed response of EHLs. Therefore, compared with the centralized frequency demand response

strategy, under the temperature queue sorting distributed demand response strategy, the operation state of EHLs depends not only on the system frequency, but also on the heating temperature of terminal EHLs. At this time, the intelligent control terminal shall not only receive the system frequency value transmitted from the dispatching center, but also receive the detected energy supply temperature of EHLs end users. At the same time, the intelligent control terminal shall send a response command to EHLs according to the transmitted real-time system frequency and user temperature. The specific implementation process is shown in Fig. 6.

EHLs are widely distributed, coupled with differences in geographical environment and heating, and the terminal heating load at different nodes at the same time is inconsistent. Under the distributed demand response strategy of temperature queue sorting, EHLs respond according to the temperature of each end user, which can avoid the impact of a large number of EHLs on the power grid and improve user comfort.

It is assumed that the minimum heating temperature and the maximum heating temperature meeting the basic comfort of end users are T_{set}^{low} and T_{set}^{high} respectively, and this temperature value is used as the temperature response threshold and recovery threshold of EHLs. There are n EHLs equipment in the system. If the system frequency $f^k \leq f_{off}$ and the end user temperature of the equipment $i (i = 1, 2, \dots, n)$ in operation meet $T_i^k \geq T_{set}^{low}$, the equipment i will exit the operation according to the principle of temperature queue sorting. If the system frequency $f^k \geq f_{on}$ and the end user temperature meet $T_i^k \leq T_{set}^{high}$, the equipment i will be put into operation again according to the principle of temperature queue sorting. The specific implementation process of temperature queue sorting is as follows:

- 1) Load Reduction Calculation. In case of disturbance or fault in multi machine power system, the measuring device can quickly detect the change of synchronous motor speed. When the frequency changes dynamically, the influence of each generator set on the power grid frequency is also different, so the term of inertia center frequency appears. In this paper, the change of inertia center frequency is regarded as the change of power grid frequency. Therefore, there are inertia frequency variation and inertia center motion equations:

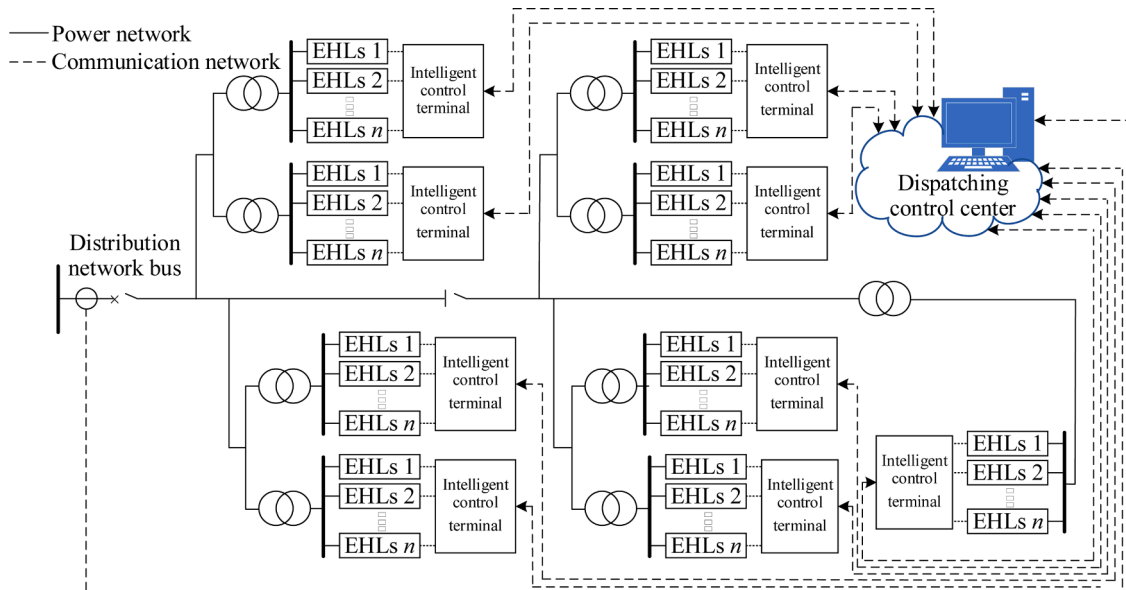


Fig. 4. Centralized frequency demand response technology of EHLs.

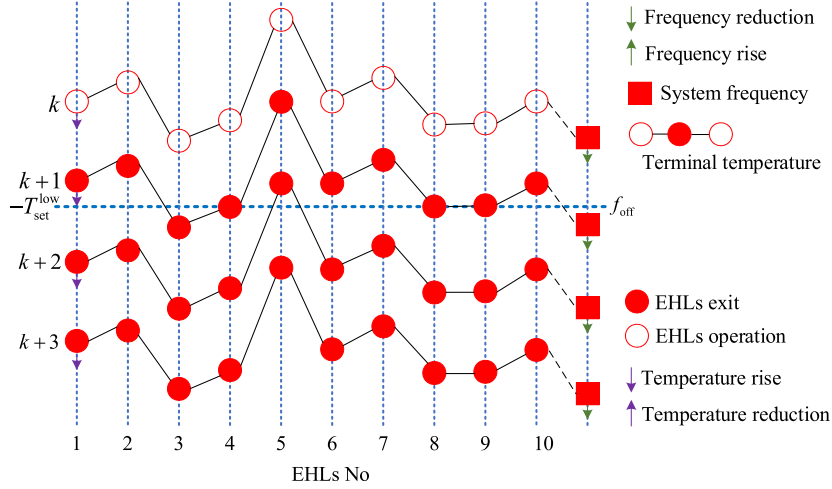


Fig 5. Illustration of centralized frequency demand response strategy of EHLs.

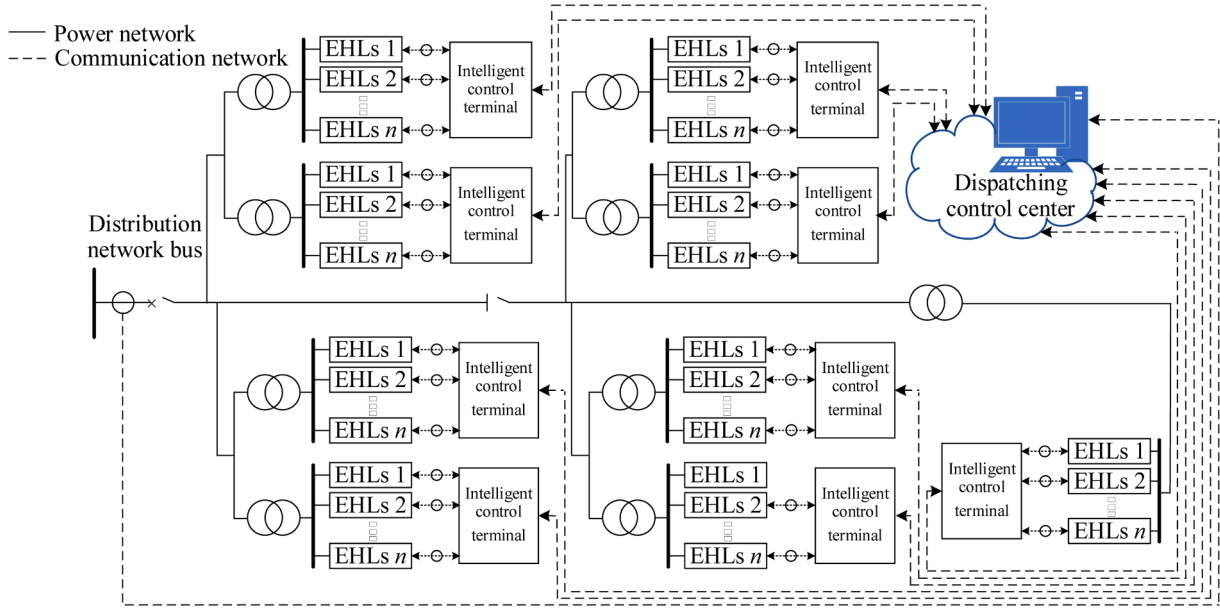


Fig 6. Distributed demand response technology based on temperature queue sorting of EHLs.

$$\begin{cases} \omega_{COI} = \frac{1}{T_J} \sum_{i=1}^I T_{Ji} \omega_i \\ T_J \frac{d\omega_{COI}}{dt} = \Delta P \end{cases} \quad (13)$$

$$f_{off} = f_{on} - \gamma f_p \quad (15)$$

$$\gamma = \sum_{i=1}^I \gamma_i \cdot \frac{P_i}{P_{off}} \quad (16)$$

Where $T_J = \sum_{i=1}^I T_{Ji}$ and $\omega_{COI} = 2\pi f_{COI}$, $\omega_{COI} = f_{COI}$ when it is expressed as per unit value, so Eq. (13) can be expressed as:

$$\begin{cases} f_{COI} = \frac{1}{T_J} \sum_{i=1}^I T_{Ji} f_i \\ T_J \frac{df_{COI}}{dt} = \Delta P \end{cases} \quad (14)$$

The load variation ΔP can be obtained according to Eq. (13), i.e. P_{target}^k . Considering the response intention and operation status of EHLs, f_{off} is expressed as:

Where γ_i represents the response intention of equipment i , with a value of 0 ~ 1, which can be obtained by evaluating the actual power consumption of the equipment. γ is the response intention of the equipment group, which can be obtained by weighting the energy consumption of each equipment. f_p represents the maximum frequency acceptable to the virtual motor, which can be obtained according to Eq. (14).

- 1) In Order of Priority. The EHLs equipment is divided into 2^n response priority levels according to the principle of binary complement. In order to avoid frequent opening (exit) of EHLs, set the temperature dead zone θ , as shown in Fig. 7. When $T_i^k \geq T_{set}^{high} - \theta$ or $T_i^k \leq T_{set}^{low} + \theta$, the response priority of device i is 0, that is, it does not participate in the response, while the EHLs between $T_{set}^{high} - \theta$ and $T_{set}^{low} + \theta$ in Fig. 7

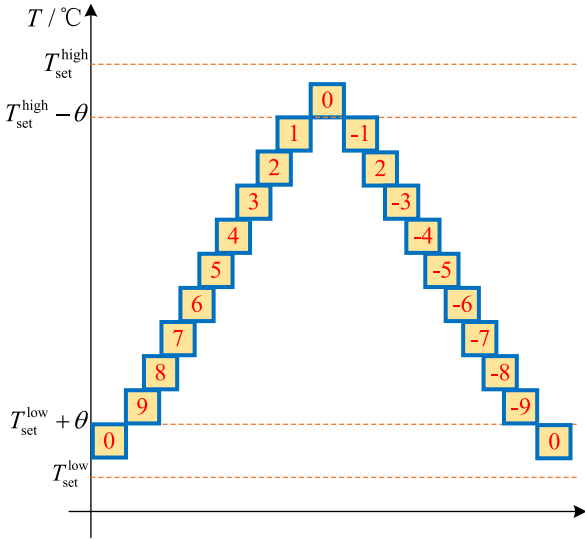


Fig 7. Temperature queue sorting method of EHLs.

are controllable and respond according to the temperature priority. If $T_i^{k+1} - T_i^k \leq 0$, the priority is positive. Conversely, if $T_i^{k+1} - T_i^k > 0$, the priority is negative. Divide the temperature areas that can be controlled into 2^{n-1} parts. The higher the end user's temperature is, the smaller the absolute value of EHLs priority is.

- 2) Response control. Temperature queue sorting is a control method to modify the original switching function of EHLs. In the uncontrollable range, the switching function of device i at time k can be expressed as

$$s_i^k = \begin{cases} 0, & T^k > T_{set}^{high} \\ 1, & T^k < T_{set}^{low} \\ s_i^{k-1}, & \text{otherwise} \end{cases} \quad (17)$$

- 3) If the system frequency is low and EHLs need to be reduced, consider exiting EHLs with positive priority and exiting EHLs with higher priority first. If the system frequency is too high and EHLs need to be added, consider putting EHLs with negative priority into operation, and put EHLs with higher priority into operation first.
- 4) The number of response devices is determined. When the switching state of device i changes from on to off at time k , the number of devices in the open device group A^k decreases by 1, while the number of devices in the closed device group B^k increases by 1, and the power P_i^k in group A^k is reduced, while the power P_i^k in group B^k is increased. The change process of equipment from off to on is opposite to that of equipment from on to off. Therefore, some EHLs are turned on or off according to the control target, which will increase or reduce their power consumption. When EHLs need to reduce power consumption, the number of EHLs to be closed is determined by Eq. (18):

$$\begin{cases} \sum_{i=1}^{N_A+1} P_{ch,i} \geq P_{target}^k \\ \sum_{i=1}^{N_A} P_{ch,i} < P_{target}^k \end{cases} \quad (18)$$

The first N_A EHLs devices of device group N_A are closed, and the power consumption P_{target}^k of EHLs is reduced. If the system needs to increase the power consumption of EHLs, the number of EHLs devices to be opened can be calculated by Eq. (19):

$$\begin{cases} \sum_{i=1}^{N_B+1} P_{ch,i} \geq P_{target}^k \\ \sum_{i=1}^{N_B} P_{ch,i} < P_{target}^k \end{cases} \quad (19)$$

The first N_B EHLs devices of device group B_k are opened, and the power consumption P_{target}^k of EHLs is increased.

Fig. 8 shows the demand response capability boundary of cluster EHLs after setting the temperature dead zone.

Because EHLs in the temperature dead zone do not participate in the response, the upper and lower power boundaries of cluster EHLs shrink to a certain extent. The orange dot indicates the power point when the temperature dead zone is not considered. Compared with the power P_{CL-u}^{k+1} when it does not participate in the response, the reduction capacity of total power consumption is expressed as shaded area I and II. After considering the temperature dead zone, some EHLs can not be regulated even if they meet the response conditions, so that the response load of cluster EHLs is "conservative", resulting in a relatively high power P_{CL-u}^{k+1} . At the same time, there is only an area I left for the reduction capacity of total electric energy consumption. In addition, the up regulation power and down regulation power of cluster EHLs are also reduced. However, the introduction of temperature dead zone avoids frequent opening (exit) of EHLs and improves user comfort to a certain extent.

Fig. 9 shows the response of 10 EHLs equipment when the system operation frequency decreases under the temperature queue sorting distributed demand response strategy.

Because the change trend of temperature index and frequency is opposite during response, in order to facilitate analysis and keep the change trend of temperature and frequency consistent, the temperature index takes the opposite number as its ordinate. It can be found that under the determined temperature response threshold, all EHLs meeting the frequency response conditions do not exit at the same time, but perform the stop action at $k+1$, $k+2$ and $k+3$ respectively, and a certain number of EHLs respond at each time.

4. Simulation and analysis

In order to verify the effectiveness of the proposed temperature queue distributed demand response strategy, a two zone test system as shown in Fig. 10 is used for simulation verification. The test system consists of 4 generator nodes, 6 load lines and 12 buses, in which the red triangle represents the EHLs carried by the load line. The total system load is 1000 MW, and the average power of EHLs is 80 kW. The minimum heating temperature to meet the basic comfort of users is 23 °C, and the maximum heating temperature is 27 °C. The temperature dead zone is 0.5 °C. Tables 1–3 show the load distribution of each node when the load proportion of EHLs is 10%, 20% and 30%. When a fault occurs and the tie line is disconnected, two isolated networks of zone 1 and 2 are generated.

4.1. Response strategy analysis under fault 1

Fault 1: When a three-phase short circuit fault occurs in the tie line between bus9 and bus10, the protection device malfunctions, and bus9-bus10 and bus6-bus8 are disconnected at the same time, resulting in two isolated networks. At this time, the power shortage of isolated networks in the area (receiving end) is small.

Fig. 11 shows the frequency response of different control strategies when the load proportion of EHLs in the system under fault 1 is 10%. Compared with the traditional low-frequency load shedding control strategy, the centralized response strategy and the temperature queue sorting distributed demand response strategy have some improvement on the frequency sag caused by fault 1.

The centralized response strategy controls the EHLs based on the

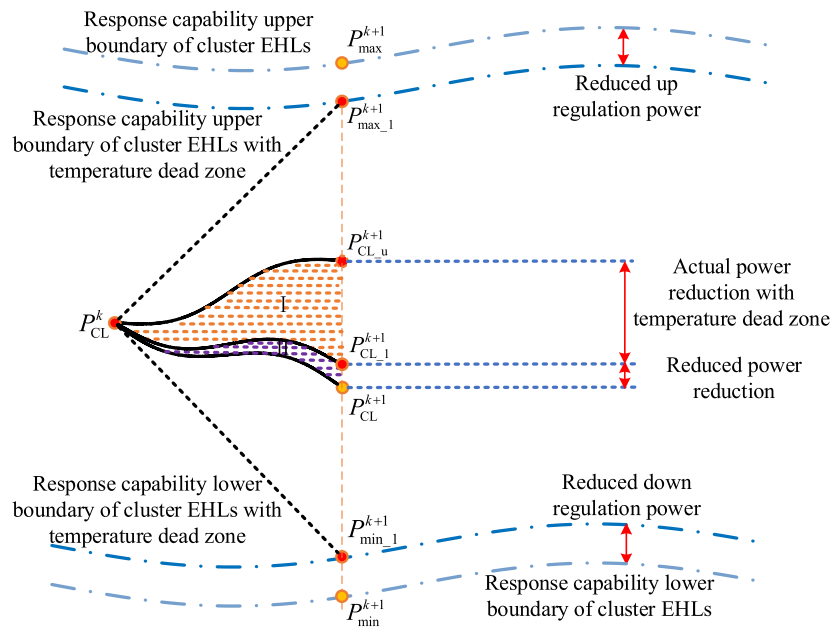


Fig 8. Demand response capability boundary considering temperature dead zone of EHLs.

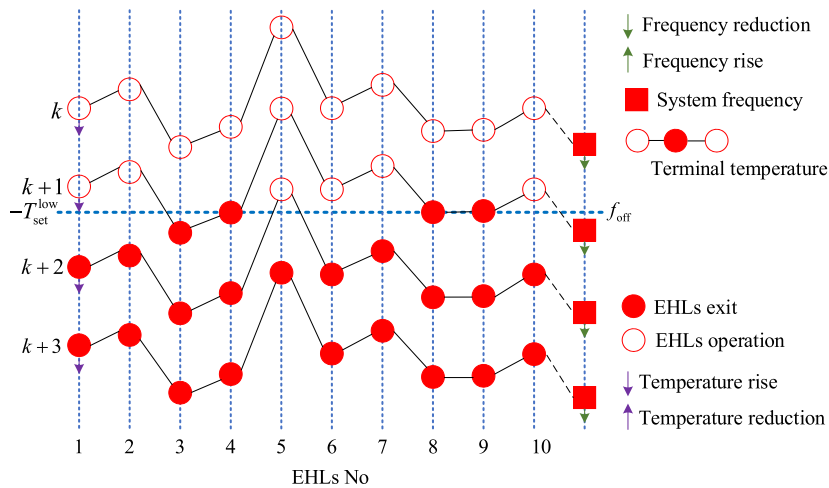


Fig 9. Illustration of EHLs temperature queue sorting distributed demand response strategy.

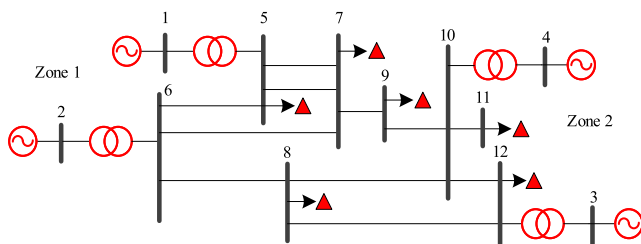


Fig 10. Test system.

Table 1

Load distribution of each node at 10% EHLs.

Node No number	Node Power/MW /MW	EHLs Number	EHLs Power/MW
5	150	183	15
7	150	185	15
8	150	190	15
9	150	187	15
11	200	250	20
12	200	255	20

reduction of system frequency. It can be found from Table 4 that the EHLs of all nodes respond and exit from operation at 1.6273 s, which effectively improves the system frequency. However, the synchronous input of EHLs at 8.2402s has a certain impact on the system, reducing the system frequency to the level when there is no response. Under the distributed response strategy of temperature queue sorting, the response time of EHLs of each node is basically the same, and the improvement of

system frequency is obvious, but the return operation time of EHLs of each node is different, which are 8.1512 s, 14.8817 s and 14.7645 s respectively. It can be seen from Fig. 11 that the asynchronous response of EHLs under the temperature queue sorting distributed response strategy effectively suppresses the impact on the system frequency and keeps the system frequency above 49.4 Hz.

When the load proportion of EHLs in the system rises to 20%, the frequency response under different control strategies is shown in Fig. 12.

Table 2
Load distribution of each node at 20% EHLs.

Node No number	Node Power/MW /MW	EHLs Number目	EHLs Power/MW
5	150	366	30
7	150	370	30
8	150	380	30
9	150	374	30
11	200	500	40
12	200	510	40

Table 3
Load distribution of each node at 30% EHLs.

Node No number	Node Power/MW /MW	EHLs Number目	EHLs Power/MW
5	150	549	45
7	150	555	45
8	150	570	45
9	150	561	45
11	200	750	60
12	200	765	60

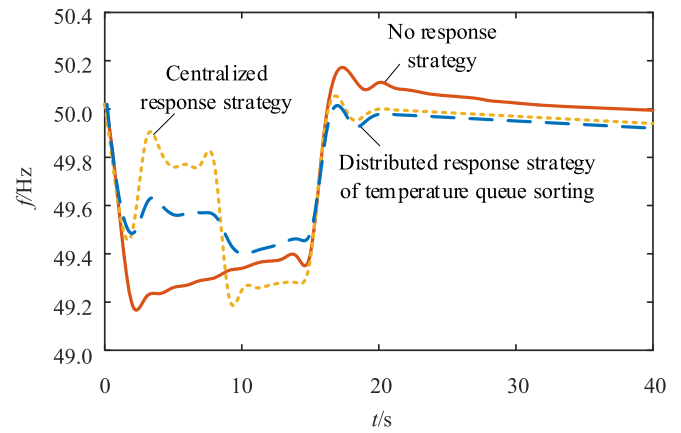


Fig 12. Frequency response curves of different control strategies when 20% EHLs participate in response under fault 1.

Table 5
Response time of each node at 20% EHLs under fault 1.

Strategy	Node No	Response Start Time /s	Response End Time /s
Centralized	8	1.6186	8.1543
	11	1.6186	8.1543
	12	1.6186	8.1543
Distributed	8	1.6175	8.1274
	11	1.7251	14.8651
	12	8.0418	14.6526

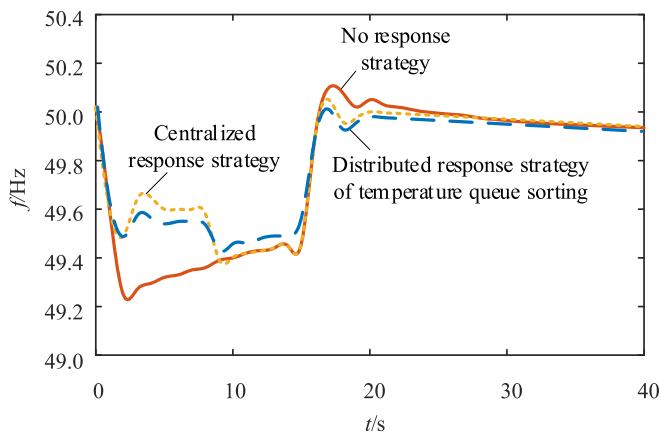


Fig 11. Frequency response curves of different control strategies when 10% EHLs participate in response under fault 1.

Table 4
Response time of each node at 10% EHLs under fault 1.

Strategy	Node No	Response Start Time /s	Response End Time /s
Centralized	8	1.6273	8.2402
	11	1.6273	8.2402
	12	1.6273	8.2402
Distributed	8	1.6224	8.1512
	11	1.6218	14.8817
	12	1.7621	14.7645

As can be seen from Fig. 12, when the load proportion of EHLs rises to 20%, the centralized response strategy and temperature queue sorting distributed response strategy can greatly improve the frequency drop caused by fault 1. It can be seen from Table 5 that the centralized response strategy controls all EHLs to exit operation at 1.6186 s at the initial time of frequency drop, so as to increase the frequency to near the rated value of stable operation. Compared with the temperature queue sorting distributed response strategy, the centralized response strategy has more obvious improvement on the frequency. However, after about 6.5 s, under the control of the centralized response strategy, the return operation of a large number of EHLs has a great impact on the system frequency, making the system frequency even lower than when EHLs do not participate in the response. Under the temperature queue sorting

distributed response strategy, the response time of EHLs at different nodes is different. Although it also has a certain impact on the system frequency, it still has a significant effect on improving the frequency compared with the case of no response, so that the frequency is always maintained above 49.4 Hz.

When the load proportion of EHLs in the system increases to 30%, the frequency response under different control strategies is shown in Fig. 13.

It can be seen from Fig. 13 that when the load proportion of EHLs rises to 30%, a large number of EHLs synchronous exit and synchronous back into operation under the control of centralized response strategy have a great impact on the system, making the frequency peak exceed 50.2 Hz and the valley lower than 49.0 Hz, indicating that EHLs is in the state of excessive response at this time. The asynchronous response under the temperature queue sorting distributed response strategy has a good effect on improving the system frequency. It can be seen from Table 6 that the asynchronous input of EHLs when resuming operation avoids a great impact on the system and keeps the frequency above 49.4

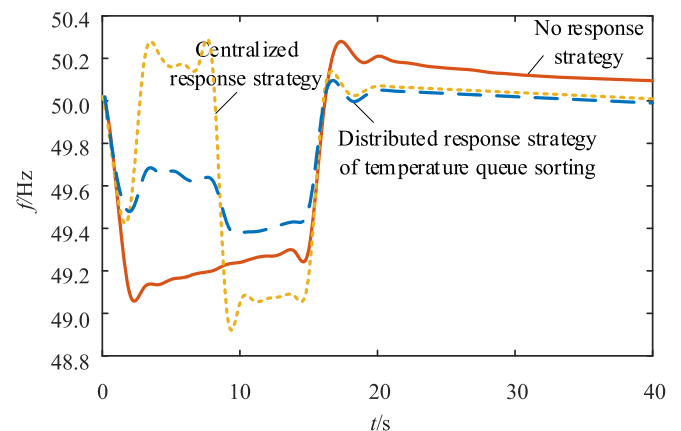


Fig 13. Frequency response curves of different control strategies when 30% EHLs participate in response under fault 1.

Table 6
Response time of each node at 30% EHLs under fault 1.

Strategy	Node No	Response Start Time /s	Response End Time /s
Centralized	8	1.6081	8.0626
	11	1.6081	8.0626
	12	1.6081	8.0626
Distributed	8	1.6254	8.2354
	11	1.7019	14.5125
	12	8.0587	14.7348

Hz.

4.2. Response strategy analysis under fault 2

Fault 2: When a three-phase short circuit fault occurs in the tie line between bus7 and bus9, the protection device misoperates, and bus7-bus9 and bus6-bus8 are disconnected at the same time, resulting in two isolated networks. At this time, the power shortage of isolated networks in the area (receiving end) is large.

Fig. 14 shows the frequency response of different control strategies when the load proportion of EHLs in the system under fault 2 is 10%. Compared with the traditional low-frequency load shedding control strategy, the centralized response strategy and temperature queue sorting distributed demand response strategy have some improvements on the frequency sag caused by fault 2.

It can be seen from Table 7 that under fault 2, EHLs of four nodes participated in the response, and EHLs of four nodes began to respond and quit operation in 1.8435 s under the centralized response strategy, which effectively improved the system frequency. However, the return operation of a large number of EHLs in 7.2374s had a certain impact on the system, making the system frequency close to the level when there was no response. Under the distributed response strategy of temperature queue sorting, the response time of EHLs of each node is basically the same, but the return operation time of EHLs of each node is different, which are 7.1602s, 7.3641 s, 11.5343 s and 11.8247 s respectively. It can be seen from Fig. 11 that under fault 2, due to the large power shortage of the system, the frequency drop is more serious than that under fault 1. Even with the improvement of the temperature queue sorting distributed response strategy, it is still lower than 49.2 Hz.

When the load proportion of EHLs in the system rises to 20%, the frequency response under different control strategies is shown in Fig. 15.

As can be seen from Fig. 15, when the load proportion of EHLs rises to 20%, the improvement effect of centralized response strategy and temperature queue sorting distributed response strategy on the frequency drop caused by fault 2 is basically the same as that in fault 1. It can be seen from Table 8 that under fault 2, the centralized response

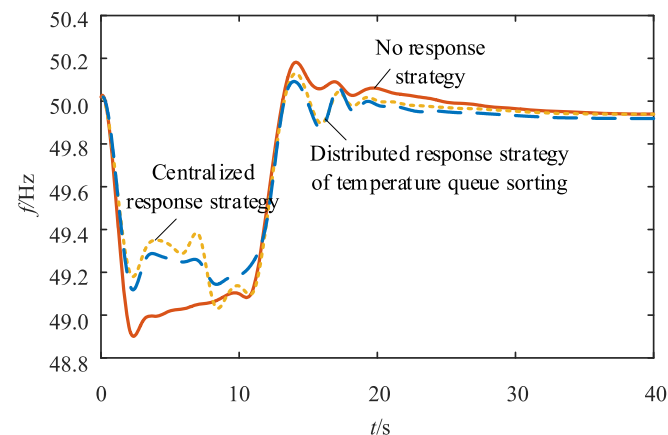


Fig 14. Frequency response curves of different control strategies when 10% EHLs participate in response under fault 2.

Table 7
Response time of each node at 10% EHLs under fault 2.

Strategy	Node No	Response Start Time /s	Response End Time /s
Centralized	8	1.8435	7.2374
	9	1.8435	7.2374
	11	1.8435	7.2374
	12	1.8435	7.2374
Distributed	8	1.7198	7.1602
	9	1.8756	7.3641
	11	1.8463	11.5343
	12	1.6526	11.8247

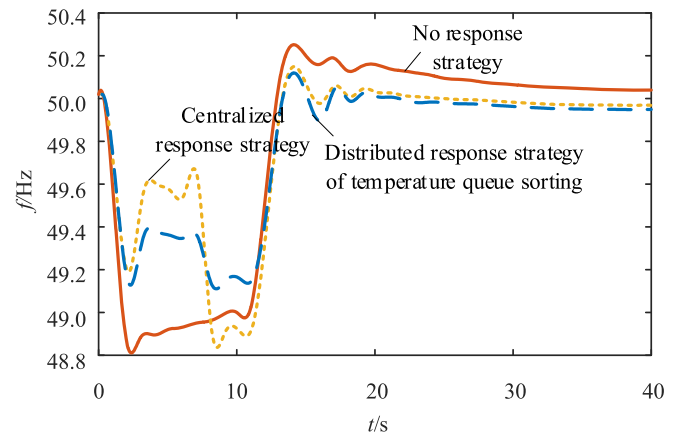


Fig 15. Frequency response curves of different control strategies when 20% EHLs participate in response under fault 2.

Table 8
Response time of each node at 20% EHLs under fault 2.

Strategy	Node No	Response Start Time /s	Response End Time /s
Centralized	8	1.8219	7.1728
	9	1.8219	7.1728
	11	1.8219	7.1728
	12	1.8219	7.1728
Distributed	8	1.8536	7.2569
	9	1.8921	7.3972
	11	7.0453	11.8343
	12	1.7695	11.7152

strategy controlled all EHLs to exit operation in 1.8219 s, so that the frequency increased to near 49.6 Hz, which was slightly lower than that of fault 1. After about 5.3 s, under the control of centralized response strategy, a large number of EHLs are put into synchronization, so that the system frequency is lower than that when EHLs do not participate in response. Under the distributed response strategy of temperature queue sorting, the asynchronous response of EHLs has less impact on the system than the centralized response strategy, keeping the frequency above 49.1 Hz, but there is a certain gap compared with the frequency value of 49.4 Hz in fault 1.

When the load proportion of EHLs in the system increases to 30%, the frequency response under different control strategies is shown in Fig. 16.

As can be seen from Fig. 16, when the load proportion of EHLs under fault 2 rises to 30%, the synchronous response of a large number of EHLs under the control of centralized response strategy has a great impact on the system as in fault 1. The synchronous exit of EHLs makes the frequency peak exceed 50.2 Hz, while the synchronous return operation of EHLs makes the valley even lower than 48.6 Hz. Compared with the valley at fault 1, the frequency drop is more serious. This is the result of large power shortage under fault 2 and excessive response of centralized response strategy. It can be seen from Table 9 that under the distributed response strategy of temperature queue sorting, although the power

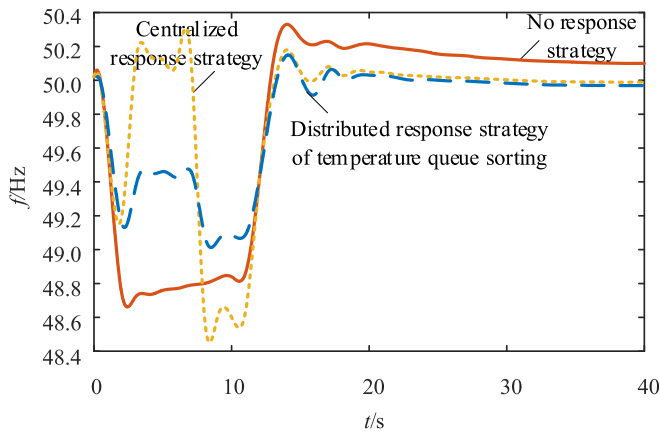


Fig. 16. Frequency response curves of different control strategies when 30% EHLs participate in response under fault 2.

Table 9

Response time of each node at 30% EHLs under fault 2.

Strategy	Node No	Response Start Time /s	Response End Time /s
Centralized	8	1.8196	7.0465
	9	1.8196	7.0465
	11	1.8196	7.0465
	12	1.8196	7.0465
Distributed	8	1.8317	7.3569
	9	1.8654	7.2468
	11	7.1928	11.6463
	12	7.0325	11.4697

shortage of fault 2 is large, the asynchronous response of EHLs has little impact on the system, so that the valley value of frequency is above 49.0 Hz.

4.3. Effect of EHLs ratio on frequency variation

Fig. 17 is the frequency variation curves when the system contains different proportions of EHLs under fault 1 and fault 2 respectively.

It can be seen from Fig. 17 that no matter whether the system has fault 1 or fault 2, the system frequency will drop sharply at the initial time of the fault, and the higher the load proportion of EHLs is in the node, the greater the frequency drop is. After the system disconnection fault, the frequency fluctuates upward in the process of recovery, and the higher the proportion of EHLs is, the more obvious the fluctuation behaves. At the same time, it can be seen that the overall response time of EHLs under fault 1 is longer, while the overall response time of EHLs under fault 2 is shorter.

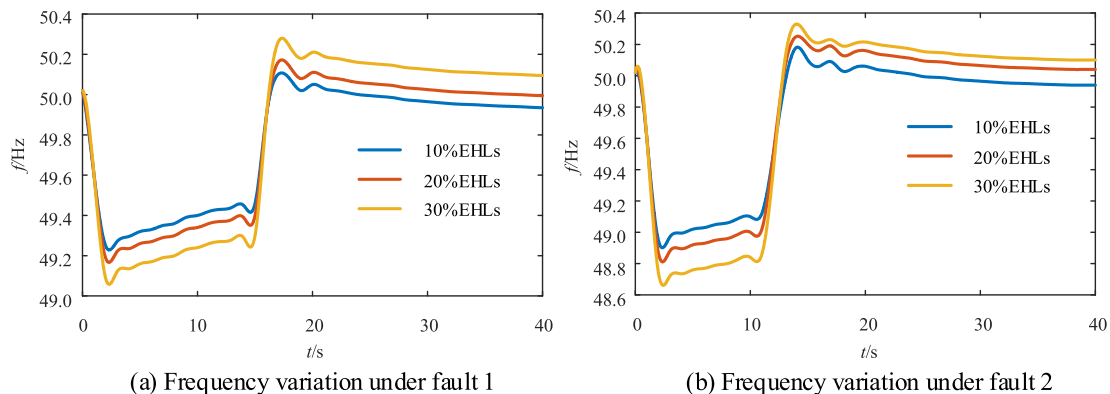


Fig. 17. Frequency variation of the system with different proportions of EHLs under fault 1 and fault 2.

4.4. EHLs power response analysis

Fig. 18 shows the power response of different proportions of EHLs under the control of temperature queue sorting distributed response strategy when system fault 1 and fault 2 occur respectively.

As can be seen from Fig. 18, in the initial stage of fault 1, due to the control of the distributed response strategy of temperature queue sorting, when the load proportion of EHLs is 10%, 20% and 30% respectively, the power of EHLs is reduced by nearly 77%, 75% and 70% respectively, indicating that the proportion of EHLs participating in the response in the total EHLs under the three proportions is 77%, 75% and 70% respectively. In the subsequent frequency recovery process, EHLs power also rebounded. Comparing power response curves under fault 1 and fault 2, it can be seen that under the control of the temperature queue sorting distributed response strategy, the power of EHLs participating in the response increases compared with that of fault 1 due to the large power shortage of the system under fault 2, and the power fluctuation is more obvious in the response process.

4.5. Room temperature regulation analysis of single EHLs

The room temperature regulation changes of single EHLs under the temperature queue sorting distributed response strategy (TQSD-RS), centralized response strategy (C-RS) and dynamic frequency response strategy (DFC-RS) are analyzed, as shown in Fig. 19.

As can be seen from Fig. 19, the initial temperature under EHLs 1 regulation is 26.1 °C, which meets the temperature requirements for the basic comfort of heating users. At this time, EHLs 1 participates in the system frequency response and exits the operation under the temperature queue sorting distributed response strategy. Under the three response strategies, the change of room temperature at each time is always consistent, showing a trend of decreasing first and then increasing. The temperature difference between other times and the initial time reaches the maximum at 30 s, at which time the user's comfort experience is the worst. Then, with the recovery of system frequency and the rise of room temperature, the comfort experience will gradually recover.

The initial temperature under EHLs 2 regulation is 22.1 °C, which does not meet the temperature requirements of basic comfort of heating users. Under the centralized response strategy, EHLs 2 needs to be out of operation, so the room temperature drop is the most serious and the comfort experience is the worst. Under the dynamic frequency response strategy, the power consumption of EHLs 2 decreases and the room temperature will decrease, but the degree of decline is smaller than that of the centralized response strategy. Therefore, the comfort experience of the dynamic frequency response strategy is better than that of the centralized response strategy. Under the temperature queue sorting distributed response strategy, EHLs 2 does not participate in the system frequency response and continues to operate. The room temperature is

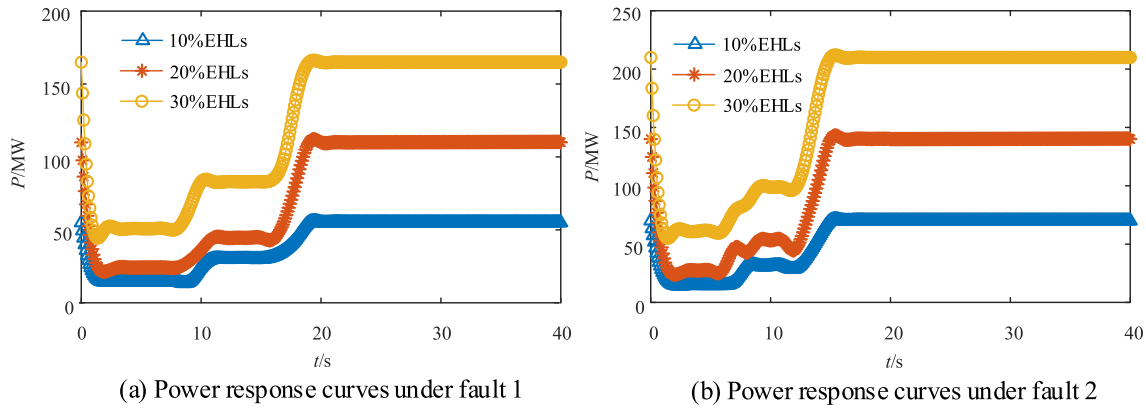


Fig 18. Power response curves of different proportions of EHLs under the control of temperature queue sorting distributed response strategy under fault 1 and fault 2.

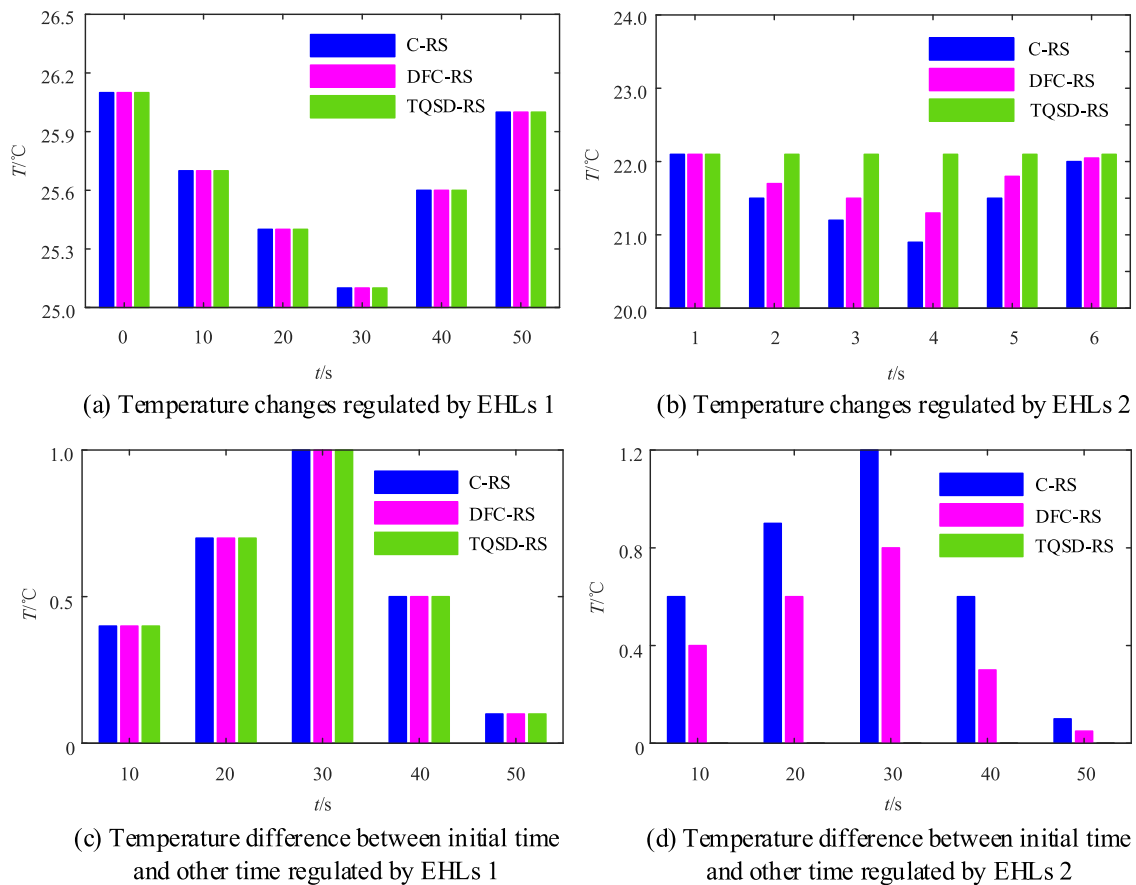


Fig 19. Room temperature changes of single EHLs regulated by three response strategies.

always kept at 22.1 °C, and the temperature difference between other times and the initial time is always 0 °C. Among the three response strategies, the comfort experience is the best.

5. Conclusion

In view of the adverse impact of the rapid growth of EHLs on the safe and stable operation of power grid under the background of the development of clean energy heating, a distributed response strategy based on temperature queue sorting is proposed to suppress the frequency drop when the system fails. The effectiveness of the proposed strategy is verified by simulation, and the following conclusions are obtained:

- 1) When system failure leads to frequency drop, the synchronous response of centralized response strategy and temperature queue sorting distributed response strategy can improve the frequency to a certain extent. In the same proportion of EHLs, the centralized response strategy has a more significant effect on frequency improvement, but compared with the temperature queue sorting distributed response strategy, a large number of EHLs synchronous exit under the control of the centralized response strategy will have excessive response.
- 2) Due to the large power shortage of the system under fault 2, the frequency drop is more serious than that of fault 1, but the proposed

temperature queue sorting distributed response strategy can still effectively improve the system frequency level.

- 3) When the system fails, the higher the load proportion of EHLs is in the node, the greater the frequency fluctuation is.

CRediT authorship contribution statement

Shoudong Li: Conceptualization, Methodology, simulation, data curation, writing-original draft preparation. **Guangqing Bao:** Supervision & reviewing. **Xiaoying Zhang:** Simulation & data curation. **Guodong Wu:** Validation & editing. **Bing Ren:** Reviewing & editing.

Declaration of Competing Interest

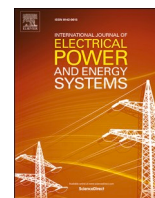
This paper is completed by the author and our team without any plagiarism. We declare that we do not have any commercial or associative interest that represents a conflict of interest in connection with the work submitted.

Acknowledgements

This work was supported in part by the National Natural Science Foundation of China under Grant 51867015.

References

- [1] Y. Liu, S. You, Y. Liu, Study of wind and PV frequency control in U.S. power grids—EI and TI case studies, *IEEE Power and Energy Technol. Syst. J.* 4 (3) (2017) 65–73.
- [2] G. Dehnavi, H.L. Ginn, Distributed load sharing among converters in an autonomous microgrid including PV and wind power units, *IEEE Trans. Smart Grid* 10 (4) (2019) 4289–4298.
- [3] L. Cheng, T. Yu, H. Jiang, S. Shi, Z. Tan, Z. Zhang, Energy Internet access equipment integrating cyber-physical systems: concepts, key technologies, system development, and application prospects, *IEEE Access* 7 (2019) 23127–23148.
- [4] J. Yang, W. Yuan, Y. Sun, H. Han, X. Hou, J.M. Guerrero, A novel quasi-master-slave control frame for pv-storage independent microgrid, *Int. J. Electrical Power & Energy Syst.* 97 (2018) 262–274.
- [5] A. Merabet, K.T. Ahmed, H. Ibrahim, R. Beguenane, A. Ghias, Energy management and control system for laboratory scale microgrid based wind-pv-battery, *IEEE Trans. Sustain. Energy* 8 (1) (2017) 145–154.
- [6] P. Li, Z. Wang, N. Wang, W. Yang, M. Li, X. Zhou, Y. Yin, J. Wang, T. Guo, Stochastic robust optimal operation of community integrated energy system based on integrated demand response, *Int. J. Electrical Power & Energy Syst.* 128 (2021), 106735.
- [7] D.H. Blum, T. Zakula, L.K. Norford, Opportunity cost quantification for ancillary services provided by heating, ventilating, and air-conditioning systems, *IEEE Trans. Smart Grid* 8 (3) (2017) 1264–1273.
- [8] E.S. Parizy, H.R. Bahrami, S. Choi, A low complexity and secure demand response technique for peak load reduction, *IEEE Trans. Smart Grid* 10 (3) (2019) 3259–3268.
- [9] D. Wu, J. Lian, Y. Sun, T. Yang, J. Hansen, Hierarchical control framework for integrated coordination between distributed energy resources and demand response, *Electric Power Syst. Res.* 150 (2017) 45–54.
- [10] M.H. Albadi, E.F. El-Saadany, A summary of demand response in electricity markets, *Electric Power Syst. Res.* 78 (11) (2008) 1989–1996.
- [11] O. Alkadi, N. Cappers, P. Denholm, Demand response for ancillary services, *IEEE Trans. Smart Grid* 4 (4) (2013) 1988–1995.
- [12] J. Wang, H. Zhang, Z. Yue, J. Sun, W. Dan, Evaluation of the potential regulation capacity of water heater loads, in: 2013 5th International Conference on Power Electronics Systems and Applications (PESA) New Energy Conversion for the 21st Century, IEEE, 2013, pp. 1–5.
- [13] X. Huang, Z. Xu, Y. Sun, Y. Xue, Z. Wang, Z. Liu, Z. Li, W. Ni, Heat and power load dispatching considering energy storage of district heating system and electric boilers, *J. Modern Power Syst. Clean Energy* 5 (6) (2018) 992–1003.
- [14] J. Li, Y. Fu, Z. Xing, X. Zhang, X. Fan, Coordination scheduling model of multi-type flexible load for increasing wind power utilization, *IEEE Access* 7 (7) (2019) 105840–105850.
- [15] W. Gu, Z. Wang, Z. Wu, Z. Luo, Y. Tang, J. Wang, An online optimal dispatch schedule for CCHP microgrids based on model predictive control, *IEEE Trans. Smart Grid* 5 (8) (2017) 2332–2342.
- [16] J. Hao, Q. Chen, K. He, L. Chen, Y. Dai, F. Xu, Y. Min, A heat current model for heat transfer/storage systems and its application in integrated analysis and optimization with power systems, *IEEE Trans. Sustain. Energy* 1 (11) (2020) 175–184.
- [17] S.A. Pourmousavi, M.H. Nehrir, Real-time central demand response for primary frequency regulation in microgrids, *IEEE Trans. Smart Grid* 3 (4) (2012) 1988–1996.
- [18] N. Lu, Y. Zhang, Design considerations of a centralized load controller using thermostatically controlled appliances for continuous regulation re-serves, *IEEE Trans. Smart Grid* 4 (2) (2013) 914–921.
- [19] J. Kondoh, N. Lu, D.J. Hammerstrom, An evaluation of the water heater load potential for providing regulation service, *IEEE Trans. Power Syst.* 26 (3) (2011) 1309–1316.
- [20] N. Lu, An evaluation of the HVAC load potential for providing load balancing service, *IEEE Trans. Smart Grid* 3 (3) (2012) 1263–1270.
- [21] A. Molina-Garcia, F. Bouffard, D.S. Kirschen, Decentralized demand-side contribution to primary frequency control, *IEEE Trans. Power Syst.* 26 (1) (2011) 411–419.
- [22] J.A. Short, D.G. Infield, L.L. Freris, Stabilization of grid frequency through dynamic demand control, *IEEE Trans. Power Syst.* 22 (3) (2007) 1284–1293.
- [23] C. Meng, J. Wu, S.J. Galsworthy, C.E. Ugalde-Loo, N. Gargov, W.W. Hung, N. Jenkins, Power system frequency response from the control of bitumen tanks, *IEEE Trans. Power Syst.* 31 (3) (2016) 1769–1778.
- [24] C. Meng, S.S. Sami, J. Wu, Benefits of using virtual energy storage system for power system frequency response, *Appl. Energy* 194 (2016) 376–385, 2016.
- [25] D.G. Infield, J. Short, C. Horne, L.L. Freris, in: Potential for domestic dynamic demand-side management in the UK. Power Engineering Society General Meeting, IEEE, 2007, pp. 1–6.
- [26] Z. Xu, R. Diao, S. Lu, J. Lian, Y. Zhang, Modeling of electric water heaters for demand response: a baseline PDE model, *IEEE Trans. Smart Grid* 5 (5) (2014) 2203–2210.
- [27] Y.Q. Bao, Y. Li, FPGA-based design of grid friendly appliance controller, *IEEE Trans. Smart Grid* 2 (5) (2014) 924–931.



Consensus-based distributed coordinated operation of active distribution networks with electric heating loads

Shoudong Li^{a,b}, Guangqing Bao^{a,c,*}, Anan Zhang^c

^a School of Electrical and Information Engineering, Lanzhou University of Technology, Lanzhou 730050, China

^b School of Automation and Electrical Engineering, Lanzhou Jiaotong University, Lanzhou 730070, China

^c School of Electronics and Information Engineering, Southwest Petroleum University, Chengdu 610500, China

ARTICLE INFO

Keywords:

Communication failure
Active distribution network
Consensus algorithm
Electric heating loads
Correction variable

ABSTRACT

Aiming at the problems of a large amount of communication information, changeable network topology, and communication failures in active distribution networks with electric heating loads, a consensus distributed coordinated operation method for active distribution networks considering communication failures is proposed. Firstly, a coordinated optimization model is established with the goal of maximizing the comprehensive benefits of agents in the active distribution network with electric heating loads. Then, the consensus variable for each agent is defined based on the coordinated optimization model. On this basis, the consensus variable of each agent is extracted using the Lagrange multiplier method and KKT optimal conditions; Finally, considering the impact of communication failures on the consensus-distributed coordinated operation of active distribution networks with electric heating loads, a modified variable is introduced in the iterative process to improve the consensus-distributed algorithm so as to eliminate the unbalanced power of the system. A 5-machine active distribution network example system is constructed for simulation verification. The results show that the improved consensus distributed method can eliminate the imbalance between supply and demand in the system under communication failures, and the application scenarios have strong robustness. After electric heating loads participate in the coordinated operation, it can promote the accommodation of new energy power and the economic operation of the system.

1. Introduction

With the continuous improvement of the penetration rate of new energy power and the access to various loads, the security and stability of the power grid have been seriously challenged [1,2]. Flexible loads in smart grids can use their responsiveness to improve the flexibility of the system, achieving a balance between supply and demand in the event of system failures or disturbances [3,4]. Currently, most research on the scheduling and operation of distribution networks is based on energy storage and demand response technology to achieve system power balance. Reference [5] uses hydrogen energy as an energy storage carrier, utilizing the coupling and interaction between multiple energy sources to improve the utilization rate of renewable energy during scheduling and operation, achieving a balance between the supply and demand of the system. Reference [6] models common energy storage resources, including centralized and distributed energy storage equipment, pipe network energy storage, and building thermal capacity, as centralized

energy storage to ensure supply and demand balance and long-term stable operation of the system. Reference [7] considers the synergistic effects of electrical energy storage, thermal energy storage, and EV and improves the system's resistance to extreme weather. Reference [8] proposes a new integrated demand response day ahead energy management framework for remote off grid power systems, which uses probabilistic fuzzy inference systems to estimate user responses to price based incentives, so as to coordinate and manage the energy system more effectively. Reference [9] establishes a demand management model with the participation of energy storage systems and proposed peak shaving and valley filling factors to describe the degree of demand management. Reference [10] formulates optimization strategies through reasonable electricity prices to orderly guide the charging and discharging behavior of electric vehicles, thereby achieving peak shaving and valley filling of the power grid and balancing supply and demand. However, traditional configuration energy storage and demand response technologies to maintain system power balance can lead to a

* Corresponding author at: School of Electrical and Information Engineering, Lanzhou University of Technology, Lanzhou 730050, China.
E-mail address: baogq03@163.com (G. Bao).

<https://doi.org/10.1016/j.ijepes.2023.109393>

Received 29 October 2022; Received in revised form 25 May 2023; Accepted 22 July 2023

Available online 28 July 2023

0142-0615/© 2023 Elsevier Ltd. This is an open access article under the CC BY-NC-ND license (<http://creativecommons.org/licenses/by-nc-nd/4.0/>).

reduced economy. As a new type of flexible and adjustable load generated under the development trend of clean heating, electric heating loads (EHLs) have grown rapidly in recent years, and have become an important load resource that cannot be ignored on the demand side. They have significant adjustment capabilities while meeting the energy comfort of users [11]. EHLs are divided into space heating EHLs and domestic hot water EHLs according to their uses [12]. In developed and developing countries, space heating EHLs and domestic hot water EHLs are two major components of household energy consumption. In China, space heating EHLs are the largest component of household energy consumption, accounting for 54% of total household energy consumption [13]. Domestic hot water EHLs are the third largest component, accounting for 14% of total household energy consumption [13]. In Europe and the United States, space heating EHLs and domestic hot water EHLs account for approximately 80% and 60% of the final energy use of residential buildings, respectively [14]. The load forms of space heating EHLs are mainly electric heat storage boilers, heat pumps, and air conditioners, and the comfort measure is the heating temperature [15]. The load form of domestic hot water EHLs is mainly electric water heaters, and the comfort measure is the hot water temperature [16].

EHLs, as a clean heating technology under the substitution of electric energy, utilize electric energy to achieve clean heating through the electrothermal conversion of electric heating equipment during the peak period of electricity prices. This heating method has significant advantages over traditional coal-fired boilers and configured heat storage. Configuring heat storage devices only improves the flexibility of cogeneration, and the effect of promoting the consumption of new energy power is mainly reflected in the improvement of the peak shaving capacity of cogeneration units without fundamentally expanding the consumption space of new energy power [17]. EHLs technology can not only ensure the sustainability of heating but also save on electricity costs under the guidance of electricity pricing mechanisms. EHLs technology achieves peak shaving and valley filling in the power grid, expands space for the accommodation of new energy power, and reduces the occurrence of wind and light waste. However, EHLs in the system are widely distributed, with strong spatiotemporal dispersion and diversity, which poses challenges for EHLs to participate in the coordinated operation of the distribution network. Therefore, studying how to use distributed computing methods to achieve EHLs participating in the coordinated operation of distribution networks is of great significance for solving the problems of supply and demand balance and local accommodation of high-permeability new energy power systems.

Centralized operation mode has been widely used in traditional economic dispatching of power systems, such as the Newton-Raphson method, quadratic programming, Lagrange relaxation method, genetic algorithm, tabu search algorithm, and particle swarm optimization algorithm. In this mode, each distributed unit needs to upload its own parameters and constraints to the central controller that solves the economic scheduling problem [18] and then, after obtaining the optimal solution, send the output instructions back to each distributed unit. Due to a large number of distributed devices and the high requirements for communication capacity and central storage in a centralized manner, a single point of failure in the center can also lead to system crashes [19]. In addition, the submission of parameter and constraint information will expose the privacy of distributed unit owners. In response to the shortcomings of centralized methods, researchers have conducted a lot of research on the application of consistently distributed algorithms to energy management, especially in supporting and gradually replacing the traditional centralized framework of power systems with the coordinated operation of microgrids and active distribution systems [20]. Compared to the classical centralized method, the consistency-based distributed method is superior to the centralized algorithm in terms of solving speed and solving the coordinated operation of active distribution networks containing large-scale distributed resources [21]. Secondly, centralized methods require high-bandwidth communication to process information collected within the system, while consistency-

based distributed methods only require local information exchange between neighbors, reducing the necessary communication costs [22]. In addition, future power grids and communication networks may have a variable topology, and consistency-based distributed methods are more suitable for handling topology changes and adapting to plug-and-play functionality [23]. Therefore, distributed methods based on consistency algorithms have broad application prospects in solving the coordinated operation problem of active distribution networks with large-scale EHLs. Reference [24] uses consistency-based energy management algorithms to maximize social welfare by coordinating supplier generations and customer needs. Reference [25] proposes to select marginal cost as a consistent variable to solve the distributed economic scheduling problem, but it requires a centralized statistical system for the active deficit of a leader node. Therefore, reference [26] improves the consistency algorithm on the basis of reference [25] and proposes communication information traversal statistics based on connected networks to eliminate "Leader" agents. In [27], considering storage devices, the single-time step economic scheduling problem was extended to a multi-time step scheduling problem. Reference [28] improves the convergence speed by adding gradient terms to the consistent algorithm, but this largely depends on the selection of step size. Although decreasing step size can achieve a compromise between optimality and convergence speed, it is necessary to find the optimal step size through offline research [29].

Although consistency-based energy management algorithms have attracted a lot of attention, most existing studies assume that communication is completely reliable, and communication failures (manifested as link failures or packet loss) may occur randomly in practical applications [30]. Therefore, communication failure is an important factor to consider in power system applications. Reference [31] indicates that in power system control based on wide-area measurement systems, packet loss during data transmission may lead to transient instability issues. Reference [32] demonstrates the importance of reliable communication for demand response control in Heating Ventilation and Air Conditioning (HVAC) systems. In the case of a communication failure, the actual power consumption deviates from the target power consumption and does not meet the user's comfort level.

Therefore, it is necessary to study the impact of communication failures on consistency-based energy management algorithms. Reference [33] introduces Bernoulli random variable and piecewise constant function for correction in case of communication failure to ensure that the consistency algorithm converges to the average value, thereby improving the robustness of the algorithm. However, the above algorithms neither consider constraints on agent status nor any optimization criteria, both of which are indispensable in energy management issues. Reference [34] demonstrates the impact of incomplete communication networks on consistency-based economic scheduling algorithms. However, the impact of communication failures on scheduling results is not provided. Reference [35] proposes a robust distributed economic scheduling method based on the push-sum method. However, only the single-stage optimization problem is considered, which limits its application in distribution networks.

In summary, the current research on consistently distributed optimization computing for power systems has hardly considered the impact of communication failures on system operation results. At the same time, after configuring EHLs in active distribution networks, problems such as large amounts of communication information and variable network topology may arise. Therefore, based on the establishment of a coordinated and optimized operation model for active distribution networks with EHLs, this paper uses the Lagrange multiplier method and KKT optimal conditions to extract the consistent variables of each agent in the active distribution network and considers the impact of communication failures on system operation. In the iterative process, modified variables are introduced to propose an improved method of consistent distributed operation. Compared to the methods in [33–35], the proposed method does not require reconfiguration of communication or

retransmission of lost data and can find feasible solutions in the event of communication failures to achieve the optimal results of coordinated operation of EHLs active distribution networks.

2. Distributed optimal operation modeling of the active distribution network with EHLs

EHLs can be divided into space heating EHLs and domestic hot water EHLs according to their uses. The active distribution network structure with EHLs studied in this paper is shown in Fig. 1.

2.1. Coordinated and optimized operation model

When coordinating and optimizing the operation of various intelligent agents in the active distribution network, they will be constrained by overall power balance and other constraints. While pursuing maximum self-interest, they also need to achieve maximum comprehensive system benefits. The comprehensive benefits of coordinated operation of active distribution networks consider the benefits of EHLs and non electric heating flexible loads, the operating costs of new energy generation units, the operating costs of energy storage devices, and the power exchange costs between active distribution networks and transmission grids. The goal of active distribution network coordinated optimization operation is to maximize the comprehensive benefits of the system, specifically expressed as:

$$\max \left[\sum_{i=1}^{N_{bl}} C_i^{bl}(T_i^{bl}) + \sum_{i=1}^{N_{el}} C_i^{el}(T_i^{el}) + \sum_{i=1}^{N_l} C_i^f(L_i) - \sum_{i=1}^{N_h} C_i^h(P_i) - \sum_{i=1}^{N_w} C_i^w(W_i) - \sum_{i=1}^{N_{es}} C_i^{es}(E_i) + C_{grid}(P_{grid}) \right]$$

(1)

where $C_i^{bl}(T_i^{bl})$ is the benefit of coordinated operation of the space heating EHLs agent, and T_i^{bl} is the set temperature of the space heating EHLs agent. $C_i^{el}(T_i^{el})$ is the benefit of the coordinated operation of EHLs agent for making domestic hot water, and T_i^{el} is the set temperature of EHLs agent for making domestic hot water. $C_i^f(L_i)$ is the benefit of a coordinated-operation of the non-electric heating flexible load agent, and L_i is the power of a non-electric heating flexible load agent. $C_i^h(P_i)$ is the power generation cost of conventional thermal power unit agents, and P_i is the power generation power of thermal power unit agents. $C_i^w(W_i)$ is the cost of wind and light discarding of the new energy generator unit agent, and W_i is the power regulation for the new energy generator unit agent. $C_i^{es}(E_i)$ is the operation cost of the energy storage agent, and E_i is the power transmitted by the energy storage agent to the active distribution network. $C_{grid}(P_{grid})$ is the power exchange cost between the active distribution network and the transmission network. P_{grid} is the exchange of power between the active distribution network and the transmission network. $P_{grid} > 0$ indicates that the active distribution network transmits power to the transmission network, and conversely $P_{grid} < 0$.

The profit and cost functions of each part of the active distribution network can be expressed as follows:

(1) Revenue function of EHLs

The benefits of EHLs in active distribution networks are directly related to the comfort of users. Therefore, the benefits of EHLs in active distribution networks are also directly related to their set temperatures. If the set temperature is closer to the user's optimal temperature, the benefits of EHLs will be greater. When the set temperature is equal to the user's optimal temperature, the EHLs revenue reaches its peak. If the set temperature deviates from the user's optimal temperature, the EHLs will benefit less. When the set temperature is equal to the ambient

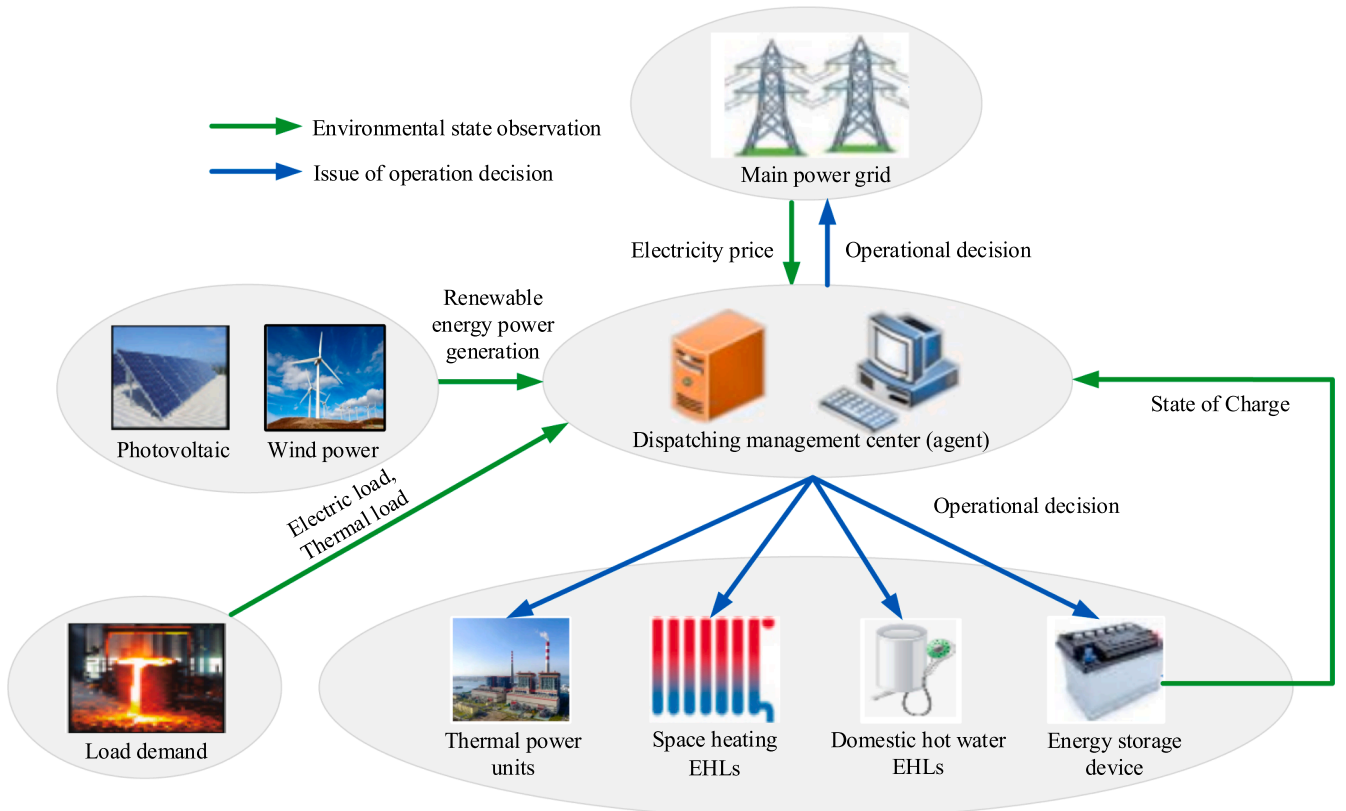


Fig. 1. Schematic diagram of an active distribution network with EHLs.

temperature, the EHLs return is 0. According to the above principles, the income functions of space heating EHLs and domestic hot water EHLs are respectively expressed as [36]:

$$C_i^{\text{bl}}(T_i^{\text{bl}}) = k^{\text{bl}}[(T_{\text{out},i}^{\text{bl}} - T_s^{\text{bl}})^2 - (T_i^{\text{bl}} - T_s^{\text{bl}})^2] \quad (2)$$

$$C_i^{\text{el}}(T_i^{\text{el}}) = k^{\text{el}}[(T_{\text{out},i}^{\text{el}} - T_s^{\text{el}})^2 - (T_i^{\text{el}} - T_s^{\text{el}})^2] \quad (3)$$

where k^{bl} and k^{el} are the profit coefficients of space heating EHLs and domestic hot water EHLs, respectively. $T_{\text{out},i}^{\text{bl}}$ and $T_{\text{out},i}^{\text{el}}$ are the outdoor temperatures of space heating EHLs and domestic hot water EHLs, respectively. T_i^{bl} and T_i^{el} are the set temperatures of space heating EHLs and domestic hot water EHLs, respectively. T_s^{bl} and T_s^{el} are the optimal temperatures for space heating EHLs and domestic hot water EHLs, respectively.

(2) Revenue function of non-electric heating flexible load

The benefit of a flexible non-electric heating load is that it is independent of temperature and has general characteristics that can be fitted with a quadratic function as follows [37]:

$$C_i^f(L_i) = a_{L,i}L_i^2 + b_{L,i}L_i + c_{L,i} \quad (4)$$

where $a_{L,i}$, $b_{L,i}$, and $c_{L,i}$ are the profit coefficients of a non-electric heating flexible load.

(3) The cost function of thermal power units is [38]:

$$C_i^h(P_i) = a_i P_i^2 + b_i P_i + c_i \quad (5)$$

where a_i , b_i , and c_i are the generation cost coefficients of thermal power units.

(4) Cost function of new energy-generating units

In order to facilitate modeling and analysis, wind power and photovoltaic units are uniformly modeled as new energy unit agents in this paper. The power of new energy units is divided into an adjustable part and a fixed grid-connected part. Its regulated power can be disposed of by discarding wind and light. In order to improve the wind and solar energy consumption rates, discarding wind and light will result in a certain penalty cost. Therefore, the cost of new energy units is mainly the penalty cost, which can be expressed as:

$$C_i^w(W_i) = k^w(W_{i,\text{max}} - W_i)^2 \quad (6)$$

where k^w is the cost coefficient of new energy units. $W_{i,\text{max}}$ is the maximum adjustable power of new energy units.

(5) The cost function of an energy storage device is [39]:

$$C_i^{\text{es}}(E_i) = a_{\text{es},i}E_i^2 \quad (7)$$

where $a_{\text{es},i}$ is the cost coefficient of the energy storage device. E_i is the discharge power of the energy storage device.

(6) The power exchange cost of the active distribution network and transmission network is [39]:

$$C_{\text{grid}}(P_{\text{grid}}) = \rho_{\text{grid}}P_{\text{grid}} \quad (8)$$

where ρ_{grid} is the price of the power exchanged between the active distribution network and the transmission network.

When the agents in the active distribution network operate in coor-

dination, the following constraints should also be considered [36–39]:

$$\sum_{i=1}^{N_h} P_i + \sum_{i=1}^{N_w} W_{g,i} + \sum_{i=1}^{N_w} W_i + \sum_{i=1}^{N_{\text{es}}} E_i - \sum_{i=1}^{N_{\text{bl}}} V_i^{\text{bl}} - \sum_{i=1}^{N_{\text{el}}} V_i^{\text{el}} - \sum_{i=1}^{N_l} L_i = P^{\text{grid}} \quad (9)$$

$$\begin{cases} V_i^{\text{bl}} = \eta^{\text{bl}}(T_i^{\text{bl}} - T_{\text{out},i}^{\text{bl}})^2 \\ V_i^{\text{el}} = \eta^{\text{el}}(T_i^{\text{el}} - T_{\text{out},i}^{\text{el}})^2 \end{cases} \quad (10)$$

$$\begin{cases} V_{i,\text{min}}^{\text{bl}} \leq V_i^{\text{bl}} \leq V_{i,\text{max}}^{\text{bl}} \\ V_{i,\text{min}}^{\text{el}} \leq V_i^{\text{el}} \leq V_{i,\text{max}}^{\text{el}} \end{cases} \quad (11)$$

$$W_{i,\text{min}} \leq W_i \leq W_{i,\text{max}} \quad (12)$$

$$P_{i,\text{min}} \leq P_i \leq P_{i,\text{max}} \quad (13)$$

$$E_{i,\text{min}} \leq E_i \leq E_{i,\text{max}} \quad (14)$$

$$E_i^{\text{pre}} - E_i^{\text{full}} \leq E_i \leq E_i^{\text{pre}} \quad (15)$$

$$\begin{cases} T_{i,\text{min}}^{\text{bl}} \leq T_i^{\text{bl}} \leq T_{i,\text{max}}^{\text{bl}} \\ T_{i,\text{min}}^{\text{el}} \leq T_i^{\text{el}} \leq T_{i,\text{max}}^{\text{el}} \end{cases} \quad (16)$$

where $W_{g,i}$ is the fixed grid-connected power of new energy units. V_i^{bl} and V_i^{el} are the power consumption of space heating EHLs and domestic hot water EHLs for temperature regulation, respectively. η^{bl} and η^{el} are the power consumption coefficients of space heating EHLs and domestic hot water EHLs, respectively. $V_{i,\text{max}}^{\text{bl}}$ and $V_{i,\text{min}}^{\text{bl}}$ are the upper and lower limits of V_i^{bl} . $V_{i,\text{max}}^{\text{el}}$ and $V_{i,\text{min}}^{\text{el}}$ are the upper and lower limits of V_i^{el} . $W_{i,\text{max}}$ and $W_{i,\text{min}}$ are the upper and lower limits of W_i ; $P_{i,\text{max}}$ and $P_{i,\text{min}}$ are the upper and lower limits of thermal power unit output. $E_{i,\text{max}}$ and $E_{i,\text{min}}$ are the upper and lower limits of E_i . E_i^{pre} is the current state of charge of the energy storage agent, and E_i^{full} is its capacity of energy storage agent. $T_{i,\text{max}}^{\text{bl}}$ and $T_{i,\text{min}}^{\text{bl}}$ are the upper and lower limits of T_i^{bl} . $T_{i,\text{max}}^{\text{el}}$ and $T_{i,\text{min}}^{\text{el}}$ are the upper and lower limits of T_i^{el} . Constraint (9) represents the power balance during coordinated operation of the active distribution network. Constraint (10) represents the power consumption expression during temperature regulation of space heating EHLs and domestic hot water EHLs. Constraint (11) represents the operating power limit of space heating EHLs and domestic hot water EHLs. Constraints (12) and (13) represent the operating power limit of new energy units and thermal power units, respectively. Constraint (14) represents the regulating power limit of energy storage intelligent agents. Constraint (15) represents the state of charge constraint of the energy storage intelligent agent. Constraint (16) represents the temperature limits for space heating EHLs and domestic hot water EHLs.

2.2. Consensus variable extraction based on KKT optimal condition

During the distributed and coordinated operation of the active distribution network, the incremental benefits (IB) of space heating EHLs, domestic hot water EHLs, and non-electric heating flexible loads and the incremental costs (IC) of thermal power units, new energy generating units, and energy storage devices are taken as the consensus variables of each agent, which are Lagrangian multipliers. The consensus variables are extracted based on KKT optimal conditions, and the model is solved using the consensus distributed algorithm. When inequality constraints (10) - (15) are ignored, the optimization problem of active distribution network load coordination is as follows:

$$\begin{aligned} \min \varpi = & - \sum_{i=1}^{N_{bl}} C_i^{bl}(T_i^{bl}) - \sum_{i=1}^{N_{el}} C_i^{el}(T_i^{el}) - \sum_{i=1}^{N_f} C_i^f(L_i) + \sum_{i=1}^{N_h} C_i^h(P_i) + \\ & \sum_{i=1}^{N_w} C_i^w(W_i) + \sum_{i=1}^{N_{es}} C_i^{es}(E_i) - C_{grid}(P_{grid}) + \\ & \lambda [P_{grid} - (\sum_{i=1}^{N_h} P_i + \sum_{i=1}^{N_w} W_{g,i} + \sum_{i=1}^{N_w} W_i + \sum_{i=1}^{N_{es}} E_i - \sum_{i=1}^{N_{bl}} V_i^{bl} - \sum_{i=1}^{N_{el}} V_i^{el} - \sum_{i=1}^{N_f} L_i)] \end{aligned} \quad (17)$$

Without considering inequality constraints, the Lagrangian multiplier method is applied, and partial derivatives are calculated for each decision variable based on KKT optimal conditions. The optimal conditions of equation (17) are as follows:

$$\left\{ \begin{aligned} \frac{\partial \varpi}{\partial T_i^{bl}} = -\frac{\partial C_i^{bl}(T_i^{bl})}{\partial T_i^{bl}} + \frac{\partial V_i^{bl}(T_i^{bl})}{\partial T_i^{bl}} = -\frac{\partial C_i^{bl}(T_i^{bl})}{\partial T_i^{bl}} + \lambda [2\eta^{bl}(T_i^{bl} - T_{out,i}^{bl})] = 0 \\ \frac{\partial \varpi}{\partial T_i^{el}} = -\frac{\partial C_i^{el}(T_i^{el})}{\partial T_i^{el}} + \frac{\partial V_i^{el}(T_i^{el})}{\partial T_i^{el}} = -\frac{\partial C_i^{el}(T_i^{el})}{\partial T_i^{el}} + \lambda [2\eta^{el}(T_i^{el} - T_{out,i}^{el})] = 0 \\ \frac{\partial \varpi}{\partial L_i} = -\frac{\partial C_i^f(L_i)}{\partial L_i} + \lambda = 0 \\ \frac{\partial \varpi}{\partial P_i} = \frac{\partial C_i^h(P_i)}{\partial P_i} - \lambda = 0 \\ \frac{\partial \varpi}{\partial W_i} = \frac{\partial C_i^w(W_i)}{\partial W_i} - \lambda = 0 \\ \frac{\partial \varpi}{\partial E_i} = \frac{\partial C_i^{es}(E_i)}{\partial E_i} - \lambda = 0 \end{aligned} \right. \quad (18)$$

$$\begin{aligned} \lambda = \frac{\frac{\partial C_i^{bl}(T_i^{bl})}{\partial T_i^{bl}}}{2\eta^{bl}(T_i^{bl} - T_{out,i}^{bl})} = \frac{\frac{\partial C_i^{el}(T_i^{el})}{\partial T_i^{el}}}{2\eta^{el}(T_i^{el} - T_{out,i}^{el})} = \frac{\partial C_i^f(L_i)}{\partial L_i} = \frac{\partial C_i^h(P_i)}{\partial P_i} = \frac{\partial C_i^w(W_i)}{\partial W_i} \\ = \frac{\partial C_i^{es}(E_i)}{\partial E_i} \end{aligned} \quad (19)$$

According to equations (18) and (19), the consensus variables of each agent extracted from space heating EHLs, domestic hot water EHLs, non-electric heating flexible loads, thermal power units, new energy generating units, and energy storage devices are:

$$\left\{ \begin{aligned} \lambda_{bl,i} = \frac{\frac{\partial C_i^{bl}(T_i^{bl})}{\partial T_i^{bl}}}{2\eta^{bl}(T_i^{bl} - T_{out,i}^{bl})} = \frac{k^{bl}(T_s^{bl} - T_i^{bl})}{2\eta^{bl}(T_i^{bl} - T_{out,i}^{bl})} \\ \lambda_{el,i} = \frac{\frac{\partial C_i^{el}(T_i^{el})}{\partial T_i^{el}}}{2\eta^{el}(T_i^{el} - T_{out,i}^{el})} = \frac{k^{el}(T_s^{el} - T_i^{el})}{2\eta^{el}(T_i^{el} - T_{out,i}^{el})} \\ \lambda_{f,i} = \frac{\partial C_i^f(L_i)}{\partial L_i} = 2a_{L,i}L_i + b_{L,i} \\ \lambda_{h,i} = \frac{\partial C_i^h(P_i)}{\partial P_i} = 2a_iP_i + b_i \\ \lambda_{w,i} = \frac{\partial C_i^w(W_i)}{\partial W_i} = 2k^w(W_{i,max} - W_i) \\ \lambda_{es,i} = \frac{\partial C_i^{es}(E_i)}{\partial E_i} = 2a_{es,i}E_i \end{aligned} \right. \quad (20)$$

3. A consensus-based distributed algorithm considering communication failures

3.1. Agent information transmission considering communication failures

The communication failure problem on the network can be modeled as an independent Bernoulli process [40]. The binary variable $d_{i-j}(k) \rightarrow (0, 1)$ represents the communication state of the communication link $i \leftrightarrow j$ at iteration k , and $d_{i-j}(k) = 0$ represents the communication link $i \leftrightarrow j$, which has communication failure, and $d_{i-j}(k) = 1$ represents the data transmission between nodes i and j as normal. The probability of the communication state is:

$$\begin{cases} \pi_r \{d_{i-j}(k) = 0\} = \rho_{i-j} \\ \pi_r \{d_{i-j}(k) = 1\} = 1 - \rho_{i-j} \end{cases} \quad (21)$$

where ρ_{i-j} is the probability of communication failure in the communication link $i \leftrightarrow j$.

Let $A_i(k)$ denote the set of neighbors that fail to deliver the information to node i at iteration k , and let $B_i(k)$ denote the set of neighbors that succeed. The set of adjacent nodes of node i is expressed as $N_i = A_i(k) \cup B_i(k)$. Node i can only use the data transmitted by the information set $B_i(k)$ to update the information due to the communication failure of the information set $A_i(k)$ at iteration k .

The updating rules of consensus variables and the unbalanced power of agents under communication failure are shown in Equations (22) and (23):

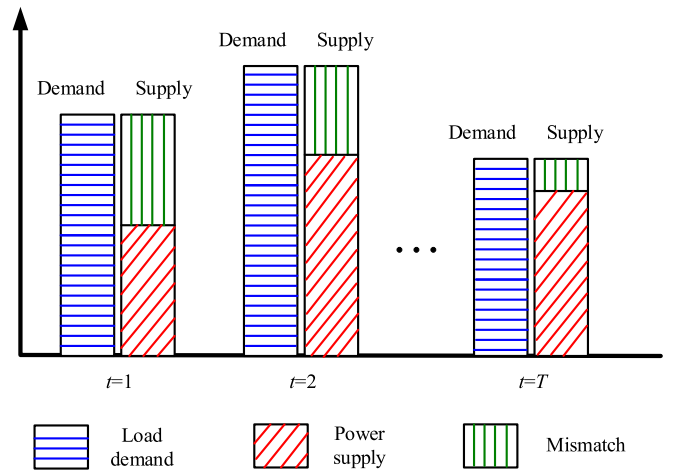


Fig. 2. Explanation of the impact of communication failures on coordinated operation results.

$$\forall t \in T : \left\{ \begin{array}{l} \lambda_{bl,i}^t(k+1) = \lambda_{bl,i}^t(k) + \sum_{j \in B_i(k)} \alpha_{bl,ij} (\lambda_{bl,j}^t(k) - \lambda_{bl,i}^t(k)) + \omega \Delta P_{bl,i}^t(k) \\ \lambda_{cl,i}^t(k+1) = \lambda_{cl,i}^t(k) + \sum_{j \in B_i(k)} \alpha_{cl,ij} (\lambda_{cl,j}^t(k) - \lambda_{cl,i}^t(k)) + \omega \Delta P_{cl,i}^t(k) \\ \lambda_{f,i}^t(k+1) = \lambda_{f,i}^t(k) + \sum_{j \in B_i(k)} \alpha_{L,ij} (\lambda_{L,j}^t(k) - \lambda_{L,i}^t(k)) + \omega \Delta P_{L,i}^t(k) \\ \lambda_{h,i}^t(k+1) = \lambda_{h,i}^t(k) + \sum_{j \in B_i(k)} \alpha_{P,ij} (\lambda_{P,j}^t(k) - \lambda_{P,i}^t(k)) + \omega \Delta P_{P,i}^t(k) \\ \lambda_{w,i}^t(k+1) = \lambda_{w,i}^t(k) + \sum_{j \in B_i(k)} \alpha_{W,ij} (\lambda_{W,j}^t(k) - \lambda_{W,i}^t(k)) + \omega \Delta P_{W,i}^t(k) \\ \lambda_{es,i}^t(k+1) = \lambda_{es,i}^t(k) + \sum_{j \in B_i(k)} \alpha_{E,ij} (\lambda_{E,j}^t(k) - \lambda_{E,i}^t(k)) + \omega \Delta P_{E,i}^t(k) \end{array} \right. \quad (22)$$

$$\forall t \in T : \left\{ \begin{array}{l} \lim_{k \rightarrow \infty} \sum_{i \in N} V_{bl,i}^t(k) = \lim_{k \rightarrow \infty} \sum_{s=0}^k \sum_{i \in N} \sum_{j \in A_i(s)} \alpha_{bl,ij} (\Delta V_{bl,j}^t(s) - \Delta V_{bl,i}^t(s)) \\ \lim_{k \rightarrow \infty} \sum_{i \in N} V_{cl,i}^t(k) = \lim_{k \rightarrow \infty} \sum_{s=0}^k \sum_{i \in N} \sum_{j \in A_i(s)} \alpha_{cl,ij} (\Delta V_{cl,j}^t(s) - \Delta V_{cl,i}^t(s)) \\ \lim_{k \rightarrow \infty} \sum_{i \in N} L_i^t(k) = \lim_{k \rightarrow \infty} \sum_{s=0}^k \sum_{i \in N} \sum_{j \in A_i(s)} \alpha_{L,ij} (\Delta L_j^t(s) - \Delta L_i^t(s)) \\ \lim_{k \rightarrow \infty} \sum_{i \in N} P_i^t(k) = \lim_{k \rightarrow \infty} \sum_{s=0}^k \sum_{i \in N} \sum_{j \in A_i(s)} \alpha_{P,ij} (\Delta P_j^t(s) - \Delta P_i^t(s)) \\ \lim_{k \rightarrow \infty} \sum_{i \in N} W_i^t(k) = \lim_{k \rightarrow \infty} \sum_{s=0}^k \sum_{i \in N} \sum_{j \in A_i(s)} \alpha_{W,ij} (\Delta W_j^t(s) - \Delta W_i^t(s)) \\ \lim_{k \rightarrow \infty} \sum_{i \in N} E_i^t(k) = \lim_{k \rightarrow \infty} \sum_{s=0}^k \sum_{i \in N} \sum_{j \in A_i(s)} \alpha_{E,ij} (\Delta E_j^t(s) - \Delta E_i^t(s)) \end{array} \right. \quad (25)$$

$$\forall t \in T : \left\{ \begin{array}{l} \Delta V_{bl,i}^t(k+1) = \Delta V_{bl,i}^t(k) + \sum_{j \in B_i(k)} \alpha_{bl,ij} (\Delta V_{bl,j}^t(k) - \Delta V_{bl,i}^t(k)) + V_{bl,i}^t(k+1) - V_{bl,i}^t(k) \\ \Delta V_{cl,i}^t(k+1) = \Delta V_{cl,i}^t(k) + \sum_{j \in B_i(k)} \alpha_{cl,ij} (\Delta V_{cl,j}^t(k) - \Delta V_{cl,i}^t(k)) + V_{cl,i}^t(k+1) - V_{cl,i}^t(k) \\ \Delta L_i^t(k+1) = \Delta L_i^t(k) + \sum_{j \in B_i(k)} \alpha_{L,ij} (\Delta L_j^t(k) - \Delta L_i^t(k)) + L_i^t(k+1) - L_i^t(k) \\ \Delta P_i^t(k+1) = \Delta P_i^t(k) + \sum_{j \in B_i(k)} \alpha_{P,ij} (\Delta P_j^t(k) - \Delta P_i^t(k)) + P_i^t(k+1) - P_i^t(k) \\ \Delta W_i^t(k+1) = \Delta W_i^t(k) + \sum_{j \in B_i(k)} \alpha_{W,ij} (\Delta W_j^t(k) - \Delta W_i^t(k)) + W_i^t(k+1) - W_i^t(k) \\ \Delta E_i^t(k+1) = \Delta E_i^t(k) + \sum_{j \in B_i(k)} \alpha_{E,ij} (\Delta E_j^t(k) - \Delta E_i^t(k)) + E_i^t(k+1) - E_i^t(k) \end{array} \right. \quad (23)$$

where α_{ij} is the connection strength between nodes i and j , to ensure convergence, the value is $0 \leq \alpha_{ij} < (\max_{i=1, \dots, N} |N_i|)^{-1}$ [41]. $t \in [1, T]$ is the scheduling period in the scheduling cycle. For the consensus convergence coefficient ω , select a value that is small enough to make the iteration result converge to the global optimum. $\Delta V_{bl,i}^t(k)$, $\Delta V_{cl,i}^t(k)$, $\Delta L_i^t(k)$, $\Delta P_i^t(k)$, $\Delta W_i^t(k)$, and $\Delta E_i^t(k)$ are the unbalanced power of space heating EHLs, domestic hot water EHLs, non-electric heating flexible loads, thermal power units, new energy generating units, and energy storage device agents, respectively.

The local unbalanced power can be initialized as the originally generated power and load consumption before coordinated operation:

$$\forall t \in T : \left\{ \begin{array}{l} \Delta V_{bl,i}^t(0) = V_{bl,i}^t(0) = V_{bl,i}^t \\ \Delta V_{cl,i}^t(0) = V_{cl,i}^t(0) = V_{cl,i}^t \\ \Delta L_i^t(0) = L_i^t(0) = L_i^t \\ \Delta P_i^t(0) = P_i^t(0) = P_i^t \\ \Delta W_i^t(0) = W_i^t(0) = W_i^t \\ \Delta E_i^t(0) = E_i^t(0) = 0 \end{array} \right. \quad (24)$$

3.2. Influence of communication failures on the consensus-distributed coordinated operation

When the consensus-distributed method shown in equations (22) and (23) converges in the case of communication failure, the power supply of the system cannot meet the load demand, and the mismatch between supply and demand meets the following requirements:

where the left term is the actual unbalanced power of the system at iteration k , the right item includes all communication failures of the system at iteration k .

The impact of communication failures on the coordinated operation results is shown in Fig. 2. In the final coordinated operation, the total generation power and total load demand of the system cannot be balanced, resulting in the system cannot operate safely and stably. It can be seen from equation (25) that the impact on the final coordinated operation is determined by the local unbalanced power:

$$\forall t \in T : \left\{ \begin{array}{l} \lim_{k \rightarrow \infty} \sum_{i \in N} V_{bl,i}^t(k) = \alpha_{bl,ij} (\Delta V_{bl,j}^t(k) - \Delta V_{bl,i}^t(k)) \\ \lim_{k \rightarrow \infty} \sum_{i \in N} V_{cl,i}^t(k) = \alpha_{cl,ij} (\Delta V_{cl,j}^t(k) - \Delta V_{cl,i}^t(k)) \\ \lim_{k \rightarrow \infty} \sum_{i \in N} L_i^t(k) = \alpha_{L,ij} (\Delta L_j^t(k) - \Delta L_i^t(k)) \\ \lim_{k \rightarrow \infty} \sum_{i \in N} P_i^t(k) = \alpha_{P,ij} (\Delta P_j^t(k) - \Delta P_i^t(k)) \\ \lim_{k \rightarrow \infty} \sum_{i \in N} W_i^t(k) = \alpha_{W,ij} (\Delta W_j^t(k) - \Delta W_i^t(k)) \\ \lim_{k \rightarrow \infty} \sum_{i \in N} E_i^t(k) = \alpha_{E,ij} (\Delta E_j^t(k) - \Delta E_i^t(k)) \end{array} \right. \quad (26)$$

Under a non-ideal communication environment, communication failure will lead to power deviation. The communication failure problem in the distributed iterative calculation process will have a cumulative impact on the coordinated operation results. Suppose there are two independent communication failure problems, one of which occurs when nodes i and j communicate with each other at iteration k_1 , and another

communication failure problem occurs when nodes i and j communicate with each other at iteration k_2 . It can be seen from equation (25) that the impact on coordinated operation is the addition of two communication failure problems in the communication process:

It can be seen from the update rules in Equations (22) and (23) that the local unbalanced power $\Delta P_i^t(k_1)$ of each node will be affected by the unbalanced power $\Delta P_j^t(k_1)$ ($j \in N_i$) of its adjacent nodes in each iteration. To indicate the impact on adjacent nodes, set a correction variable

$$\forall t \in T : \left\{ \begin{array}{l} \lim_{k \rightarrow \infty} \sum_{i \in N} V_{bl,i}^t(k) = \alpha_{bl,ij}(\Delta V_{bl,j}^t(k_1) - \Delta V_{bl,i}^t(k_1)) + \alpha_{bl,mn}(\Delta V_{bl,n}^t(k_2) - \Delta V_{bl,m}^t(k_2)) \\ \lim_{k \rightarrow \infty} \sum_{i \in N} V_{cl,i}^t(k) = \alpha_{cl,ij}(\Delta V_{cl,j}^t(k_1) - \Delta V_{cl,i}^t(k_1)) + \alpha_{cl,mn}(\Delta V_{cl,n}^t(k_2) - \Delta V_{cl,m}^t(k_2)) \\ \lim_{k \rightarrow \infty} \sum_{i \in N} L_i^t(k) = \alpha_{L,ij}(\Delta L_j^t(k_1) - \Delta L_i^t(k_1)) + \alpha_{L,mn}(\Delta L_n^t(k_2) - \Delta L_m^t(k_2)) \\ \lim_{k \rightarrow \infty} \sum_{i \in N} P_i^t(k) = \alpha_{ij}(\Delta P_j^t(k_1) - \Delta P_i^t(k_1)) + \alpha_{P,mn}(\Delta P_n^t(k_2) - \Delta P_m^t(k_2)) \\ \lim_{k \rightarrow \infty} \sum_{i \in N} W_i^t(k) = \alpha_{W,ij}(\Delta W_j^t(k_1) - \Delta W_i^t(k_1)) + \alpha_{W,mn}(\Delta W_n^t(k_2) - \Delta W_m^t(k_2)) \\ \lim_{k \rightarrow \infty} \sum_{i \in N} E_i^t(k) = \alpha_{E,ij}(\Delta E_j^t(k_1) - \Delta E_i^t(k_1)) + \alpha_{E,mn}(\Delta E_n^t(k_2) - \Delta E_m^t(k_2)) \end{array} \right. \quad (27)$$

3.3. Improvement of the consensus-distributed algorithm under communication failures

A series of communication failure problems that occurred in the communication process will produce serious local unbalanced power. In order to maintain the accuracy of system unbalanced power estimation, a correction variable is introduced in the iterative process to eliminate the impact of communication failure problems on the results of distributed coordinated operations.

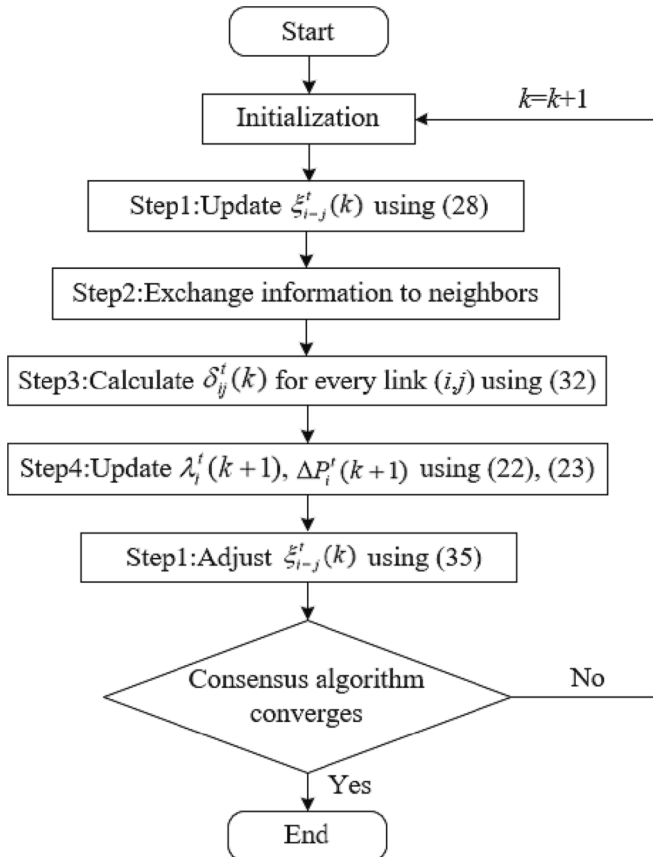


Fig. 3. Flowchart of the proposed improvement method.

$\xi_{i-j}^t(k)$:

$$\forall t \in T : \xi_{i-j}^t(k) = \begin{cases} \xi_{i-j}^t(k-1) + \alpha_{ij}(\Delta P_j^t(k-1) - \Delta P_i^t(k-1)), & j \in B_i(k-1) \\ \xi_{i-j}^t(k-1), & j \in A_i(k-1) \end{cases} \quad (28)$$

where $B_i(k-1)$ is the set of neighboring nodes that successfully transferred the information to node i at iteration $k-1$; $A_i(k-1)$ refers to the set of neighboring nodes that failed to transfer the information to node i accurately.

The modified variable $\xi_{i-j}^t(k)$ represents the change in the unbalanced power $\Delta P_i^t(k)$ due to the influence of the adjacent node j before the iteration is k . Before the iteration, there is no information exchange between adjacent nodes, so the value of the correction variable is:

$$\forall t \in T : \xi_{i-j}^t(0) = 0 \quad (29)$$

In an ideal communication environment, there is no data quality problem. It can be seen that:

$$\forall t \in T : \xi_{i-j}^t(k) + \xi_{j-i}^t(k) = \sum_{s=0}^{k-1} \alpha_{ij}((\Delta P_j^t(s) - \Delta P_i^t(s)) + (\Delta P_i^t(s) - \Delta P_j^t(s))) = 0 \quad (30)$$

However, in the actual communication environment, there will be more or less communication failures, namely $\xi_{i-j}^t(k) + \xi_{j-i}^t(k) \neq 0$. Therefore, the adjustment variable $\delta_{ij}^t(k)$ is set to adjust the local unbalanced power caused by communication failure:

$$\forall t \in T : \delta_{ij}^t(k) = \xi_{i-j}^t(k) + \xi_{j-i}^t(k) \quad (31)$$

Due to the addition of correction variables $\xi_{i-j}^t(k)$ in the information transmission, the node i receives $\xi_{j-i}^t(k)$ ($j \in N_i$) from its adjacent nodes and calculates $\delta_{ij}^t(k)$ for adjacent nodes (i,j) at iteration k . Under the adjustment of $\delta_{ij}^t(k)$, node i receives the error signal caused by the local communication failure. Node i uses $\delta_{ij}^t(k)$ to adjust the local unbalanced power $\Delta P_i^t(k+1)$ to ensure the accuracy of the system unbalanced power estimation. Fig. 3 shows the main steps of the proposed improvement method.

The details of adjusting the original update rules are described as follows:

Step 1: Considering the final result of information transmission under communication failure, use equation (26) to update the impact of

adjacent nodes.

Step 2: Exchange information with neighboring nodes, including consensus variables $\Delta P_i^t(k-1)$, $\lambda_i^t(k-1)$ and final auxiliary variables $\xi_{i-j}^t(k)$.

Step 3: Calculate the adjustment variable $\delta_{ij}^t(k)$ to master the final result of information transmission under communication failure:

$$\forall t \in T : \delta_{ij}^t(k) = \begin{cases} \xi_{i-j}^t(k) + \xi_{j-i}^t(k), & j \in B_i(k-1) \\ 0, & j \in A_i(k-1) \end{cases} \quad (32)$$

Step 4: Update consensus variables $\Delta P_i^t(k-1)$ and $\lambda_i^t(k-1)$ according to the following rules:

$$\begin{aligned} \forall t \in T : \Delta P_i^t(k+1) &= \Delta P_i^t(k) + \sum_{j \in B_i(k-1)} \alpha_{ij} (\Delta P_j^t(k-1) \\ &\quad - \Delta P_i^t(k-1)) + P_i^t(k+1) - P_i^t(k) - \sum_{j \in B_i(k-1)} \delta_{ij}^t(k) \end{aligned} \quad (33)$$

$$\forall t \in T : \lambda_i^t(k+1) = \lambda_i^t(k) + \sum_{j \in B_i(k-1)} \alpha_{ij} (\lambda_j^t(k-1) - \lambda_i^t(k-1)) + \omega \Delta P_i^t(k-1) \quad (34)$$

Step 5: At the end of each iteration, adjust the correction variable $\xi_{i-j}^t(k)$:

$$\forall t \in T : \xi_{i-j}^t(k) = \begin{cases} \xi_{i-j}^t(k-1) - \delta_{ij}^t(k), & j \in B_i(k-1) \\ \xi_{i-j}^t(k-1), & j \in A_i(k-1) \end{cases} \quad (35)$$

For two-way communication (i, j), nodes i and j have their own adjustment variables. Node i updates its adjustment variables $\delta_{ij}^t(k)$ to eliminate the impact of communication failure on information transmission between nodes i and j . Node j updates its corresponding adjustment variable $\delta_{ji}^t(k)$ to eliminate the impact of communication failures on information transmission between nodes j and i .

Compared with the unmodified, consistent, distributed algorithm, this method does not significantly increase the communication and computing burden. At each iteration, only one additional variable is added. For the increased calculation burden, the improved consistency algorithm also introduces only three updates, namely Formulas (28), (32), and (35).

In a non-ideal communication environment, the proposed improved consistent distributed algorithm is used to eliminate the imbalance between the supply and demand of system power, thus meeting the constraint of the supply and demand balance equation. It is hereby certified that:

The sum of the unbalanced powers of all nodes at iteration k is:

$$\begin{aligned} \forall t \in T : \sum_{i \in N} \Delta P_i^t(k+1) &= \sum_{i \in N} \Delta P_i^t(k) + \sum_{i \in N} \sum_{j \in B_i(k-1)} \alpha_{ij} (\Delta P_j^t(k-1) - \Delta P_i^t(k-1)) + \\ &\quad \sum_{i \in N} P_i^t(k+1) - \sum_{i \in N} P_i^t(k) - \sum_{i \in N} \sum_{j \in B_i(k-1)} \delta_{ij}^t(k) \end{aligned} \quad (36)$$

The second term of equation (36) can be expressed as follows:

$$\begin{aligned} \sum_{i \in N} \sum_{j \in B_i(k-1)} \alpha_{ij} (\Delta P_j^t(k-1) - \Delta P_i^t(k-1)) &= \sum_{j \in B_i(k-1)} \alpha_{ij} (\Delta P_j^t(k-1) - \Delta P_i^t(k-1) + \Delta P_i^t(k-1) - \Delta P_j^t(k-1)) + \\ &\quad \sum_{j \in B_i(k-1)} \alpha_{ij} (\Delta P_j^t(k-1) - \Delta P_i^t(k-1)) = 0 + \sum_{j \in B_i(k-1)} \alpha_{ij} (\Delta P_j^t(k-1) - \Delta P_i^t(k-1)) \\ &\quad \sum_{i \in A_j(k-1)} \alpha_{ij} (\Delta P_j^t(k-1) - \Delta P_i^t(k-1)) \end{aligned} \quad (37)$$

The last item of equation (36) can be expressed as follows:

$$\sum_{i \in N} \sum_{j \in B_i(k-1)} \delta_{ij}^t(k) = \sum_{\substack{j \in B_i(k-1), \\ i \in A_j(k-1)}} \alpha_{ij} (\Delta P_j^t(k-1) - \Delta P_i^t(k-1)) \quad (38)$$

Substituting equations (37) and (38) into (36), we can get

$$\forall t \in T : \sum_{i \in N} \Delta P_i^t(k+1) = \sum_{i \in N} \Delta P_i^t(k) + \sum_{i \in N} P_i^t(k+1) - \sum_{i \in N} P_i^t(k) \quad (39)$$

It can be seen that

$$\forall t \in T : \sum_{i \in N} \Delta P_i^t(k) = \sum_{i \in N} P_i^t(k) \quad (40)$$

According to equation (40), the total unbalanced power of all nodes is equal to the actual unbalanced power of the system.

Suppose that the local incremental cost $\lambda_i^t(k)$ eventually converges to a certain value $\varepsilon(t)$:

$$\forall t \in T : \lim_{k \rightarrow \infty} \lambda_i^t(k) = \varepsilon(t) \quad (41)$$

Considering the constraints on both sides of equation (22), it can be seen that

$$\begin{aligned} \forall t \in T : \varepsilon(t) &= \varepsilon(t) + \sum_{j \in B_i(k)} \alpha_{ij} (\varepsilon(t) - \varepsilon(t)) + \omega \lim_{k \rightarrow \infty} \Delta P_i^t(k) \Leftrightarrow \forall t \in T \\ &: \lim_{k \rightarrow \infty} \Delta P_i^t(k) = 0 \end{aligned} \quad (42)$$

Considering the constraints on both sides of equation (40), it can be seen that

$$\forall t \in T : \lim_{k \rightarrow \infty} \sum_{i \in N} P_i^t(k) = \lim_{k \rightarrow \infty} \sum_{i \in N} \Delta P_i^t(k) = \sum_{i \in N} 0 = 0 \quad (43)$$

According to the definition and extraction process of consensus variables, the power of each agent in the active distribution network is updated as follows:

$$\left\{ \begin{aligned} V_i^{\text{bl}}(k+1) &= \eta^{\text{bl}} [T_i^{\text{bl}}(k+1) - T_{\text{out},i}^{\text{bl}}]^2, T_i^{\text{bl}}(k+1) = \frac{k^{\text{bl}} T_s^{\text{bl}} + \eta^{\text{bl}} \lambda_{\text{bl},i}(k+1) T_{\text{out},i}^{\text{bl}}}{\eta^{\text{bl}} \lambda_{\text{bl},i}(k+1) + k^{\text{bl}}} \\ V_i^{\text{el}}(k+1) &= \eta^{\text{el}} [T_i^{\text{el}}(k+1) - T_{\text{out},i}^{\text{el}}]^2, T_i^{\text{el}}(k+1) = \frac{k^{\text{el}} T_s^{\text{el}} + \eta^{\text{el}} \lambda_{\text{el},i}(k+1) T_{\text{out},i}^{\text{el}}}{\eta^{\text{el}} \lambda_{\text{el},i}(k+1) + k^{\text{el}}} \\ L_i(k+1) &= \frac{\lambda_{f,i}(k+1) - b_{L,i}}{2a_{L,i}} \\ P_i(k+1) &= \frac{\lambda_{n,i}(k+1) - b_i}{2a_i} \\ W_i(k+1) &= \frac{\lambda_{w,i}(k+1)}{2k^w} + W_{i,\max} \\ E_i(k+1) &= \frac{\lambda_{\text{es},i}(k+1)}{2a_{\text{es},i}} \end{aligned} \right. \quad (44)$$

After the consensus variables are updated iteratively, it is necessary to calculate the power of the updated space heating EHLs, domestic hot water EHLs, non-electric heating flexible loads, thermal power units,

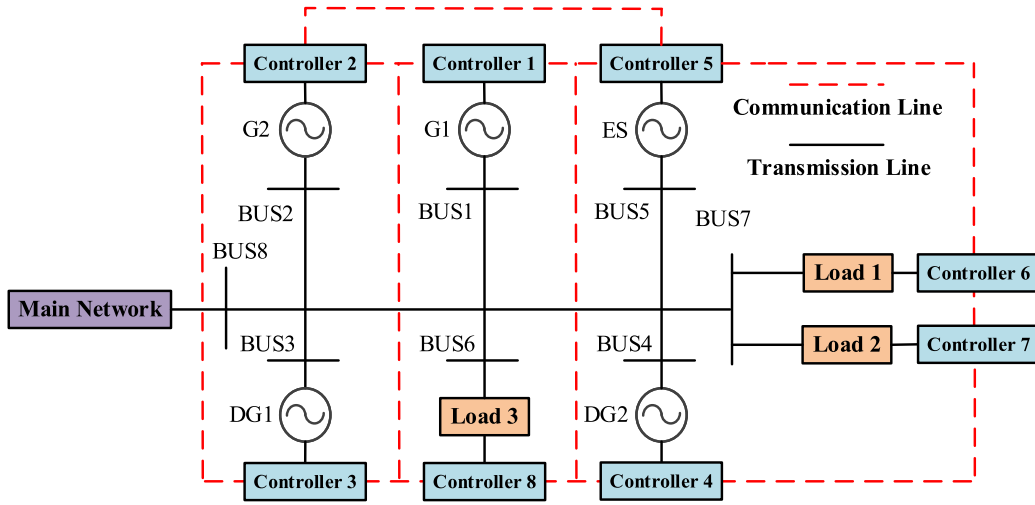


Fig. 4. Active distribution network communication topology (I).

Table 1
Relevant parameters.

Parameters	Value	Parameters	Value
k^{bl}	0.03	$P_{2,max}/MW$	120
k^{el}	0.02	$P_{1,min}/MW$	75
k^w	0.03	$P_{2,min}/MW$	55
$\eta^{bl}/(MW/^\circ C)$	0.8	E_{max}/MW	40
$\eta^{el}/(MW/^\circ C)$	0.6	E_{min}/MW	-40
L_{max}/MW	20	V_{max}^{bl}/MW	35
L_{min}/MW	5	V_{min}^{bl}/MW	2
$W_{g,1}/MW$	20	V_{max}^{el}/MW	30
$W_{g,2}/MW$	10	V_{min}^{el}/MW	1
$T_{max}^{bl}/^\circ C$	25	$W_{1,max}/MW$	60
$T_{max}^{el}/^\circ C$	60	$W_{1,min}/MW$	10
$T_{min}^{bl}/^\circ C$	21	$W_{2,max}/MW$	65
$T_{min}^{el}/^\circ C$	45	$W_{2,min}/MW$	15
$P_{1,max}/MW$	160	-	-

Table 2
Communication link failure rate.

Communication link	1 ↔ 2	1 ↔ 3	1 ↔ 4	1 ↔ 5	1 ↔ 8
Failure rate	0.1	0.1	0.1	0.15	0.15
Communication link	2 ↔ 3	2 ↔ 5	2 ↔ 8	3 ↔ 8	4 ↔ 5
Failure rate	0.15	0.2	0.2	0.2	0.25
Communication link	4 ↔ 7	4 ↔ 8	5 ↔ 6	5 ↔ 8	6 ↔ 7
Failure rate	0.25	0.25	0.3	0.3	0.3

new energy generating units, and energy storage devices according to equation (44). At the same time, it is necessary to judge whether V_i^{bl} , V_i^{el} , L_i , P_i , W_i , and E_i are out of bounds according to inequality constraints. If there is an out-of-limit situation, it is necessary to correct the out-of-limit power. Taking space heating EHLs power V_i^{bl} as an example, the inequality constraint is modified as follows:

$$V_i^{bl}(k+1) = \begin{cases} \eta^{bl}[T_i^{bl}(k+1) - T_{out,i}^{bl}]^2, & V_{i,min}^{bl} \leq \eta^{bl}[T_i^{bl}(k+1) - T_{out,i}^{bl}]^2 \leq V_{i,max}^{bl} \\ V_{i,max}^{bl}, & \eta^{bl}[T_i^{bl}(k+1) - T_{out,i}^{bl}]^2 > V_{i,max}^{bl} \\ V_{i,min}^{bl}, & \eta^{bl}[T_i^{bl}(k+1) - T_{out,i}^{bl}]^2 < V_{i,min}^{bl} \end{cases} \quad (45)$$

Inequality constraints on domestic hot water EHLs, non-electric heating flexible loads, thermal power units, new energy power generation units, and energy storage device agents are also modified according to the above method and will not be repeated.

Using the improved consensus distributed algorithm proposed in this paper, the final result satisfies the supply and demand balance constraints and inequality constraints in the original problem, and the final convergence of the incremental cost is consistent, indicating that the final result is the optimal solution.

4. Simulation and analysis

4.1. Example setting

To verify the effectiveness of the proposed consensus distributed coordinated operation method, a 5-machine active distribution network

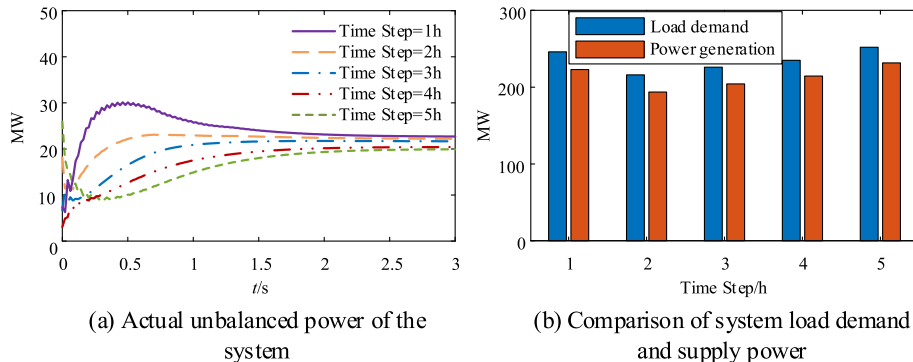


Fig. 5. Iteration process of system unbalanced power under traditional consistency method.

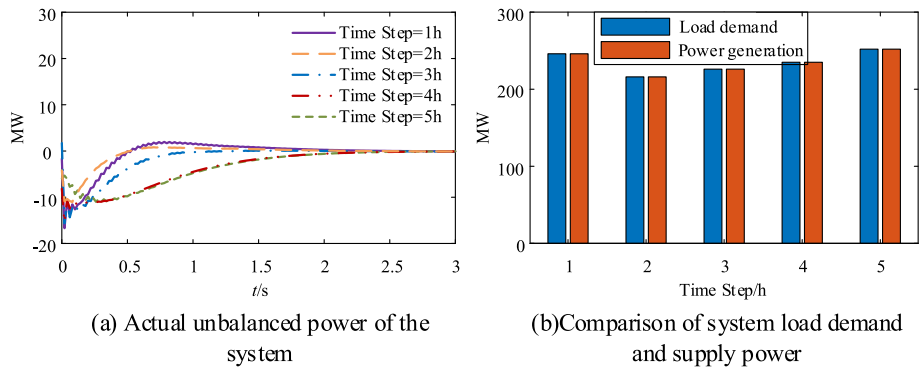


Fig. 6. Iteration process of system unbalanced power under improved consistency method.

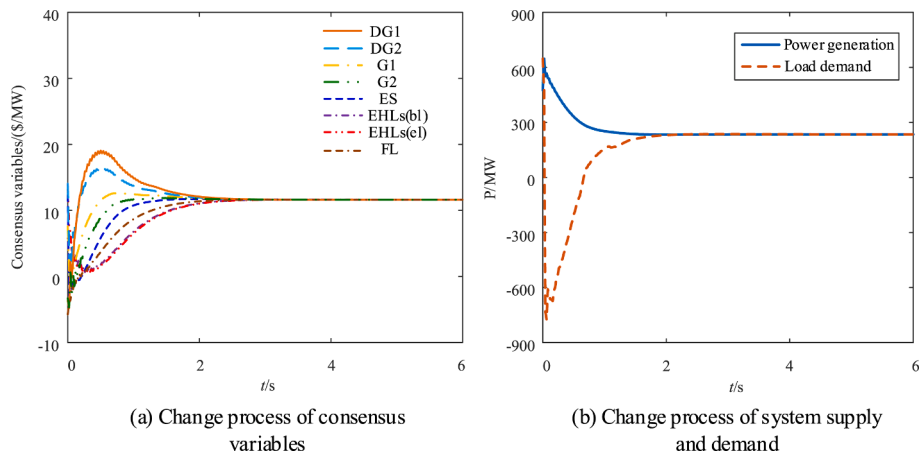


Fig. 7. Iteration process of system variables under scenario 1.

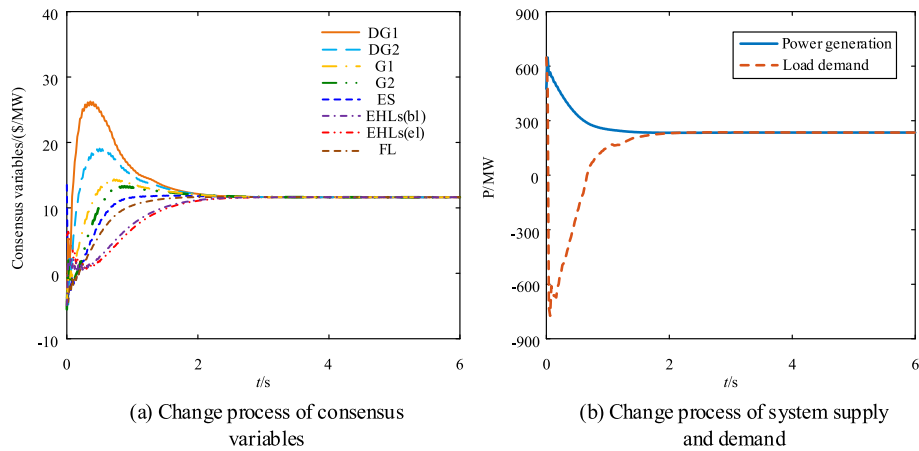


Fig. 8. Iteration process of system variables in scenario 2.

example system, as shown in Fig. 4, is built for simulation verification. Among them, G1 and G2 are conventional thermal power unit agents, DG1 and DG2 are new energy unit agents, ES is an energy storage agent, load 1 is a space heating electric heating load (EHLs (bl)) agent, load 2 is a domestic heating electric heating load (EHLs (el)) agent, and load 3 is a non-electric heating flexible load (FL) agent. T_s^{bl} is 23°C, T_s^{el} is 50°C, the initial load of the active distribution network is 200 MW, and other parameters are shown in Table 1.

4.2. Comparison of the actual unbalanced power of the system under communication failures

In order to verify the effectiveness of the proposed correction method for different communication failure rates, the probability of failure of different communication links is different. For example, a communication link 4 ↔ 5 is more susceptible to communication failure problems than a communication link 1 ↔ 4. The failure rates of each communication link are shown in Table 2. In case of communication failure, the iterative changes in the actual unbalanced power of the system before and after correction are shown in Figs. 5 and 6, respectively.

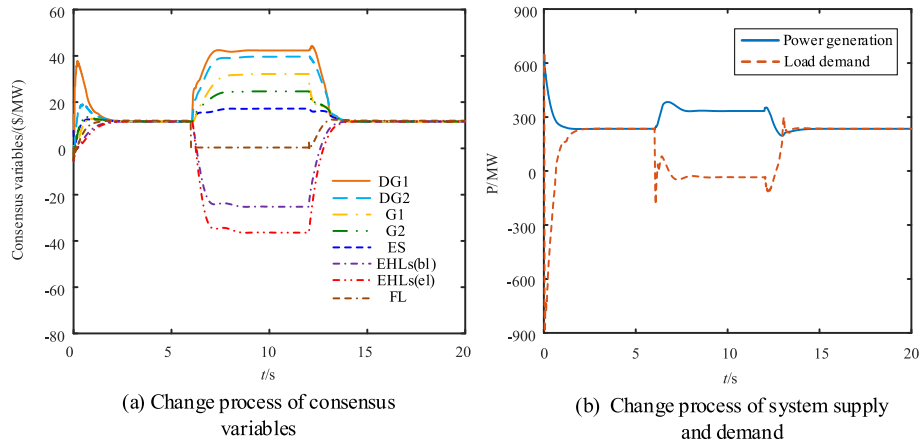


Fig. 9. Iteration process of system variables in scenario 3.

In order to facilitate the analysis, five scheduling periods are selected for analysis. By comparing Figs. 5 and 6, it can be seen that under the traditional consensus distribution method, the actual unbalanced power of the system does not converge to zero, and the supply power in each dispatching period is always less than the load demand, which indicates that there is a certain unbalance between the power supply and load demand of the system. After introducing the correction variable, the actual unbalanced power of the system finally converges to 0, and the supply power in each dispatching period is always equal to the load demand, indicating that the imbalance between supply and demand in the system is eliminated.

4.3. Improved consensus-distributed method testing

As shown in Table 2, when the communication link fails, four scenarios are set up to simulate and verify the effectiveness of the proposed improved consensus distributed operation method. Let the consensus convergence coefficient $be\omega = 0.005$, the sampling step Δk be 0.02 s, and the simulation calculation time be the product of iteration k and the sampling step Δk . When the centralized optimal operation method is adopted, $\lambda=11.64$ \$/MW corresponds to the optimal solution for system operation.

Scenario 1: The effectiveness of the improved consensus-distributed method

In Scenario 1, the effectiveness of the proposed consensus method of distributed operation for an active distribution network with an electric heating load is simulated, and the simulation results are shown in Fig. 7. Fig. 7 (a) shows the iterative change process of the consistency variable of each agent in the active distribution network, and Fig. 7 (b) shows the iterative change process of the generation power and load demand in the active distribution network.

It can be seen from Fig. 7 (a) that $\lambda = 11.64$ \$/MW corresponds to the optimal solution for system operation. When the calculation time is 3.92 s, that is, when the number of iterations is 196, the consensus variables of all agents converge to the best. It can be seen from Fig. 7 (b) that the final convergence results of the system's generation power and load demand remain balanced, and the consensus distributed method with the introduction of modified variables achieves the same results as the centralized optimal operation method. It shows that under the fully distributed optimization operation method, each agent can also obtain satisfactory optimization results by avoiding centralized communication.

Scenario 2: Range constraints of generator units and loads are considered

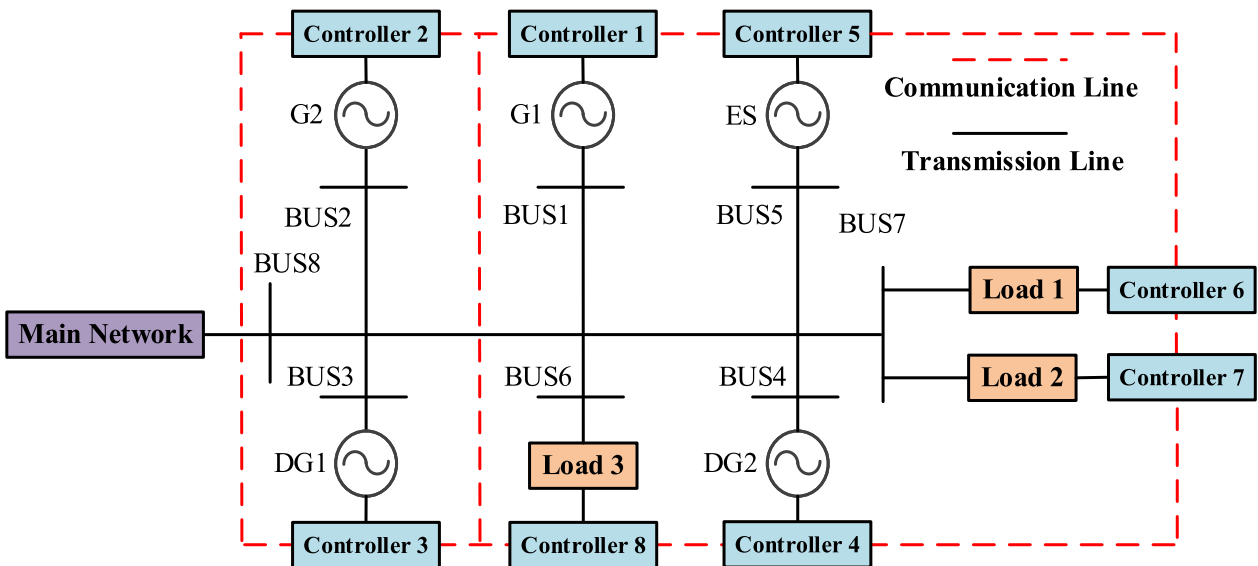


Fig. 10. Active distribution network communication topology (II).

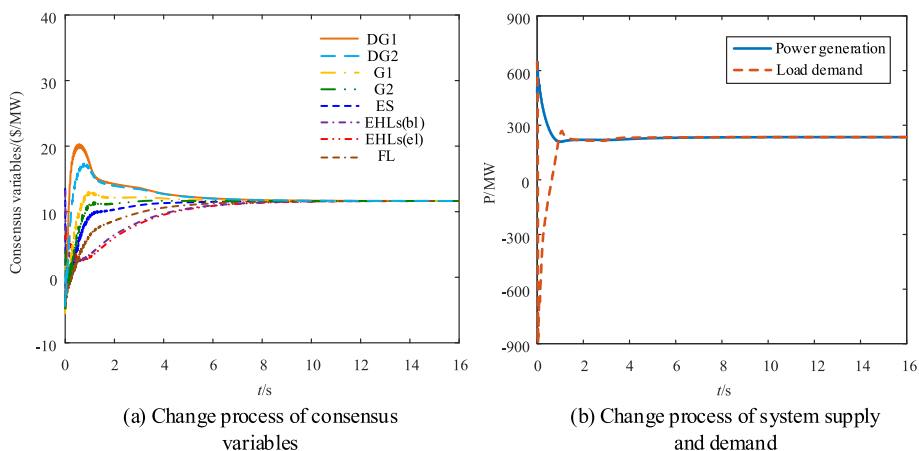


Fig. 11. Iteration process of system variables in scenario 4.

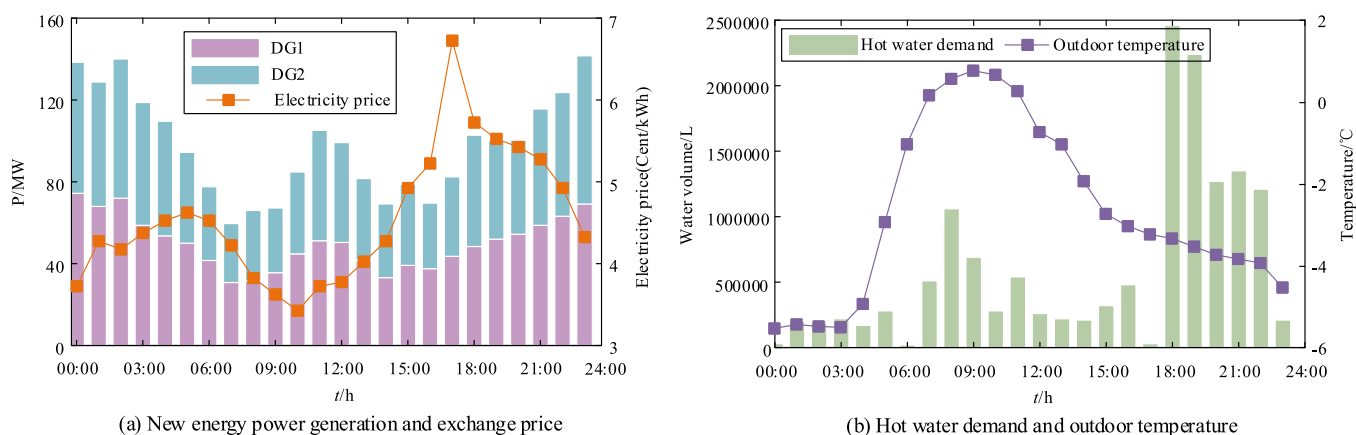


Fig. 12. Overview of typical days in winter.

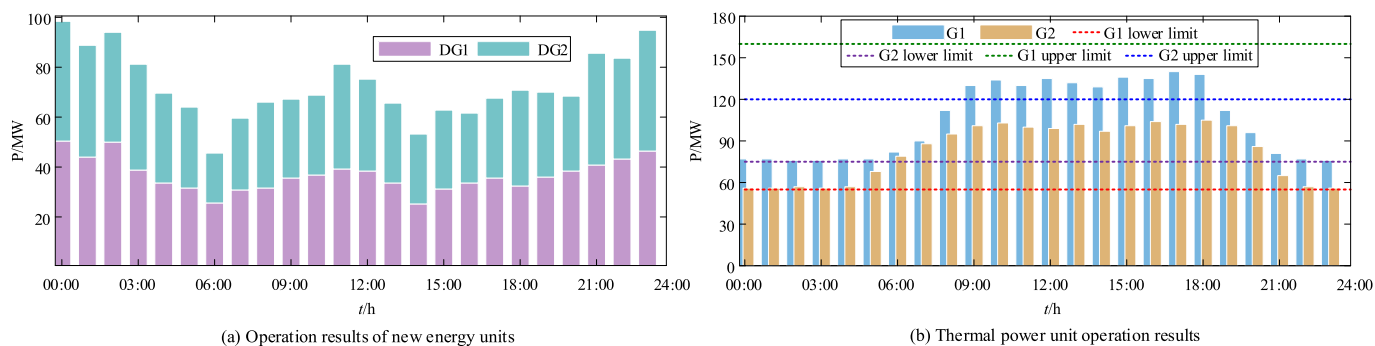


Fig. 13. Results of EHLs not participating in system-coordinated operation.

Table 3

Consumption of new energy electricity when EHLs do not participate in system coordination operation.

New energy unit	Electricity generation / MW-h	Grid-connected operating electricity /MW-h	The electricity of discarded wind and light /MW-h	The consumption rate of new energy / %
DG1	1204.32	883.31	321.01	73.35
DG2	1151.63	861.17	290.46	74.78
DG1 + DG2	2355.95	1744.48	611.47	74.05

In Scenario 2, considering the power inequality constraints of generator sets and various loads, the effectiveness of the consensus distributed operation method is simulated using the communication topology in Scenario 1. The simulation results are shown in Fig. 8.

It can be seen from Fig. 8 that when considering the power range constraints of various agents, such as space heating EHLs, domestic hot water EHLs, non-electric heating flexible loads, thermal power units, new energy generating units, and energy storage devices, the consensus variable corresponding to the optimal solution of the system operation can still converge to the best, that is, $\lambda=11.64$ \$/MW, and the supply and demand powers of the system can also converge to the equilibrium state.

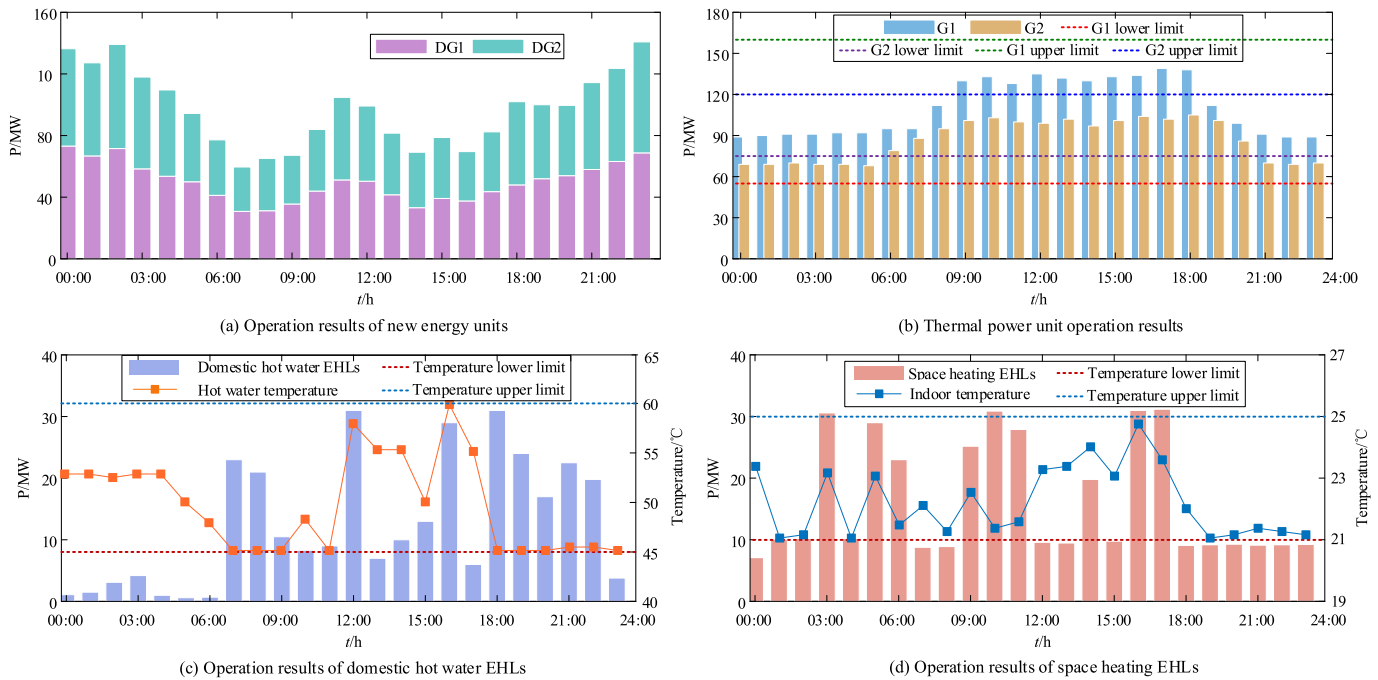


Fig. 14. Results of EHLs participating in system-coordinated operations.

Table 4

Consumption of new energy electricity when EHLs participate in system coordination operation.

New energy unit	Electricity generation / MW-h	Grid-connected operating electricity /MW-h	The electricity of discarded wind and light /MW-h	The consumption rate of new energy / %
DG1	1204.32	1197.45	6.87	99.43
DG2	1151.63	1147.31	4.32	99.62
DG1 + DG2	2355.95	2344.76	11.19	99.53

Scenario 3: “Plug and Play” function test

In Scenario 3, the “Plug and Play” function of the proposed consensus distributed operation method is simulated, and the simulation results are shown in Fig. 9. Using the communication topology in Scenario 1, when $t = 6$ s, the non-electric heating flexible load (FL) agent exits the operation; when $t = 12$ s, the FL agent is connected to the grid again.

It can be seen from Fig. 9 that when $t = 6$ s, the FL agent exits the power grid, and the consensus variable of each agent in the system runs to a new convergence value $\lambda = 11.66$ \$/MW; When $t = 12$ s, FL agent is connected to the grid again, and the consensus variable of each agent converges to the operation value before FL agent exits, that is, $\lambda=11.64$ \$/MW. At the same time, the supply and demand powers of the system converge on the equilibrium state. This shows that the proposed consensus distributed operation method can meet the “plug and play” function requirements of active distribution networks.

Scenario 4: Robustness of communication topology changes

In Scenario 4, the communication topology of the active distribution network is changed to verify the robustness of the proposed consensus distributed operation method with different communication topologies. The changed communication topology is shown in Fig. 10, and the simulation results are shown in Fig. 11.

It can be seen from Fig. 11 that although the communication topology of the active distribution network is different, the consensus variable can still converge to the optimal operation point, that is, $\lambda=11.64$ \$/MW, and the supply and demand power in the active distribution network can also converge to the equilibrium state. Compared with Scenarios 1–3, there are four fewer communication links ($1 \leftrightarrow 4, 2 \leftrightarrow 5, 4 \leftrightarrow 5, 5 \leftrightarrow 8$) in Scenario 4, so the communication conditions in Scenario 4 are worse than those in Scenarios 1–3. Although there are few communication links in Scenario 4, the communication topology still has connectivity and can eventually converge to the optimal value.

4.4. Analysis of distributed coordinated operation results

In order to verify the performance of the proposed consensus distributed operation method for an active distribution network with an electric heating load and also to illustrate the positive significance of EHLs and other active loads participating in system operation for new energy power consumption and system economic operation, two cases are designed to simulate and analyze the results before and after space heating EHLs and domestic hot water EHLs participated in system coordinated operation. The data on generating power of new energy units, power exchange price between the active distribution network and main network, hot water demand, and outdoor temperature on a typical day in winter are shown in Fig. 12.

Case 1: EHLs do not participate in the coordinated operation of the system

In Case 1, EHLs do not participate in the coordinated operation of the system. The coordinated operation results for new energy units and thermal power units are shown in Fig. 13, and the consumption of new energy power is shown in Table 3.

It can be seen from Fig. 13 (a) and Table 3 that when EHLs do not participate in the coordinated operation of the system due to the lack of flexibility of the system compared with the generating power of new energy units in Fig. 12 (a), there is a serious phenomenon of wind and light rejection. During the dispatching operation period, the wind and light rejections of DG1 and DG2 respectively reach 321.01 MW-h and

290.46 MW-h, and the new energy power consumption rate is only 74.05%. It can be seen from Fig. 13 (b) that in order to improve the system's situation by discarding wind and light and making room for new energy power, the operating power of conventional thermal power units G1 and G2 has also been forced to be limited. At 00:00–04:00 and 22:00–24:00, it is located near the lower limit of power for a long time. This mode of deep regulation will cause disadvantages and harm to the operation and maintenance of thermal power units.

Case 2: EHLs participate in the coordinated operation of the system

In Case 2, EHLs participate in the coordinated operation of the system. The coordinated operation results for new energy units, thermal power units, domestic hot water EHLs, and space heating EHLs are shown in Fig. 14, and the consumption of new energy power is shown in Table 4.

It can be seen from Fig. 14 (a) and Table 4 that when EHLs participate in the coordinated operation of the system, due to the strong flexibility of the system compared with the generating power of new energy units in Fig. 12 (a), the phenomenon of wind and light rejection has been greatly improved. During the dispatching operation period, the amount of wind and light rejection at DG1 and DG2 is only 6.87 MW-h and 4.32 MW-h, and the consumption rate of new energy power has been improved to 99.53%, which can be basically completely consumed. At the same time, it can be seen from Fig. 14 (b) that the improvement of system flexibility due to the participation of EHLs in coordinated operations can relieve the operating pressure of thermal power units to a certain extent, increase their output power, and improve the status of the long-term operations (such as 00:00–04:00 and 22:00–24:00) near the lower power limit. It can be seen from Fig. 14 (c) that during the operation time (such as 18:00–22:00) when the hot water demand is high and the electricity price is high, the domestic hot water EHLs will continue to operate so as to keep the temperature of the hot water not lower than the lower temperature limit (45°C). In Fig. 14 (d), the space heating EHLs stopped running when the electricity price was high, and the electricity price at 10:00 was the lowest during the whole day. The power value of space heating EHLs was high, so the indoor temperature quickly rose to 24.6°C, close to the upper-temperature limit (25°C).

5. Conclusion

Based on the consistency algorithm, a distributed coordinated operation method for active distribution networks with electric heating loads considering communication failures is proposed. The effectiveness of the proposed method is verified through simulation, and the following conclusions are obtained:

- (1) When a communication failure occurs in the system, after introducing a modified variable to improve the consensus-distributed method, the imbalance between supply and demand in the system is eliminated. Compared with the unmodified consensus-distributed method, this method does not significantly increase the communication and computing burdens, but only adds an additional variable in the iteration process.
- (2) After considering power constraints, the proposed improved consensus-distributed coordinated operation method can still obtain the same optimal solution as the centralized method when the network communication topology changes and can also meet the functional requirements of an active distribution network “plug and play”, indicating that the application scenario of the proposed method has strong robustness.
- (3) After participating in the coordinated operation of the system, electric heating loads will play a positive role in the consumption of new energy power and the economic operation of the system.
- (4) To avoid the negative impact of some bad data generated during operation on the consistency coordination of active distribution

networks, methods such as data mining and state estimation can be used to identify and correct the bad data. Subsequent research will be carried out in this direction.

CRediT authorship contribution statement

Shoudong Li: Conceptualization, Methodology, Data curation, Software, Writing - original draft. **Guangqing Bao:** Supervision. **Anan Zhang:** Validation.

Declaration of Competing Interest

The authors declare that they have no known competing financial interests or personal relationships that could have appeared to influence the work reported in this paper.

Data availability

No data was used for the research described in the article.

Acknowledgements

This work was supported in part by the Science and Technology Project of SGCC (52272220002T) and in part by the Central Government Funds for Guiding Local Scientific and Technological Development of China (2021ZYD0042).

References

- [1] Dehnavi G, Ginn HL. Distributed load sharing among converters in an autonomous microgrid including PV and wind power units. *IEEE Trans Smart Grid* 2019;10(4):4289–98.
- [2] Liu J, Cheng HZ, Zeng PL, Yao LZ. Rapid assessment of maximum distributed generation output based on security distance for interconnected distribution networks. *Int J Electr Power Energy Syst* 2018;101:13–24.
- [3] Yang J, Yuan WB, Sun Y, Han H, Hou XC, Guerrero JM. A novel quasi-master-slave control frame for pv-storage independent microgrid. *Int J Electr Power Energy Syst* 2018;97:262–74.
- [4] Li P, Wang ZX, Wang N, Yang WH, Li MZ, Zhou XC, et al. Stochastic robust optimal operation of community integrated energy system based on integrated demand response. *Int J Electr Power Energy Syst* 2021;128:106735.
- [5] Wang ZX, Hu JJ, Liu BZ. Stochastic optimal dispatching strategy of electricity-hydrogen-gas-heat integrated energy system based on improved spectral clustering method. *Int J Electr Power Energy Syst* 2021;126:106495.
- [6] Huang WJ, Zhang X, Li KP, Zhang N, Strbac G, Kang CQ. Resilience oriented planning of urban multi-energy systems with generalized energy storage sources. *IEEE Trans Power Syst* 2022;37(4):2906–18.
- [7] Masrur H, Shafie-Khah M, Hossain MJ, Senju T. Multi-energy microgrids incorporating EV integration: optimal design and resilient operation. *IEEE Trans Smart Grid* 2022;13(5):3508–18.
- [8] Kaluthanthrige R, Rajapakse AD. Demand response integrated day-ahead energy management strategy for remote off-grid hybrid renewable energy systems. *Int J Electr Power Energy Syst* 2021;129:106731.
- [9] Yang HJ, Zhang YY, Ma YH, Zhou M, Yang X. Reliability evaluation of power systems in the presence of energy storage system as demand management resource. *Int J Electr Power Energy Syst* 2019;110:1–10.
- [10] Seyedyazdi M, Mohammadi M, Farjah E. A combined driver-station interactive algorithm for a maximum mutual interest in charging market. *IEEE Trans Intell Transp Syst* 2020;21(6):2534–44.
- [11] Huang XZ, Xu ZF, Sun Y, Xue YL, Wang Z, Liu ZJ, et al. Heat and power load dispatching considering energy storage of district heating system and electric boilers. *J Modern Power Syst Clean Energy* 2018;5(6):992–1003.
- [12] Wang JD, Liu JX, Li CH, Zhou Y, Wu JZ. Optimal scheduling of gas and electricity consumption in a smart home with a hybrid gas boiler and electric heating system. *Energy* 2020;204:117951.
- [13] Zheng XY, Wei C, Qin P, Guo J, Yu YH, Song F, et al. Characteristics of residential energy consumption in China: findings from a household survey. *Energy Pol* 2014;75(14):126–35.
- [14] International Energy Agency (IEA). Energy balances of OECD countries, vol. 2014; 2014.
- [15] Yu L, Xie WW, Xie D. Deep reinforcement learning for smart home energy management. *IEEE Internet Things J* 2020;7(4):2751–62.
- [16] Su YX, Zhou Y, Tan M. An interval optimization strategy of household multi-energy system considering tolerance degree and integrated demand response. *Appl Energy* 2020;260:114144.

- [17] Chen XY, Kang CQ, O'Malley M, Xia Q, Bai JH, Liu C, et al. Increasing the flexibility of combined heat and power for wind power integration in China: Modeling and implications. *IEEE Trans Power Syst* 2015;30(4):1848–57.
- [18] Chen CY, Chen Y, Zhao JB, Zhang KF, Ni M, Ren B. Data-driven resilient automatic generation control against false data injection attacks. *IEEE Trans Industr Inform* 2021;17(12):8092–101.
- [19] Yu X, Xue Y. Smart grids: A cyber-physical systems perspective. *Proc IEEE* 2016; 104(5):1058–70.
- [20] Rahbari-Asr N, Zhang Y, Chow MY. Cooperative distributed scheduling for storage devices in microgrids using dynamic KKT multipliers and consensus networks. In: *Proc IEEE power energy soc gen conference*; 2015. p. 1–5.
- [21] Molzahn DK, Dorfler F, Sandberg H, Low SH, Chakrabarti S, Baldick R, et al. A survey of distributed optimization and control algorithms for electric power systems. *IEEE Trans Smart Grid* 2017;8(6):2941–62.
- [22] Zhao CC, He JP, Cheng P, Chen JM. Consensus-based energy management in smart grid with transmission losses and directed communication. *IEEE Trans Smart Grid* 2017;8(5):2049–61.
- [23] Guo FH, Wen CY, Mao JF, Song YD. Distributed economic dispatch for smart grids with random wind power. *IEEE Trans Smart Grid* 2016;7(3):1572–83.
- [24] Zhang W, Xu YL, Liu WX, Zang CZ, Yu HB. Distributed online optimal energy management for smart grids. *IEEE Trans Ind Informat* 2015;11(3):717–27.
- [25] Zhang Z, Chow MY. Convergence analysis of the incremental cost consensus algorithm under different communication network topologies in a smart grid. *IEEE Trans Power Syst* 2012;27(4):1761–8.
- [26] Binetti G, Davoudi A, Lewis FL, Naso D, Turchiano B. Distributed consensus-based economic dispatch with transmission losses. *IEEE Trans Power Syst* 2014;29(4): 1711–20.
- [27] Rahbari-Asr N, Zhang Y, Chow MY. Consensus-based distributed scheduling for cooperative operation of distributed energy resources and storage devices in smart grids. *IET Gener Transm Distrib* 2016;10(5):1268–77.
- [28] Ma K, Yu Y, Zhu S, Yang J, Guan X. Consensus based distributed algorithm for economic dispatch in power systems. In: *IEEE Int Conf Control Autom*; 2018. p. 544–9.
- [29] Zhang W, Liu WX, Wang X, Liu LM, Ferrese F. Online optimal generation control based on constrained distributed gradient algorithm. *IEEE Trans Power Syst* 2015; 30(1):35–45.
- [30] Kar S, Moura JMF. Sensor networks with random links: Topology design for distributed consensus. *IEEE Trans Signal Process* 2008;56(7):3315–26.
- [31] Wang SB, Meng XY, Chen TW. Wide-area control of power systems through delayed network communication. *IEEE Trans Control Syst Technol* 2012;20(2):495–503.
- [32] Zheng L, Lu N, Cai L. Reliable wireless communication networks for demand response control. *IEEE Trans Smart Grid* 2013;4(1):133–40.
- [33] Zhang WB, Tang Y, Huang TW, Kurths J. Sampled-data consensus of linear multi-agent systems with packet losses. *IEEE Trans Neural Netw Learn Syst* 2017;28(11): 2516–27.
- [34] Hamdi M, Chaoui M, Idoumghar L, Kachouri A. Coordinated consensus for smart grid economic environmental power dispatch with dynamic communication network. *IET Gener Transm Distrib* 2018;12(11):2603–13.
- [35] Wu JF, Yang T, Wu D, Kalsi K, Johansson KH. Distributed optimal dispatch of distributed energy resources over lossy communication networks. *IEEE Trans Smart Grid* 2017;8(6):3125–37.
- [36] Zhu JQ, Duan P, Liu MB, Xia YR, Guo Y, Mo XM. Bi-level real-time economic dispatch of VPP considering uncertainty. *IEEE Access* 2019;7:15282–91.
- [37] Xia SW, Bu SQ, Wan C, Lu X, Chan KW, Zhou B. A fully distributed hierarchical control framework for coordinated operation of DERs in active distribution power networks. *IEEE Trans Power Syst* 2019;34(6):5184–97.
- [38] Wang Y, Ai X, Tan ZF, Yan L, Liu ST. Interactive dispatch modes and bidding strategy of multiple virtual power plants based on demand response and game theory. *IEEE Trans Smart Grid* 2016;7(1):510–9.
- [39] Yong CS, Kong XY, Chen Y, E ZJ, Cui K, Wang X. Multiobjective scheduling of an active distribution network based on coordinated optimization of source network load. *Appl Sci* 2018; 8(10): 1888.
- [40] Singh AK, Singh R, Pal BC. Stability analysis of net-worked control in smart grids. *IEEE Trans Smart Grid* 2015;6(1):381–90.
- [41] Olfati-Saber R, Fax JA, Murray RM. Consensus and cooperation in networked multi-agent systems. *Proc IEEE* 2007;95(1):215–33.

Article

Distributed Coordinated Operation of Active Distribution Networks with Electric Heating Loads Based on Dynamic Step Correction ADMM

Shoudong Li ^{1,2}, Guangqing Bao ^{3,*} and Yanwen Hu ²

¹ School of Electrical and Information Engineering, Lanzhou University of Technology, Lanzhou 730050, China; lisd@mail.lzjtu.cn

² School of Automation and Electrical Engineering, Lanzhou Jiaotong University, Lanzhou 730070, China; huyw@mail.lzjtu.cn

³ School of Electronics and Information Engineering, Southwest Petroleum University, Chengdu 610500, China

* Correspondence: baogq@swpu.edu.cn

Abstract: In order to change the centralized operation framework of the active distribution network with electric heating loads (EHLs), a distributed optimization method is proposed for the coordinated operation of the active distribution network with EHLs. Firstly, considering the thermal delay effect and heat loss of the thermal system, a centralized optimization operation model for active distribution networks with EHLs is established. Then, based on the centralized optimization operation model, it is rephrased as a standard sharing problem, and a distributed optimization operation model for the EHL active distribution network is established based on the alternating direction multiplier method (ADMM) solution. In the process of solving ADMM, dynamic step correction was further considered. By updating the steps during the iteration process, the number of iterations was reduced, and the convergence and computational efficiency of ADMM were improved. Finally, the effectiveness of the distributed coordinated operation method proposed in this paper was simulated and verified by constructing an IEEE33 distribution system. The results showed that the proposed distributed coordinated operation method has strong robustness to the randomness of the number of distributed units and parameters, and EHLs participating in coordinated operation can expand the consumption space of wind power and photovoltaic power, and improve the economic efficiency of system operation.



Citation: Li, S.; Bao, G.; Hu, Y.

Distributed Coordinated Operation of Active Distribution Networks with Electric Heating Loads Based on Dynamic Step Correction ADMM.

Energies **2024**, *17*, 533. <https://doi.org/10.3390/en17020533>

Academic Editor: Andrea Mariscotti

Received: 15 December 2023

Revised: 11 January 2024

Accepted: 13 January 2024

Published: 22 January 2024



Copyright: © 2024 by the authors. Licensee MDPI, Basel, Switzerland. This article is an open access article distributed under the terms and conditions of the Creative Commons Attribution (CC BY) license (<https://creativecommons.org/licenses/by/4.0/>).

Keywords: active distribution network; distributed coordinated operation; electric heating loads; alternating direction multiplier method; dynamic step correction

1. Introduction

The increasing proportion of new energy generation and the integration of multiple types of loads have had a serious impact on the safe and stable operation of the power grid [1,2]. Flexible loads in active distribution networks are balanced between supply and demand through demand response technology [3,4], maintaining the safe and stable operation of the system in the event of disturbances or faults in the power grid [5,6]. The current scheduling operation of active distribution networks mainly improves the system's regulation ability by utilizing energy storage and flexible load demand response [7–9]. With the development of electric heating technology, EHLs have become a demand response resource with significant regulation ability on the load side [10]. EHLs mainly include two categories: space heating EHLs and domestic hot water EHLs [11]. Whether in European and American countries or China, space heating and domestic hot water production account for a large proportion of household energy consumption. In China, space heating accounts for 54% of household energy consumption and is the main source of household energy consumption. Hot water production accounts for 14% of household energy consumption, making it the third largest part of household energy consumption [12]. In

developed countries in Europe and America, the proportion of space heating and domestic hot water production in household energy consumption is 80% and 60%, respectively [13].

EHLs belong to clean heating methods, which use electricity to heat electric heating conversion equipment for user heating during periods of relatively low electricity prices. Compared with the heating method of configuring heat storage devices and coal-fired boilers, using EHLs for heating has significant advantages. The configuration of heat storage devices in cogeneration only reduces the coupling characteristic of heat to electricity in cogeneration units and does not generate new load space for the consumption of new energy electricity [14]. The use of EHLs for heating can not only maintain the stability of heating, but also reduce costs through the adjustment of market electricity prices, expand the consumption space of new energy from the load side, and have a positive effect on peak shaving and valley filling of the power grid. However, the distribution of EHLs is relatively scattered, with a variety of types and significant differences, making it difficult for EHLs to participate in the coordinated operation of active distribution networks. Therefore, using distributed methods to solve the coordinated operation problem of active distribution networks containing EHLs is of great significance for achieving safe and efficient operation of new energy power systems.

The scheduling operation of traditional power systems adopts a centralized operation mode, which is achieved through traditional planning methods and intelligent optimization algorithms. In the centralized operation mode, each distributed unit reports parameters and boundary conditions to the central controller responsible for coordination [15], obtains the optimal solution for coordinated operation through the centralized solving method, and transmits it to each distributed device. Due to the presence of a large number of distributed devices in the active distribution network, the centralized operation mode requires a large communication capacity and storage space. Once a central single point of failure occurs, it will cause the system to crash [16]. In addition, the submission of parameter and constraint information will expose the privacy of distributed unit owners. Therefore, it is necessary to achieve coordinated and optimized operation of active distribution networks with EHLs by shifting the operating mode from centralized to distributed. At present, the main methods for solving distributed optimization include Alternating Direction Multiplier Method (ADMM), Analysis Objective Cascading Method (ATC), Near End Message Passing Method (PMP), Auxiliary Problem Principle (APP), Optimality Condition Decomposition Method (OCD), and so on. The ATC usually requires the establishment of a higher-level coordination center that can grasp some boundary information. PMP, APP, and OCD do not require a higher-level coordination center and only rely on various regions to jointly complete information transmission and optimization calculations. However, their convergence is relatively poor, and the optimization results obtained may not be ideal. ADMM has a natural decoupling structure and stable convergence performance and has been widely used in distributed optimization operations of energy systems [17–19]. Reference [20] conducted research on the coordinated operation of power and natural gas systems based on ADMM. A decentralized optimal power flow method is proposed in reference [21] to reduce the communication burden between multiple integrated energy systems. Reference [22] established a day-ahead optimization scheduling model for the integrated energy system of electricity and natural gas and used an improved ADMM solution model to obtain the minimum operating cost.

In the above references, the interaction between different energy systems is only coupled through gas turbine units or cogeneration units. However, at the level of active distribution networks with EHLs, the coupling of multi-vector energy may be more complex. This operation involves the collaborative optimization of different forms of energy, including electricity and heat. The central operator is responsible for managing this operation. Meanwhile, with the continuous increase in various coupling devices, there are more and more operational entities in active distribution networks with EHLs. Therefore, the original ADMM cannot be directly applied to active distribution networks with EHLs, and the interaction between energy demand and the power grid should be addressed.

Meanwhile, as the scale of distributed units in the system increases, the central coordinator in the distributed framework is expected to incur more communication costs. In addition, with the increase in data exchange, communication failures have become increasingly common. Therefore, it is necessary to propose a distributed operation framework to reduce the communication pressure of the system and achieve coordinated operation of active distribution networks with EHLs. In order to address these issues, the contributions made in this article are as follows:

- (1) Considering the thermal delay effect and heat loss of the thermal system, the centralized optimization operation model of active distribution networks containing EHLs is formulated as a standard sharing problem, and a distributed optimization operation model of EHLs active distribution networks based on ADMM solution is established.
- (2) The iterative process is improved by dynamically updating the step, which results in fewer iterations and better convergence performance compared to the original ADMM. In addition, this method can not only obtain the optimal solution with the minimum number of iterations under normal operation but also obtain the optimal solution with the minimum number of iterations in the case of communication failures.
- (3) The effectiveness of the distributed coordinated operation method proposed in this paper was simulated and verified by constructing an IEEE33 distribution system. The results showed that the proposed distributed coordinated operation method has strong robustness to the randomness of the number of distributed units and parameters. Moreover, EHLs participating in coordinated operation can expand the consumption space of wind power and photovoltaic power, and improve the economic efficiency of system operation.

2. Centralized Optimal Operation Model for Active Distribution Networks with EHLs

Due to the existence of electrothermal coupling characteristics in active distribution networks with EHLs, in order to obtain a reliable operation plan, it is necessary to consider the thermal delay effect and heat loss of the thermal system when establishing an optimized operation model for active distribution networks with EHLs. Firstly, establish a centralized optimization operation model for active distribution networks with EHLs, and then rephrase it as a standard sharing problem based on the centralized optimization operation model. Finally, establish a distributed optimization operation model for active distribution networks with EHLs based on ADMM.

The centralized optimization of active distribution networks with EHLs is based on the power constraints of each distributed unit in the virtual power plant, taking into account the day-ahead load forecasting and real-time price, to achieve the minimum comprehensive operation cost of active distribution networks with EHLs.

2.1. Objective Function

The Equation (1) is shown as below:

$$\min \sum_{i=1}^N (C_i^G + C_i^{\text{CHP}} + C_i^{\text{WF}} + C_i^{\text{PV}} + C_i^{\text{EHLs}} + C_i^{\text{EP}}) \quad (1)$$

where N is the total number of virtual power plants in the active distribution network. C_i^G , C_i^{CHP} , C_i^{WF} , C_i^{PV} and C_i^{EHLs} are the operating costs of conventional units, Cogeneration units, wind turbine units, photovoltaic generator units, and EHLs in virtual power plant

i , respectively. C_i^{EP} is the cost of purchasing energy for virtual power plant i from other virtual power plants, that is, the cost of energy sharing.

$$\begin{cases} C_i^{\text{G}} = \sum_{t=1}^T U_{i,t} [f(P_{i,t}^{\text{G}}) + (1 - U_{i,t-1})S_i], f(P_{i,t}^{\text{G}}) = a_i(P_{i,t}^{\text{G}})^2 + b_i P_{i,t}^{\text{G}} + c_i \\ C_i^{\text{WF}} = \sum_{t=1}^T \kappa_i^{\text{WF}} P_{i,t}^{\text{WF}} \\ C_i^{\text{PV}} = \sum_{t=1}^T \kappa_i^{\text{PV}} P_{i,t}^{\text{PV}} \\ C_i^{\text{EP}} = \sum_{t=1}^T [\rho_t^{\text{EE}} (P_{i,t}^{\text{EE,P}} - P_{i,t}^{\text{EE,S}}) + \rho_t^{\text{HE}} (H_{i,t}^{\text{HE,P}} - H_{i,t}^{\text{HE,S}})] \end{cases} \quad (2)$$

where T is the total number of running periods. $P_{i,t}^{\text{G}}$ is the generating power of conventional units in virtual power plant i in period t . A represents the cost of changing the operating status of a conventional unit from static to operational during time t . $U_{i,t}$ is the operating status of conventional units in period t ; $U_{i,t} = 1$ and $U_{i,t} = 0$ represent the operating and shutdown states, respectively. S_i is the start-up cost for conventional units. $f(P_{i,t}^{\text{G}})$ is the power generation cost of conventional units in period t . a_i , b_i and c_i are the generation cost coefficient of conventional units. $P_{i,t}^{\text{WF}}$ and $P_{i,t}^{\text{PV}}$ are the output of wind power and photovoltaic generator units of virtual power plant i in period t . κ_i^{WF} and κ_i^{PV} is the output maintenance cost coefficient of wind power and photovoltaic generator units in virtual power plant i . ρ_t^{EE} and ρ_t^{HE} are the energy sharing prices of the virtual power plant in the active distribution network, representing electric energy and thermal energy respectively. $P_{i,t}^{\text{EE,P}}$ and $P_{i,t}^{\text{EE,S}}$ are, respectively, the power received and provided by virtual power plant i for energy sharing in period t . $H_{i,t}^{\text{HE,P}}$ and $H_{i,t}^{\text{HE,S}}$ are respectively the heat received and provided by virtual power plant i for energy sharing in period t .

$$C_i^{\text{CHP}} = \sum_{t=1}^T [k_{i,1} + k_{i,2} P_{i,t}^{\text{CHP}} + k_{i,3} H_{i,t}^{\text{CHP}} + k_{i,4} (P_{i,t}^{\text{CHP}})^2 + k_{i,5} (H_{i,t}^{\text{CHP}})^2 + k_{i,6} P_{i,t}^{\text{CHP}} H_{i,t}^{\text{CHP}}] \quad (3)$$

where $k_{i,1}$, $k_{i,2}$, $k_{i,3}$, $k_{i,4}$, $k_{i,5}$ and $k_{i,6}$ are the operating cost coefficients of cogeneration units in virtual power plant i . $P_{i,t}^{\text{CHP}}$ and $H_{i,t}^{\text{CHP}}$ are the electrical output and thermal output of cogeneration units in virtual power plant i in period t .

EHLs consider the thermal inertia and thermal delay effects of the thermal system while meeting user comfort and operational constraints, and fully tap into the regulatory potential of EHLs.

$$C_i^{\text{EHLs}} = \sum_{t=1}^T \lambda_{e,h,i,t}^{\text{EHLs}} P_{i,t}^{\text{EHLs}} \quad (4)$$

where, $P_{i,t}^{\text{EHLs}}$ is the active power of EHLs in virtual power plant i in period t . $\lambda_{e,h,i,t}^{\text{EHLs}}$ is the compensation price for EHLs.

According to the Weber–Fechner law, a more effective and reasonable pricing method is determined, specifically expressed as:

$$\lambda_{e,h,t}^{\text{EHLs}} = \lambda_{e,h} \cdot \ln(\rho_{e,h,t}) + K \quad (5)$$

where the compensation price $\lambda_{e,t}^{\text{EHLs}}$ of EHLs in the power system is related to the electricity price $\rho_{e,t}$, while the compensation price $\lambda_{h,t}^{\text{EHLs}}$ of EHLs in the thermal system is related to the heating price; $\lambda_{e,h}$ is the compensation coefficient of electrothermal coupled EHLs, taken as 0.5. The constant K is generally taken as 1 based on the experience of Weber-Fechner law.

According to the coordinated operation requirements of the system, the actual controlled EHLs during the t period can be expressed as follows in Equation (4):

$$P_{i,t}^{\text{EHLs}} = \sum_{i=1}^N s_{i,t} P_{i,\max}^{\text{EHLs}}, s_{i,t} \in [0, 1] \quad (6)$$

where $P_{i,\max}^{\text{EHLs}}$ is the maximum regulating power of EHLs in virtual power plant i . $s_{i,t}$ is the regulation rate.

For rebound loads, there is currently no precise mathematical model to describe them, and a three-stage autoregressive model is generally used to fit them as follows:

$$P_{b,i,t}^{\text{EHLs}} = \alpha P_{i,t-1}^{\text{EHLs}} + \beta P_{i,t-2}^{\text{EHLs}} + \gamma P_{i,t-3}^{\text{EHLs}} \quad (7)$$

where $P_{b,i,t}^{\text{EHLs}}$ is the rebound load of EHLs in virtual power plant i in period t . $P_{i,t-1}^{\text{EHLs}}$, $P_{i,t-2}^{\text{EHLs}}$ and $P_{i,t-3}^{\text{EHLs}}$ are the regulated power of EHLs in period $t-1$, $t-2$, and $t-3$, respectively. α , β and γ are the rebound coefficients.

2.2. Constraints

2.2.1. Power Balance Constraints

The Equation (8) is shown as below:

$$P_{i,t}^{\text{G}} + P_{i,t}^{\text{CHP}} + P_{i,t}^{\text{WF}} + P_{i,t}^{\text{PV}} + (P_{i,t}^{\text{EE,P}} - P_{i,t}^{\text{EE,S}}) = P_{i,t}^{\text{load}} + P_{i,t}^{\text{EHLs}} \quad (8)$$

where $P_{i,t}^{\text{load}}$ is the load of virtual power plant i in period t .

2.2.2. Thermal Power Balance Constraints Considering Thermal Loss and Thermal Delay Effects

The Equations (9) and (10) are shown as below:

$$H_{i,t}^{\text{CHP}} + H_{i,t}^{\text{EHLs}} + (H_{i,t}^{\text{HE,P}} - H_{i,t}^{\text{HE,S}}) - H_{i,t-TD}^{\text{loss}} = H_{i,t}^{\text{load}} \quad (9)$$

$$H_{i,t}^{\text{loss}} = \eta_{i,t}^{\text{loss}} (H_{i,t}^{\text{CHP}} + H_{i,t}^{\text{EHLs}}) \quad (10)$$

where $H_{i,t}^{\text{load}}$ is the thermal load of virtual power plant i in period t . $H_{i,t}^{\text{CHP}}$ and $H_{i,t}^{\text{EHLs}}$ are the heating capacity of cogeneration units and EHLs in virtual power plant i in time period t , respectively. $H_{i,t-TD}^{\text{loss}}$ is the heat loss when virtual power plant i supplies heat to the user in time period t . TD is the delay time of heat transfer, which depends on the parameters of heat pipes. $\eta_{i,t}^{\text{loss}}$ is the heat loss coefficient of the thermal system. Constraint (9) considers the heat loss and thermal delay effects of the thermal system.

2.2.3. Conventional Unit Operation Constraints

The Equation (11) is shown as below:

$$P_{i,\min}^{\text{G}} \leq P_{i,t}^{\text{G}} \leq P_{i,\max}^{\text{G}} \quad (11)$$

where $P_{i,\max}^{\text{G}}$ and $P_{i,\min}^{\text{G}}$ are the upper and lower limits of conventional unit output.

$$\begin{cases} (U_{i,t-1} - U_{i,t}) (T_{i,t}^{\text{on}} - T_{i,\min}^{\text{on}}) \geq 0 \\ (U_{i,t} - U_{i,t-1}) (T_{i,t}^{\text{off}} - T_{i,\min}^{\text{off}}) \geq 0 \end{cases} \quad (12)$$

where $T_{i,t}^{\text{on}}$ and $T_{i,t}^{\text{off}}$, respectively, represent the continuous start and stop times of conventional units. $T_{i,\min}^{\text{on}}$ and $T_{i,\min}^{\text{off}}$ are the minimum continuous start and stop times for conventional units. Equation (12) represents the minimum start and stop time constraint for conventional units.

2.2.4. Operation Constraints of Cogeneration Units

The feasible range of output of cogeneration units is shown in Figure 1.

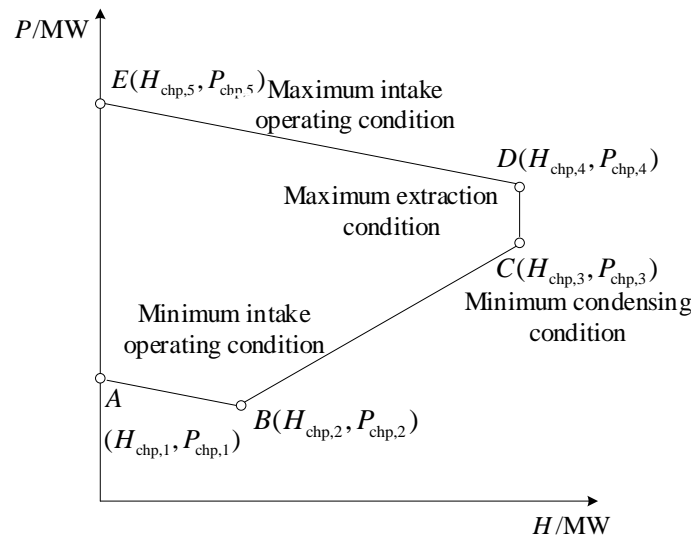


Figure 1. Cogeneration output feasibility region.

The operation of cogeneration units shall be included in the feasible range of output:

$$\begin{cases} P_{i,t}^{CHP} = \sum_{k \in S_{chp}} \eta_{k,i,t} P_k^{CHP} \\ H_{i,t}^{CHP} = \sum_{k \in S_{chp}} \eta_{k,i,t} H_k^{CHP} \\ \sum_{k \in S^{CHP}} \eta_{k,i,t} = 1 \\ 0 \leq \eta_{k,i,t} \leq 1, \forall k \in S^{CHP} \end{cases} \quad (13)$$

where P_k^{CHP} and H_k^{CHP} are the extreme points of cogeneration power and thermal output range, respectively. $\eta_{k,i,t}$ is the output coefficient of the extreme point. S^{CHP} is the set of vertices in the feasible region of output.

2.2.5. Operational Constraints for Wind and Photovoltaic Power Generation

The Equations (14) and (15) are shown as below:

$$0 \leq P_{i,t}^{WF} \leq P_{i,t,max}^{WF} \quad (14)$$

$$0 \leq P_{i,t}^{PV} \leq P_{i,t,max}^{PV} \quad (15)$$

where $P_{i,t,max}^{WF}$ and $P_{i,t,max}^{PV}$, respectively, represent the predicted power of wind and photovoltaic power generation.

2.2.6. EHLs Operational Constraints

The Equation (16) is shown as below:

$$P_{i,t,min}^{EHLs} U_{i,t}^{EHLs} \leq P_{i,t}^{EHLs} \leq P_{i,t,max}^{EHLs} U_{i,t}^{EHLs} \quad (16)$$

where $P_{i,t,min}^{EHLs}$ and $P_{i,t,max}^{EHLs}$ are, respectively, the minimum and maximum controlled quantities of EHLs participating in regulation in virtual power plant i in period t . $U_{i,t}^{EHLs}$ is the state variable of EHLs. $U_{i,t}^{EHLs} = 1$ indicates that they are in a controlled state and

$U_{i,t}^{\text{EHLs}} = 0$ indicates that they are not controlled. Equation (16) represents the controlled quantity constraint of EHLs.

$$\sum_{t=k}^{k+T_{\min}^{\text{EHLs}}-1} U_t^{\text{EHLs}} \geq T_{\min}^{\text{EHLs}} (U_k^{\text{EHLs}} - U_{k-1}^{\text{EHLs}}) \quad (17)$$

$$k = 1, \dots, T - T_{\min}^{\text{EHLs}} + 1$$

$$\sum_{t=k}^T (U_t^{\text{EHLs}} - U_k^{\text{EHLs}} + U_{k-1}^{\text{EHLs}} U_t^{\text{EHLs}}) \geq 0 \quad (18)$$

$$k = T - T_{\min}^{\text{EHLs}} + 2, \dots, T$$

$$\sum_{t=k}^{k+T_{\max}^{\text{EHLs}}} U_t^{\text{EHLs}} \geq T_{\max}^{\text{EHLs}}, k = 1, \dots, T - T_{\max}^{\text{EHLs}} \quad (19)$$

$$\sum_{t=1}^T (1 - U_{t-1}^{\text{EHLs}}) U_t^{\text{EHLs}} \leq N^{\text{EHLs}} \quad (20)$$

where T_{\min}^{EHLs} and T_{\max}^{EHLs} are the minimum and maximum interruptible duration of EHLs participating in regulation. N^{EHLs} is the maximum number of actions required for EHLs to participate in regulation. Equations (17) and (18) represent the minimum interruptible duration constraint for EHLs. Equation (19) represents the maximum interruptible duration constraint for EHLs. Equation (20) represents the number of interruption constraints for EHLs.

2.2.7. Energy Sharing Constraints

The Equations (21) and (22) are shown as below:

$$\begin{cases} 0 \leq P_{i,t}^{\text{EE,P}} \leq U_{i,t}^{\text{EE,P}} P_{i,\max}^{\text{EE,P}} \\ 0 \leq P_{i,t}^{\text{EE,S}} \leq U_{i,t}^{\text{EE,S}} P_{i,\max}^{\text{EE,S}} \\ U_{i,t}^{\text{EE,P}} + U_{i,t}^{\text{EE,S}} \leq 1 \\ \sum_{i=1}^N P_{i,t}^{\text{EE,P}} = \sum_{i=1}^N P_{i,t}^{\text{EE,S}} \end{cases} \quad (21)$$

$$\begin{cases} 0 \leq H_{i,t}^{\text{HE,P}} \leq U_{i,t}^{\text{HE,P}} H_{i,\max}^{\text{HE,P}} \\ 0 \leq H_{i,t}^{\text{HE,S}} \leq U_{i,t}^{\text{HE,S}} H_{i,\max}^{\text{HE,S}} \\ U_{i,t}^{\text{HE,P}} + U_{i,t}^{\text{HE,S}} \leq 1 \\ \sum_{i=1}^N H_{i,t}^{\text{HE,P}} = \sum_{i=1}^N H_{i,t}^{\text{HE,S}} \end{cases} \quad (22)$$

where $P_{i,\max}^{\text{EE,P}}$ and $P_{i,\max}^{\text{EE,S}}$ are the maximum electric power received and provided by virtual power plant i , respectively. $U_{i,t}^{\text{EE,P}}$ and $U_{i,t}^{\text{EE,S}}$ are the 0-1 state variables for receiving and providing electric power for virtual power plant i , respectively. $H_{i,\max}^{\text{HE,P}}$ and $H_{i,\max}^{\text{HE,S}}$ are the maximum thermal power received and provided for virtual power plant i , respectively. $U_{i,t}^{\text{HE,P}}$ and $U_{i,t}^{\text{HE,S}}$ are the 0-1 state variables for receiving and providing thermal power for virtual power plant i , respectively.

3. Distributed Optimal Operation Model for Active Distribution Networks with EHLs

The centralized optimal operation model requires all Virtual power plants to directly provide trade secret data. In most cases, virtual power plants participating in system operation may belong to different interest groups, and it is difficult to fully realize information sharing in actual operation. Directly providing data will cause data privacy disclosure. However, ADMM is used to solve the optimal operation model for active distribution networks with EHLs in a distributed manner, then the commercial privacy data of each virtual power plant can be protected. In addition, the SOCP-based AC power flow model shown in

Equations (24)–(31) is used to simulate active distribution networks with EHLs. To address the above issues, based on the ADMM, the centralized optimization operation model for active distribution networks with EHLs is rephrased as a standard sharing problem, as shown in Equations (23)–(36).

$$\begin{cases} \min \sum_{i \in N} (C_i^G + C_i^{\text{CHP}} + C_i^{\text{WF}} + C_i^{\text{PV}} + C_i^{\text{EHLs}} + C_i^{\text{EP}}) \\ \text{s.t. (8) - (9), (11) - (22), (24) - (33)} \end{cases} \quad (23)$$

$$\begin{cases} \sum_{n \in I(i)} P_{in,t} - (P_{ij,t} - R_{ij}L_{ij,t}) = P_{i,t}^{\text{net}}, \forall i \in N \\ \sum_{n \in I(i)} P_{in,t} - (P_{ij,t} - R_{ij}L_{ij,t}) = 0, \forall i \in I/N \end{cases} \quad (24)$$

$$\sum_{n \in I(i)} Q_{in,t} - (Q_{ij,t} - X_{ij}L_{ij,t}) = 0, \forall i \in I \quad (25)$$

$$V_{i,t} - 2(R_{ij}P_{ij,t} + X_{ij}Q_{ij,t}) + (R_{ij}^2 + X_{ij}^2)L_{ij,t} = V_{j,t}, \forall (i, j) \in M \quad (26)$$

$$\left\| \begin{matrix} 2P_{ij,t} \\ 2Q_{ij,t} \\ L_{ij,t} - V_{i,t} \end{matrix} \right\|_2 \leq L_{ij,t} + V_{i,t}, \forall (i, j) \in M \quad (27)$$

$$\begin{cases} \sum_{n \in N} P_{1n,t} = P_t^{\text{EM}} \\ \sum_{n \in N} Q_{1n,t} = Q_t^{\text{EM}} \end{cases} \quad (28)$$

$$|Q_t^{\text{EM}}| \leq P_t^{\text{EM}} \tan \varphi^{\text{EM}} \quad (29)$$

$$U_{i,\min}^2 \leq V_{i,t} \leq U_{i,\max}^2 \quad (30)$$

$$0 \leq L_{ij,t} \leq I_{ij,\max}^2, \forall (i, j) \in M \quad (31)$$

$$P_{i,t}^{\text{net}} = P_{i,t}^G + P_{i,t}^{\text{CHP}} + P_{i,t}^{\text{WF}} + P_{i,t}^{\text{PV}} - P_{i,t}^{\text{load}} - P_{i,t}^{\text{EHLs}} \quad (32)$$

$$H_{i,t}^{\text{net}} = H_{i,t}^{\text{CHP}} + H_{i,t}^{\text{EHLs}} - H_{i,t}^{\text{loss-TD}} - H_{i,t}^{\text{load}} \quad (33)$$

where I is the set of nodes in the active distribution network. I/N refers to the set of nodes excluding those connected to the virtual power plant. M is the collection of distribution lines. $L_{ij,t}$ is the square amplitude of the current of the distribution line (i, j) in period t . $V_{i,t}$ is the squared amplitude of the voltage at node i in period t . R_{ij} and X_{ij} , respectively, refer to the resistance and reactance of distribution lines (i, j) . φ^{EM} is the power factor of the virtual power plant. $P_{i,t}^{\text{net}}$ is the net power output of virtual power plant i in period t . $H_{i,t}^{\text{net}}$ is the net thermal output of virtual power plant i in period t . Constraints (24) and (25) represent the active and reactive power balance of each node, respectively. Constraint (26) describes the voltage drop of the distribution line. Constraint (27) provides second-order cone relaxation for nonlinear AC power flow constraints [23]. Constraint (28) represents the balance of active and reactive power at nodes of the Common Coupling Point (PCC). Constraints (29), (30), and (31) represent power factor limitations, voltage squared amplitude limitations of nodes, and current squared amplitude limitations of distribution lines, respectively.

In order to express the centralized optimization operation model of active distribution networks with EHLs as a standard sharing problem [24], two auxiliary variables $r_{i,t}^e$ and $r_{i,t}^h$ are defined, as shown in Equation (34):

$$\begin{cases} r_{i,t}^e = P_{i,t}^{\text{net}} \\ r_{i,t}^h = H_{i,t}^{\text{net}} \end{cases} \quad (34)$$

According to the defined auxiliary variables, the augmented Lagrange function of the model shown in Equations (23)–(34) can be expressed as:

$$L = \sum_{i \in N} \sum_{t \in T} C_{i,t}^U + \sum_{i \in N} \sum_{t \in T} C_{i,t}^E + \sum_{i \in N} \sum_{t \in T} \lambda_{i,t}^e (P_{i,t}^{\text{net}} - r_{i,t}^e) + \frac{\rho^e}{2} \sum_{i \in N} \sum_{t \in T} \|P_{i,t}^{\text{net}} - r_{i,t}^e\|_2^2 + \sum_{i \in N} \sum_{t \in T} \lambda_{i,t}^h (H_{i,t}^{\text{net}} - r_{i,t}^h) + \frac{\rho^h}{2} \sum_{i \in N} \sum_{t \in T} \|H_{i,t}^{\text{net}} - r_{i,t}^h\|_2^2 \quad (35)$$

where $C_{i,t}^U = C_{i,t}^G + C_{i,t}^{\text{CHP}} + C_{i,t}^{\text{WF}} + C_{i,t}^{\text{PV}} + C_{i,t}^{\text{EHLs}}$, $C_{i,t}^E = C_{i,t}^{\text{EP}}$. $\lambda_{i,t}^e$ and $\lambda_{i,t}^h$ are Lagrange multipliers. ρ^e and ρ^h are penalty coefficients.

Combine the linear term and the quadratic term, make $u_{i,t}^e = \lambda_{i,t}^e / \rho_1$, $u_{i,t}^h = \lambda_{i,t}^h / \rho_2$, and express the augmented Lagrange function (35) as a scaling form:

$$L = \sum_{i \in N} \sum_{t \in T} C_{i,t}^U + \sum_{i \in N} \sum_{t \in T} C_{i,t}^E + \frac{\rho^e}{2} \sum_{i \in N} \sum_{t \in T} \|P_{i,t}^{\text{net}} - r_{i,t}^e + u_{i,t}^e\|_2^2 - \frac{\rho^e}{2} \sum_{i \in N} \sum_{t \in T} \|u_{i,t}^e\|_2^2 + \frac{\rho^h}{2} \sum_{i \in N} \sum_{t \in T} \|H_{i,t}^{\text{net}} - r_{i,t}^h + u_{i,t}^h\|_2^2 - \frac{\rho^h}{2} \sum_{i \in N} \sum_{t \in T} \|u_{i,t}^h\|_2^2 \quad (36)$$

where $u_{i,t}^e$ and $u_{i,t}^h$ are scaled dual variables.

4. Distributed Solution Based on Dynamic Step Correction ADMM

In order to protect the privacy of the Virtual power plant during the operation of active distribution networks with EHLs, ADMM is used to solve the optimal operation model of active distribution networks with EHLs in a distributed manner. Since the step size will significantly affect the rate of convergence of ADMM, the dynamic step size modification is further considered on the basis of the original ADMM to improve the convergence performance of the algorithm.

4.1. Implementation of ADMM

The updates of each variable are shown in Equations (37)–(39):

$$\left\{ P_{i,t}^{\text{net}}(k+1), H_{i,t}^{\text{net}}(k+1) \right\} := \underset{P_{i,t}^{\text{net}}, H_{i,t}^{\text{net}}}{\text{argmin}} \sum_{i \in N} \sum_{t \in T} C_{i,t}^U + \frac{\rho^e}{2} \sum_{i \in N} \sum_{t \in T} \|P_{i,t}^{\text{net}} - r_{i,t}^e(k) + u_{i,t}^e(k)\|_2^2 + \frac{\rho^h}{2} \sum_{i \in N} \sum_{t \in T} \|H_{i,t}^{\text{net}} - r_{i,t}^h(k) + u_{i,t}^h(k)\|_2^2 \quad (37)$$

$$\left\{ r_{i,t}^e(k+1), r_{i,t}^h(k+1) \right\} := \underset{r_{i,t}^e, r_{i,t}^h}{\text{argmin}} \sum_{i \in N} \sum_{t \in T} C_{i,t}^E + \frac{\rho^e}{2} \sum_{i \in N} \sum_{t \in T} \|r_{i,t}^e - u_{i,t}^e(k) - P_{i,t}^{\text{net}}(k+1)\|_2^2 + \frac{\rho^h}{2} \sum_{i \in N} \sum_{t \in T} \|r_{i,t}^h - u_{i,t}^h(k) - H_{i,t}^{\text{net}}(k+1)\|_2^2 \quad (38)$$

$$\begin{cases} u_{i,t}^e(k+1) := u_{i,t}^e(k) + P_{i,t}^{\text{net}}(k+1) - r_{i,t}^e(k+1) \\ u_{i,t}^h(k+1) := u_{i,t}^h(k) + H_{i,t}^{\text{net}}(k+1) - r_{i,t}^h(k+1) \end{cases} \quad (39)$$

For the convenience of analysis, let:

$$\begin{cases} p^e = \sum_{i=1}^N \sum_{t=1}^T P_{i,t}^{\text{net}} \\ p^h = \sum_{i=1}^N \sum_{t=1}^T H_{i,t}^{\text{net}} \end{cases}, \quad \begin{cases} r^e = \sum_{i=1}^N \sum_{t=1}^T r_{i,t}^e \\ r^h = \sum_{i=1}^N \sum_{t=1}^T r_{i,t}^h \end{cases} \quad (40)$$

The iteration stopping standard is defined as the original residual and dual residual being less than the set tolerance. Specifically, it is determined whether the ADMM iteration has stopped based on the stopping standard shown in Equation (41).

$$\begin{cases} \|x(k+1)\|_2^2 = \max \|p^{e,h}(k+1) - r^{e,h}(k+1)\|_2^2 \leq \varepsilon^{\text{pri}} \\ \|y(k+1)\|_2^2 = \max \rho^{e,h} \|r^{e,h}(k+1) - r^{e,h}(k)\|_2^2 \leq \varepsilon^{\text{dual}} \end{cases} \quad (41)$$

The solving steps of the original ADMM are shown in Algorithm 1.

Algorithm 1. ADMM-based distributed optimization

Input: Forecast electric load $P_{i,t}^{\text{load}}$, forecast thermal load $H_{i,t}^{\text{load}}$, wind power forecast output $P_{i,t,\text{max}}^{\text{WF}}$, photovoltaic forecast output $P_{i,t,\text{max}}^{\text{PV}}$, Lagrange multiplier $\lambda_{i,t}^e$ and $\lambda_{i,t}^h$, penalty coefficient ρ^e and ρ^h , tolerance parameter ε^{pri} and $\varepsilon^{\text{dual}}$, energy price and equipment operation parameter

Output: Minimum operating cost of active distribution network with EHLs

Step 1: Initialize $\lambda_{i,t}^e = \lambda_{i,t}^h = 0$, $\rho^e = \rho^h = 0.1$, $\varepsilon^{\text{pri}} = \varepsilon^{\text{dual}} = 10^{-4}$, $P_{i,t}^{\text{net}} = H_{i,t}^{\text{net}} = 0$, $r_{i,t}^e = r_{i,t}^h = 0$, iteration number $k = 1$.

Step 2: Establish an optimization operation model for active distribution networks with EHLs, including optimization objective functions and constraint conditions.

Step 3: Parallel optimization and solution of various variables in the model.

Step 4: According to Equations (37)–(39), iteratively update variables $P_{i,t}^{\text{net}}$ and $H_{i,t}^{\text{net}}$, auxiliary variables $r_{i,t}^e$ and $r_{i,t}^h$, and dual variables $u_{i,t}^e$ and $u_{i,t}^h$.

Step 5: Update iteration number $k = k + 1$.

Step 6: According to Equation (41), determine whether the stop condition is met. If the stop condition is met, the iteration stops. Otherwise, return to Step3 for repeated calculations.

4.2. Dynamic Step Correction of ADMM

The step size will have a significant impact on the rate of convergence of ADMM [24], while the step size of the original ADMM is fixed, and the algorithm performance will deteriorate during the iteration process. Therefore, a two-stage dynamic step size correction method is adopted to improve the convergence performance of ADMM.

Stage 1: Calculate the changes in the original residual and dual residual values during each iteration process, as shown in Equation (42). If the change in the minimum values of the original and dual residuals is greater than the set value Δ (such as $\Delta = 0.1$), the step size remains unchanged because the current step size reduces the original and dual residuals. Otherwise, the current step size will worsen the convergence of the algorithm. At this time, the step size needs to be updated at Stage 2.

$$\begin{cases} \Delta \|x(k+1)\|_2^2 = \|x(k+1)\|_2^2 - \|x(k)\|_2^2 \\ \Delta \|y(k+1)\|_2^2 = \|y(k+1)\|_2^2 - \|y(k)\|_2^2 \end{cases} \quad (42)$$

Stage 2: Update the step based on the current values of the original and dual residuals, as shown in Equation (43). If the original residual is much greater than the dual residual, it will increase the step size and result in serious penalties for violating the original feasibility. If the dual residual is much greater than the original residual, then the dual feasibility

converges and the step size will decrease. At this time, the convergence of original feasibility and dual feasibility can alternate and balance.

$$\rho^{e,h}(k+1) = \begin{cases} \rho^{e,h}(k) \cdot (1 + \lg \frac{\|x(k)\|_\infty}{\|y(k)\|_\infty}) & \text{if } \|x(k)\|_\infty > 10\|y(k)\|_\infty \\ \rho^{e,h}(k) & \text{otherwise} \\ \rho^{e,h}(k) / (1 + \lg \frac{\|y(k)\|_\infty}{\|x(k)\|_\infty}) & \text{if } \|y(k)\|_\infty > 10\|x(k)\|_\infty \end{cases} \quad (43)$$

The ADMM for dynamic step size correction is shown in Algorithm 2.

Algorithm 2. ADMM based on dynamic step size correction

Step 1: Set residual variation value Δ ;

Step 2: for k

 Calculate $\Delta\|x(k+1)\|_2^2$ and $\Delta\|y(k+1)\|_2^2$ according to Equation (42)

 if $\min\{\Delta\|x(k+1)\|_2^2, \Delta\|y(k+1)\|_2^2\} \geq \Delta$

$\rho^{e,h}(k+1) = \rho^{e,h}(k)$

 else

 Update $\rho^{e,h}(k+1)$ according to Equation (43)

 end

$\rho^{e,h}(k+1)$ is sent to Algorithm 1 for step3 update

Step 3: end

5. Simulation and Analysis

5.1. Example Setting

To verify the effectiveness of the distributed coordination and optimization operation method for active distribution networks with EHLs based on ADMM, an IEEE33 distribution system as shown in Figure 2 was constructed for simulation verification. A total of 21 distributed units are aggregated into the active distribution network through three virtual power plants (VPP1, VPP2, VPP3). The parameters of conventional units (G1, G2, G3), cogeneration units (CHP1, CHP2, CHP3), wind turbines (WF1, WF2, WF3), photovoltaic power generation (PV1, PV2, PV3), and electrical heating loads (EHLs1, EHLs2, EHLs3) in distributed units are shown in Tables 1–5, and the predicted power of wind and photovoltaic is shown in Figure 3. The shared electrical power of each virtual power plant is limited to 28 MW, and the shared thermal power is limited to 5 MW. The electricity sharing price between virtual power plants is shown in Figure 4, and the heat sharing price is 0.06 \$/kW·h.

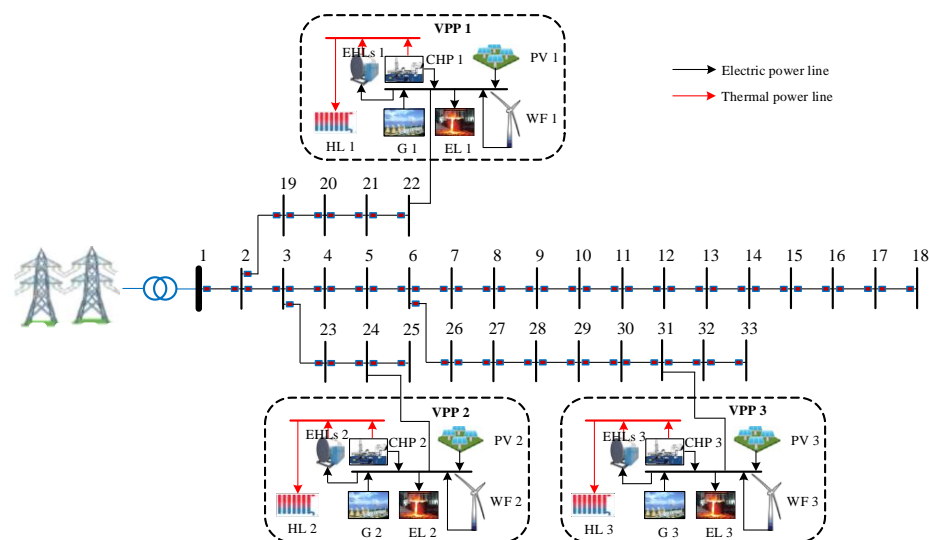


Figure 2. IEEE33 distribution system.

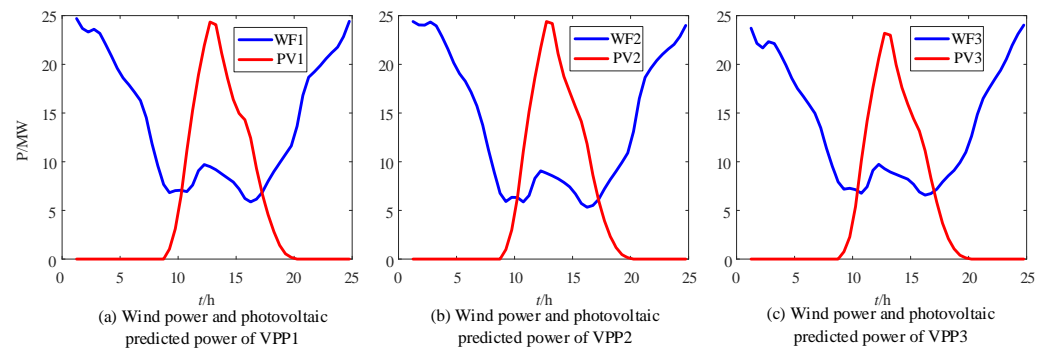


Figure 3. Wind power and photovoltaic predicted power.

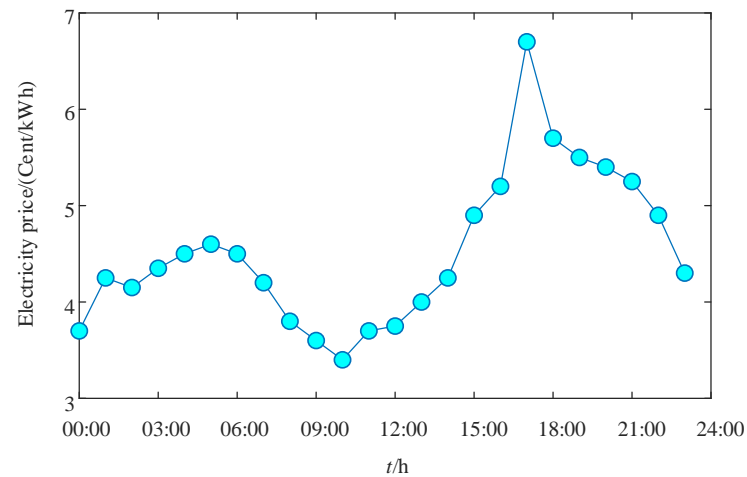


Figure 4. Electricity sharing price between virtual power plants.

Table 1. Conventional unit operating parameters.

Parameters	VPP1	VPP2	VPP3
a_i (\$/MW ²)	0.0018	0.0019	0.0021
b_i (\$/MW)	18.39	20.51	22.67
c_i (\$/h)	298	249	228
$P_{i,min}^G$ (MW)	20	15	10
$P_{i,max}^G$ (MW)	60	40	20
T_{min}^{on}/h	5	4	2
T_{min}^{off}/h	5	4	2
$S/\$$	891	540	377

Table 2. Output range of cogeneration unit.

CHP Output Range	VPP1	VPP2	VPP3
A (P/MW, H/MW)	(17.0, 0.0)	(16.0, 0.0)	(17.0, 0.0)
B (P/MW, H/MW)	(12.0, 12.0)	(11.0, 11.0)	(12.0, 12.0)
C (P/MW, H/MW)	(30.0, 61.2)	(28.0, 58.2)	(30.0, 61.2)
D (P/MW, H/MW)	(34.0, 61.2)	(33.0, 58.2)	(34.0, 61.2)
E (P/MW, H/MW)	(44.0, 0.0)	(42.0, 0.0)	(44.0, 0.0)

Table 3. Operating parameters of cogeneration unit.

CHP Unit Parameters	VPP1	VPP2	VPP3
$k_{i,1} (\$/h)$	4.07×10^2	4.03×10^2	4.07×10^2
$k_{i,2} (\$/(\text{MW} \cdot h))$	2.23×10^1	2.26×10^1	2.23×10^1
$k_{i,3} (\$/(\text{MW} \cdot h))$	5.60	5.61	5.60
$k_{i,4} (\$/(\text{MW}^2 \cdot h))$	9.90×10^{-4}	9.88×10^{-4}	9.90×10^{-4}
$k_{i,5} (\$/(\text{MW}^2 \cdot h))$	3.36×10^{-5}	3.36×10^{-5}	3.36×10^{-5}
$k_{i,6} (\$/(\text{MW}^2 \cdot h))$	3.93×10^{-4}	3.94×10^{-4}	3.93×10^{-4}

Table 4. Wind power and photovoltaic operating parameters.

Parameters	VPP1	VPP2	VPP3
$\kappa_i^{\text{WF}} (\$/(\text{kW} \cdot h))$	0.0011	0.0011	0.0011
$\kappa_i^{\text{PV}} (\$/(\text{kW} \cdot h))$	0.0012	0.0012	0.0012

Table 5. EHLs operating parameters.

Parameters	VPP1	VPP2	VPP3
$P_{l,\min}^{\text{EHLs}} (\text{MW})$	0	0	0
$P_{l,\max}^{\text{EHLs}} (\text{MW})$	10	15	20
$T_{\min}^{\text{EHLs}} (\text{h})$	2	2	2
$T_{\max}^{\text{EHLs}} (\text{h})$	5	5	5
α	0.4	0.4	0.4
β	0.3	0.3	0.3
γ	0.1	0.1	0.1

5.2. Algorithm Performance Analysis

To verify the effectiveness of the proposed distributed coordinated operation method for active distribution networks with EHLs based on dynamic step size correction ADMM (represented as A1), this method was compared with the original ADMM algorithm (represented as A2) in reference [25] and the automatically adjusted step size ADMM algorithm (represented as A3) in reference [19], as shown in Table 6.

Table 6. Operating results of different methods.

Method	Convergence Accuracy	Error	Iterations	Operating Cost (\$)
A1	10^{-5}	1.31×10^{-6}	69	2.3071×10^5
A2		9.88×10^{-6}	196	2.3080×10^5
A3		-2.37×10^{-6}	93	2.3074×10^5
A1	10^{-4}	1.31×10^{-6}	57	2.3071×10^5
A2		9.94×10^{-5}	162	2.3097×10^5
A3		2.12×10^{-5}	79	2.3084×10^5
A1	10^{-3}	1.31×10^{-6}	42	2.3071×10^5
A2		9.36×10^{-4}	121	2.3113×10^5
A3		2.43×10^{-5}	66	2.3096×10^5
A1	10^{-2}	1.31×10^{-6}	28	2.3073×10^5
A2		2.41×10^{-3}	72	2.3133×10^5
A3		2.96×10^{-5}	45	2.3114×10^5

It can be seen from Table 6 that A1 always has the fastest rate of convergence under different convergence precision, the operating cost remains stable, and the economy is optimal. Taking convergence accuracy $\epsilon^{\text{pri}} = \epsilon^{\text{dual}} = 10^{-4}$ as an example, the A2 iteration converges 162 times, the A3 iteration converges 79 times while the A1 iteration only

converges 57 times, which is significantly less than other methods. Obviously, the proposed method helps to improve the convergence of the algorithm. In addition, for A2 and A3, as the convergence accuracy decreases, the operating results gradually deteriorate. This is because their convergence is formed as each distributed unit evolves independently, while the exit condition is only based on overall error. At the same time, the intermediate results summarized by the virtual power plant layer shield the cost parameters of each distributed unit in each iteration.

To achieve convergence accuracy $\varepsilon^{\text{pri}} = \varepsilon^{\text{dual}} = 10^{-5}$, the simulation analysis shows the convergence characteristics of power output, as shown in Figures 5 and 6.

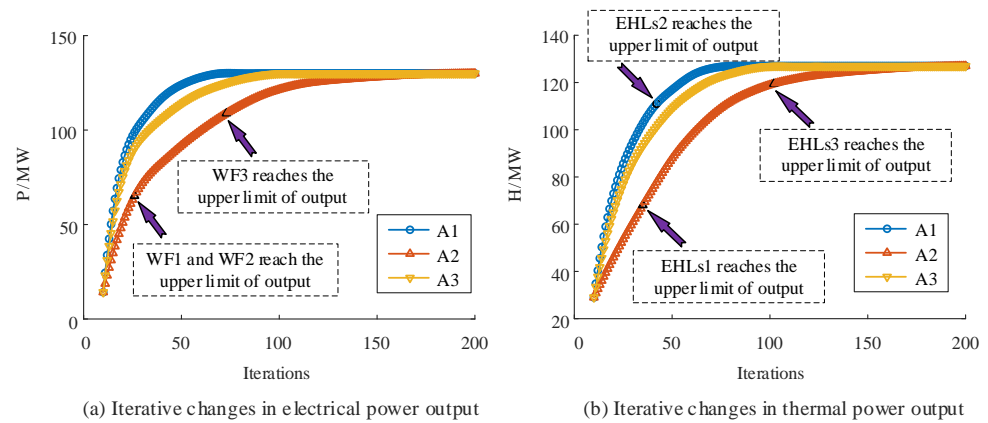


Figure 5. Convergence characteristics under normal communication.

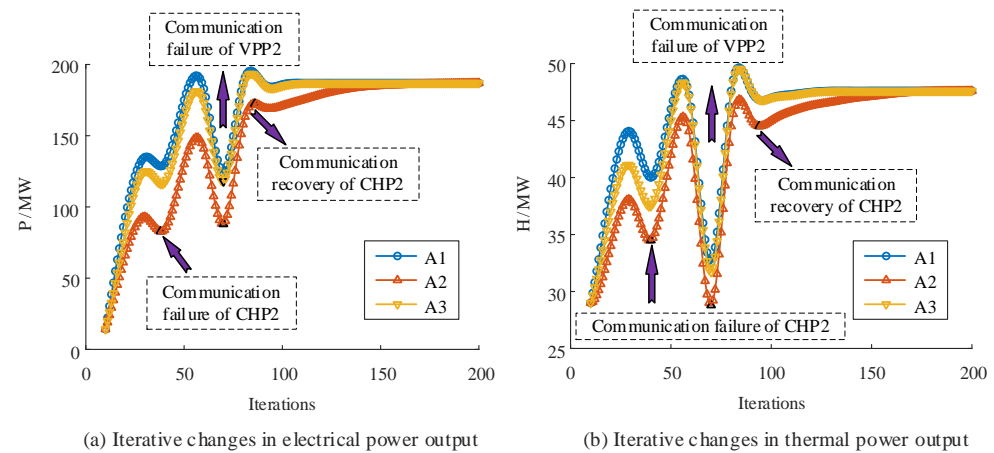


Figure 6. Convergence characteristics under communication failure.

Figure 5 shows the changes in the power output and thermal power output of the device during normal communication at 24:00 with the number of iterations. The number of iterations required for A2 and A3 power output convergence is 196 and 93, respectively, while A1 power output only needs 69 iterations to converge, which is significantly superior to the other two methods. The dynamic correction step is generated by dynamically adjusting the online distributed units from bottom to top, ensuring convergence speed. In the system economy operation, compared with conventional power generation units, wind power, and photovoltaic operation costs are lower, and the output of distributed units such as WF1, WF2, and WF3 will reach the upper limit during the iteration process.

In addition, verify the optimization effect of dynamic step size correction ADMM under communication faults. Figure 6 shows the variation of electrical and thermal power output with the number of iterations under communication faults at 12:00 pm. Assuming that there is a communication failure between CHP2 and virtual power plant 3 during the iteration process, distributed optimization is carried out based on the dynamic correction

strategy proposed in the previous section, that is, each distributed unit and virtual power plant are optimized using the latest information obtained. The dynamic correction step size can ensure that new stable operating points can be quickly reached in the event of communication connection failures in distributed units or virtual power plants. Compared with normal situations, the number of iterations under communication faults has increased, but as shown in Figure 6, the proposed method can obtain the optimal solution with the minimum number of iterations under communication faults, still outperforming other methods.

5.3. The Impact of Distributed Unit Randomness

In the three-layer distributed coordinated operation architecture, EHLs, and other distributed units in the active distribution network are widely distributed, with strong spatiotemporal dispersion and differences, which may lead to changes in the number and parameters of the underlying distributed units. Therefore, the solution speed and efficiency should have strong robustness to the randomness of the number of distributed units and parameters.

The distributed coordinated operation of active distribution networks with EHLs needs to meet the constraints of supply and demand balance and the constraints of distributed unit operation, specifically expressed as:

$$\sum_{i=1}^N s_i = S_D \quad (44)$$

$$s_i^{\min} \leq s_i \leq s_i^{\max} \quad (45)$$

where s_i is the output of distributed unit i , S_D is the system load demand, s_i^{\max} and s_i^{\min} is the upper and lower limits of the output of distributed unit i .

According to the constraints of supply and demand balance and distributed unit operation, a necessary condition that the system's economic operation must meet is:

$$\sum_{i=1}^N s_i^{\min} < S_D < \sum_{i=1}^N s_i^{\max} \quad (46)$$

Define the depth of distributed unit operation based on the above conditions (represented as $0 < m < 1$), and have

$$S_D = \sum_{i=1}^N s_i^{\min} + m \left(\sum_{i=1}^N s_i^{\max} - \sum_{i=1}^N s_i^{\min} \right) \quad (47)$$

In order to compare the influence of the number of distributed units on the algorithm convergence, assume that the parameters of different distributed units are randomly distributed in some intervals, generate a certain number of distributed units randomly from them, and form the randomness of virtual power plant simulation distributed units.

Figure 7 shows the convergence of the three methods at different operating depths when the number of distributed units changes from 20 to 100. It can be seen that the number of iterations for A2 and A3 is greatly affected by the number of distributed units. The number of iterations for A2 is approximately exponential with the number of distributed units, requiring hundreds of iterations to converge. For A3, the number of iterations is approximately linearly increasing with the number of distributed units, requiring over a hundred iterations to converge. The number of iterations for A1 is almost unaffected by the number of distributed units, and for a certain m , it can converge with only a few dozen iterations. This is because the step size of A1 is dynamically modified, which is updated from bottom to top based on the response of the underlying distributed units.

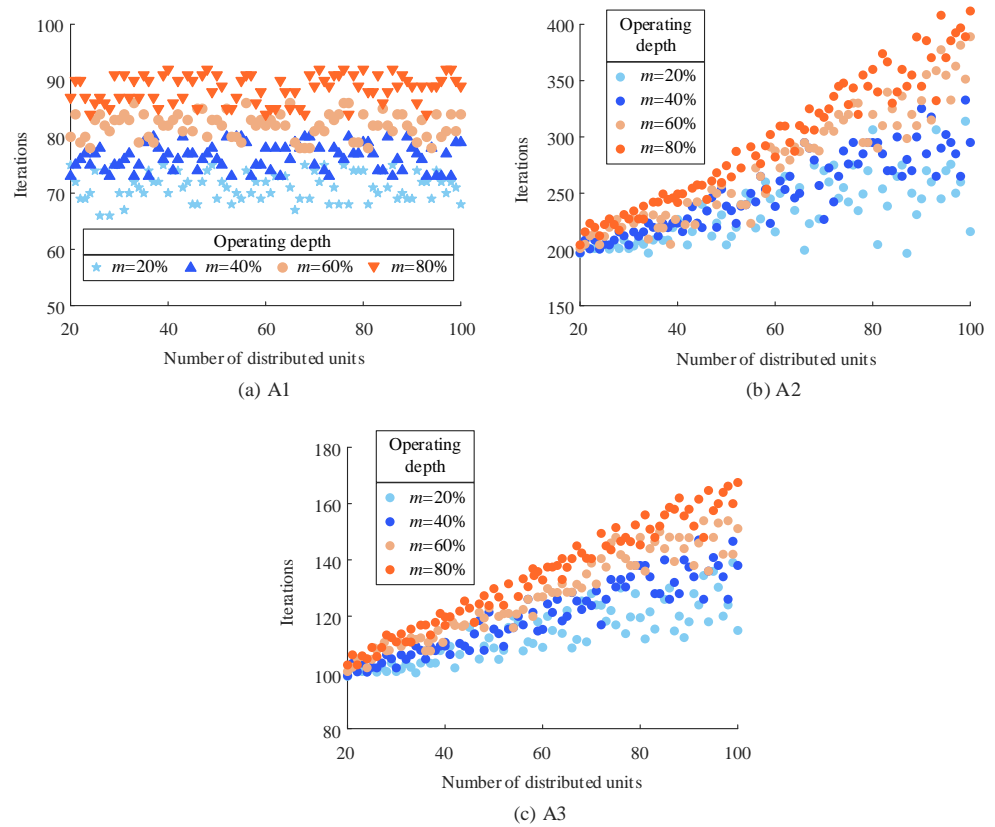


Figure 7. The impact of the number of distributed units on the number of iterations under different methods.

5.4. Distributed Coordinated Operation Results of the Active Distribution Network with EHLs

The distributed coordinated operation of active distribution networks with EHLs takes into account both thermal delay effects, thermal losses, and EHL regulation. In order to analyze the advantages of the distributed coordinated operation strategy in this paper, four operation strategies are set based on whether the thermal delay effect and heat loss of the heating system are considered during coordinated operation, and whether EHLs participate in the operation. Strategy A: The distributed coordinated operation of the system does not consider the thermal delay effect and heat loss, nor does it consider EHL regulation. Strategy B: The distributed coordinated operation of the system only considers the thermal delay effect and heat loss, without considering EHL regulation. Strategy C: The distributed coordinated operation of the system does not consider the thermal delay effect and heat loss, only EHLs regulation. Strategy D: The distributed and coordinated operation of the system takes into account the thermal delay effect, heat loss, and EHL regulation. Table 7 compares the four operating strategies in terms of system operation economy. Table 8 compares the wind abandonment situation under four operating strategies, and Table 9 compares the photovoltaic abandonment situation under four operating strategies.

Table 7. The four operating strategies in terms of system operation economy.

Strategies	Thermal Delay and Heat Loss	EHLs Operation	Operating Cost/ (\$)
A	×	×	2.3283×10^5
B	✓	×	2.3213×10^5
C	×	✓	2.3191×10^5
D	✓	✓	2.3071×10^5

Table 8. The wind abandonment situation under four operating strategies.

Strategies	Abandoned Wind Power/(MW·h)	Wind Power Abandonment Rate/%
A	270.18	27.6
B	184.03	18.8
C	141.94	14.5
D	65.59	6.7

Table 9. The photovoltaic abandonment situation under four operating strategies.

Strategies	Abandoned Photovoltaic Power/(MW·h)	Photovoltaic Abandonment Rate/%
A	70.63	19.4
B	52.06	14.3
C	42.23	11.6
D	18.57	5.1

It can be seen from Tables 7–9 that, compared with Strategy A, individually considering the thermal delay effect and heat loss of the heating system (Strategy B) and EHLs regulation (Strategy C) can both reduce the system operating costs and waste wind and solar energy to a certain extent. Compared with strategy D, the system operation economy and the potential of wind and solar energy consumption have not been fully released. Under the distributed and coordinated operation of active distribution networks with EHLs (Strategy D), the system has the lowest operating cost, only 2.3071×10^5 \$, and the wind and photovoltaic abandonment rates have further decreased to 6.7% and 5.1%.

Figure 8 shows the coordinated operation results of various distributed units in the active distribution network with EHLs.

Take virtual power plant 1 as an example to analyze the results. According to the power optimization operation results in Figure 8a, the power demand of virtual power plant 1 in the daytime is mainly met by G1, CHP1, and PV1, and the power demand of virtual power plant 1 at night is mainly met by CHP1, and WF1. This is because during the day from 11:00 to 15:00, there is sufficient sunlight, and PV1 is in the period of high power generation. At night from 20:00 to 05:00, the wind speed is high, and WF1's power generation significantly increases. In order to provide space for wind power consumption, G1 is in a shutdown state from 22:00 to 05:00. In addition, CHP1 is running all day due to providing heat to users. Virtual power plant 1 energy sharing receives 78.28 MW·h of electric energy and provides 322.80 MW·h. According to the thermal optimization operation results in Figure 8a, the thermal demand of virtual power plant 1 is mainly provided by CHP1 in the daytime, while it is in the peak heating period at night, and the thermal demand of Virtual power plant 1 is mainly provided by CHP1 and EHLs1. The heat energy received by virtual power plant 1 energy sharing is 13.72 MW·h, and the heat energy provided is 2.08 MW·h. Analysis shows that the active distribution network with EHLs achieves a distributed collaborative supply of electricity and heat energy.

The power load, EHLs controlled quantity, and rebound load are shown in Figure 9.

From Figure 9, it can be seen that the trend of rebound load is consistent with the controlled quantity of EHLs, but the rebound load is relatively delayed in time compared to the controlled quantity of EHLs, and the peak of rebound load is also smaller compared to the controlled quantity of EHLs. Due to the peak power load during the day, EHLs are mainly controlled during the day. During the controlled period of EHLs, the peak value of the power load significantly decreases, reflecting the role of EHLs control in energy conservation and emission reduction of the power system.

The thermal load and the controlled quantities of EHLs in the thermal system are shown in Figure 10.

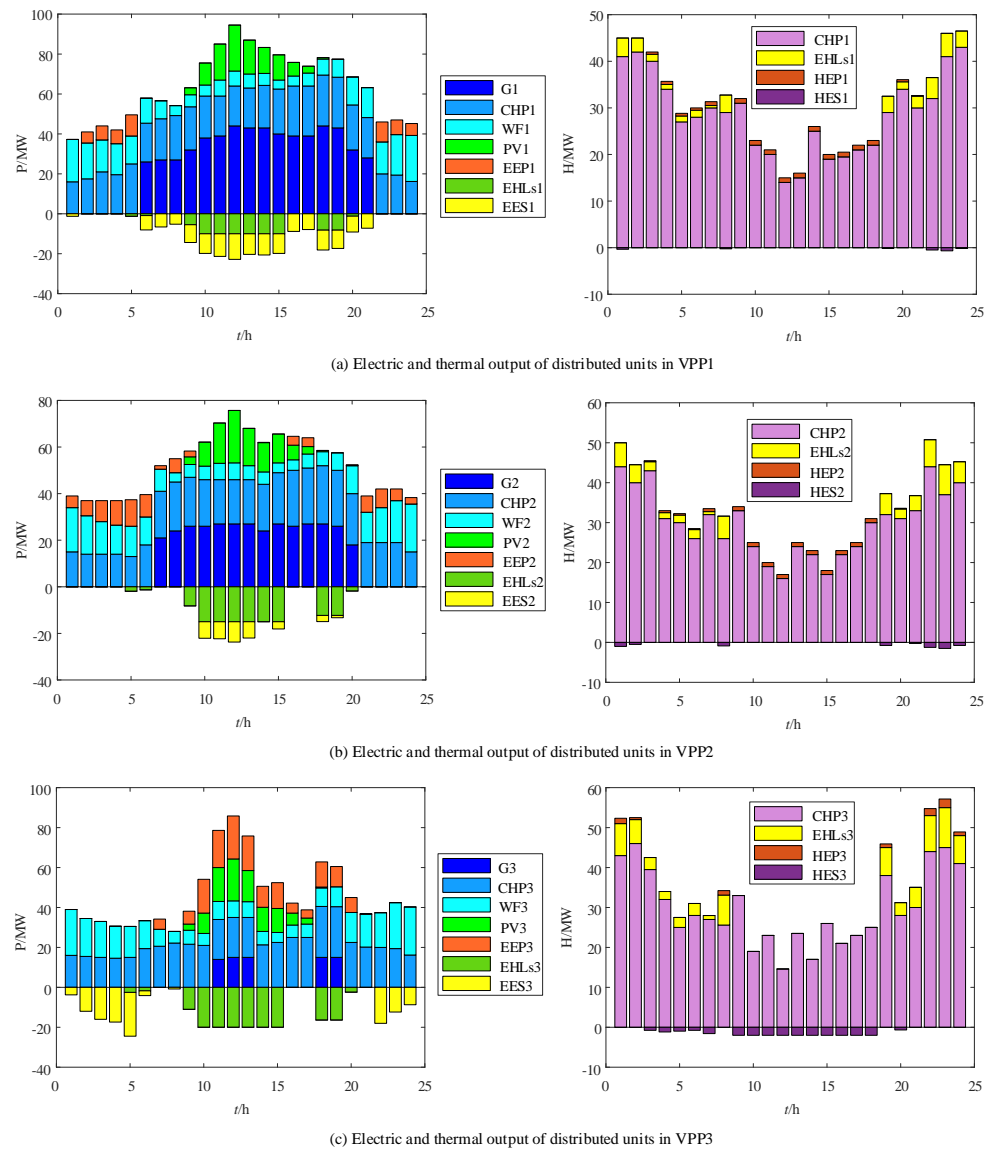


Figure 8. Distributed coordinated operation results of the active distribution network with EHLs.

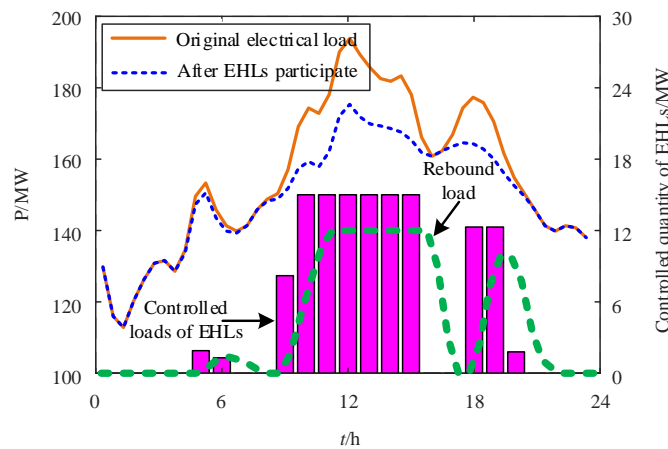


Figure 9. Power load and EHLs controlled quantity.

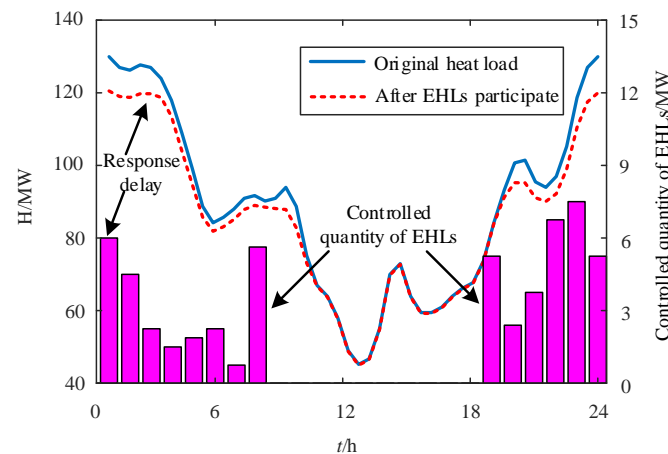


Figure 10. Thermal load and EHLs controlled quantity.

From Figure 10, it can be seen that compared to the response time of the heat load, the control time of EHLs is advanced by one hour, while the response time of the heat load is relatively delayed by one hour. Due to the peak heat load period at night, the controlled period of EHLs is mainly located at night. During the controlled period of EHLs, the peak value of thermal load significantly decreases, reflecting the role of EHLs control in energy conservation and emission reduction of the thermal system.

6. Conclusions

To solve the problem of coordinated operation of large-scale distributed units in active distribution networks with EHLs, a distributed coordinated operation method for active distribution networks with EHLs based on dynamic step correction ADMM is proposed. The effectiveness of the proposed method was verified through simulation, and the following conclusions were obtained:

- (1) In the process of solving ADMM, considering dynamic step correction can reduce the number of iterations and improve the convergence and computational efficiency of ADMM.
- (2) The proposed distributed coordinated operation method has strong robustness to the randomness of the number of distributed units and parameters.
- (3) After EHLs participate in coordinated operation, they can expand the consumption space of wind and photovoltaic power, improve the economic efficiency of system operation, and during the controlled period of EHLs, the peak values of electricity and heat loads significantly decrease, reflecting the energy-saving and emission reduction effect of EHLs on the system.

Author Contributions: Conceptualization, S.L.; methodology and data curation, S.L. and G.B.; model establishment, S.L.; data analysis, S.L. and G.B.; writing—original draft preparation, S.L.; project administration and supervision, Y.H.; visualization, G.B. and Y.H. All authors have read and agreed to the published version of the manuscript.

Funding: This research was supported by the Science and Technology Project of State Grid Corporation of China under Grant (No. 52272220002T); Sichuan Provincial key research and development program of China (No. 2022YFG0123); and in part by Central Government Funds for Guiding Local Scientific and Technological Development of China (No. 2021ZYD0042).

Data Availability Statement: Data are contained within the article.

Conflicts of Interest: This paper is completed by the author and our team without any plagiarism. We declare that we do not have any commercial or associative interest that represents a conflict of interest in connection with the work submitted.

References

1. Dehnavi, G.; Ginn, H.L. Distributed load sharing among converters in an autonomous microgrid including PV and wind power units. *IEEE Trans. Smart Grid* **2019**, *10*, 4289–4298. [[CrossRef](#)]
2. Liu, J.; Cheng, H.Z.; Zeng, P.L.; Yao, L.Z. Rapid assessment of maximum distributed generation output based on security distance for interconnected distribution networks. *Int. J. Electr. Power Energy Syst.* **2018**, *101*, 13–24. [[CrossRef](#)]
3. Wu, D.; Lian, J.; Sun, Y.; Yang, T.; Hansen, J. Hierarchical control framework for integrated coordination between distributed energy resources and demand response. *Electr. Power Syst. Res.* **2017**, *150*, 45–54. [[CrossRef](#)]
4. Albadi, M.H.; El-Saadany, E.F. A summary of demand response in electricity markets. *Electr. Power Syst. Res.* **2008**, *78*, 1989–1996. [[CrossRef](#)]
5. Yang, J.; Yuan, W.B.; Sun, Y.; Han, H.; Hou, X.C.; Guerrero, J.M. A novel quasi-master–slave control frame for PV-storage independent microgrid. *Int. J. Electr. Power Energy Syst.* **2018**, *97*, 262–274. [[CrossRef](#)]
6. Li, P.; Wang, Z.X.; Wang, N.; Yang, W.H.; Li, M.Z.; Zhou, X.C. Stochastic robust optimal operation of community integrated energy system based on integrated demand response. *Int. J. Electr. Power Energy Syst.* **2021**, *128*, 106735. [[CrossRef](#)]
7. Huang, W.J.; Zhang, X.; Li, K.P.; Zhang, N.; Strbac, G.; Kang, C.Q. Resilience oriented planning of urban multi-energy systems with generalized energy storage sources. *IEEE Trans. Power Syst.* **2022**, *37*, 2906–2918. [[CrossRef](#)]
8. Masrur, H.; Shafie-Khah, M.; Hossain, M.J.; Senjyu, T. Multi-energy microgrids incorporating EV integration: Optimal design and resilient operation. *IEEE Trans. Smart Grid* **2022**, *13*, 3508–3518. [[CrossRef](#)]
9. Seyed Yazdi, M.; Mohammadi, M.; Farjah, E. A combined driver–station interactive algorithm for a maximum mutual interest in charging market. *IEEE Trans. Intell. Transp. Syst.* **2020**, *21*, 2534–2544. [[CrossRef](#)]
10. Huang, X.Z.; Xu, Z.F.; Sun, Y.; Xue, Y.L.; Wang, Z.; Liu, Z.J. Heat and power load dispatching considering energy storage of district heating system and electric boilers. *J. Mod. Power Syst. Clean Energy* **2018**, *5*, 992–1003. [[CrossRef](#)]
11. Wang, J.D.; Liu, J.X.; Li, C.H.; Zhou, Y.; Wu, J.Z. Optimal scheduling of gas and electricity consumption in a smart home with a hybrid gas boiler and electric heating system. *Energy* **2020**, *204*, 17951. [[CrossRef](#)]
12. Zheng, X.Y.; Wei, C.; Qin, P.; Guo, J.; Yu, Y.H.; Song, F. Characteristics of residential energy consumption in China: Findings from a household survey. *Energy Policy* **2014**, *75*, 126–135. [[CrossRef](#)]
13. International Energy Agency (IEA). *Energy Balances of OECD Countries 2014*; International Energy Agency: Paris, France, 2014.
14. Chen, X.Y.; Kang, C.Q.; O'Malley, M.; Xia, Q.; Bai, J.H.; Liu, C. Increasing the flexibility of combined heat and power for wind power integration in China: Modeling and implications. *IEEE Trans. Power Syst.* **2015**, *30*, 1848–1857. [[CrossRef](#)]
15. Chen, C.Y.; Chen, Y.; Zhao, J.B.; Zhang, K.F.; Ni, M.; Ren, B. Data-driven resilient automatic generation control against false data injection attacks. *IEEE Trans. Industr. Inform.* **2021**, *17*, 8092–8101. [[CrossRef](#)]
16. Yu, X.; Xue, Y. Smart grids: A cyber–physical systems perspective. *Proc. IEEE* **2016**, *104*, 1058–1070. [[CrossRef](#)]
17. Wen, Y.; Qu, X.; Li, W.; Liu, X.; Ye, X. Synergistic operation of electricity and natural gas networks via ADMM. *IEEE Trans. Smart Grid* **2018**, *9*, 4555–4565. [[CrossRef](#)]
18. Shi, W.; Ling, Q.; Yuan, K.; Wu, G.; Yin, W. On the linear convergence of the ADMM in decentralized consensus optimization. *IEEE Trans. Signal Process* **2014**, *62*, 1750–1761. [[CrossRef](#)]
19. Du, Y.; Zhang, W.; Zhang, T. ADMM-based distributed state estimation for integrated energy system. *CSEE J. Power Energy* **2019**, *5*, 275–283. [[CrossRef](#)]
20. He, C.; Wu, L.; Liu, T.; Shahidehpour, M. Robust co-optimization scheduling of electricity and natural gas system via ADMM. *IEEE Trans. Sustain. Energy* **2017**, *8*, 658–670. [[CrossRef](#)]
21. He, Y.; Yan, M.; Shahidehpour, M.; Li, Z.; Guo, C.; Wu, L. Decentralized optimization of multi-area electricity–natural gas flows based on cone reformulation. *IEEE Trans. Power Syst.* **2018**, *33*, 4531–4542. [[CrossRef](#)]
22. Chen, J.; Zhang, W.; Zhang, Y.; Bao, G. Day-ahead scheduling of distribution level integrated electricity and natural gas system based on fast-ADMM with restart algorithm. *IEEE Access* **2018**, *6*, 17557–17569. [[CrossRef](#)]
23. Farivar, M.; Low, S.H. Branch flow model: Relaxations and convexification—Part I. *IEEE Trans. Power Syst.* **2013**, *28*, 2554–2564. [[CrossRef](#)]
24. Boyd, S.; Parikh, N.; Chu, E.; Peleato, B.; Eckstein, J. Distributed optimization and statistical learning via the alternating direction method of multipliers. *Found. Trends Mach. Learn.* **2011**, *3*, 1–122. [[CrossRef](#)]
25. Ratanakuakangwan, S.; Morita, H. Hybrid stochastic robust optimization and robust optimization for energy planning—A social impact-constrained case study. *Appl. Energy* **2021**, *298*, 117258. [[CrossRef](#)]

Disclaimer/Publisher's Note: The statements, opinions and data contained in all publications are solely those of the individual author(s) and contributor(s) and not of MDPI and/or the editor(s). MDPI and/or the editor(s) disclaim responsibility for any injury to people or property resulting from any ideas, methods, instructions or products referred to in the content.